DISSERTATION

THE INFLUENCE OF ROD PHOTORECEPTORS ON COLOR PERCEPTION

Submitted by

Lucinda Susan Baker

Department of Psychology

In partial fulfillment of the requirements

For the Degree of Doctor of Philosophy

Colorado State University

Fort Collins, Colorado

Summer 2015

Doctoral Committee:

Advisor: Vicki J. Volbrecht
Co-Advisor: Janice L. Nerger

Stuart A. Tobet
Bryan J. Dik

ABSTRACT

THE INFLUENCE OF ROD PHOTORECEPTORS ON COLOR PERCEPTION

Since the 19th century, the human visual system has been described as two separate and non-interacting visual systems, the photopic system, mediated by cone photoreceptors, and the scotopic system, mediated by rod photoreceptors. The photopic system operates at high light levels, and provides us with color perception, while the scotopic system operates in low light levels, and allows us achromatic vision. It has come to be accepted that there is some overlap, or simultaneous activity, of these two visual systems at moderate, or mesopic, light levels. Anecdotal and empirical evidence has suggested that when rod and cone photoreceptors are simultaneously active, color perception is altered in two general ways: there is an increase in the perception of blue, and there is desaturation, or overall decrease in the perception of chromatic content of colored stimuli.

Various research groups have investigated the effect of rod photoreceptor input on color perception using a variety of research methods. The studies reported here extend previous work from this laboratory, and were conducted to characterize the development of rod influences on perceived hue and saturation during the course of dark adaptation, to reveal how the relationship between achromatic and chromatic perception is altered over time. The first study, which involved collecting descriptions of observers' hue and saturation perceptions, provided data that were used to predict the results of the second set of studies, in which observers identified the particular wavelengths of light that appeared to be of pure, or unique, hues under various viewing

conditions. In addition, observers also identified wavelengths of light that appeared to be equal mixtures of two neighboring hues, e.g., blue/green and green/yellow, under the same viewing conditions. These wavelengths are called binary hues. Results from the first hue scaling study were used to derive wavelength predictions for the second set of studies, with the expectation that the results from the two different experimental methods would produce the same pattern of changes in color perception correlated with rod photoreceptor activity. This was not what was found, however.

The results of all studies described herein provide only partial support for the hypotheses that increased rod input correlates with increased perception of blue and a decrease in perceived saturation of colored stimuli. What these results do show is that there was a great deal of variability in the responses provided by the four observers who participated in the hue scaling study, and noticeable differences in the hue loci identified by the three observers who participated in the second set of studies. The predictions derived from the hue scaling study, for both unique and binary hues, did not match the loci measured with a staircase procedure for the two observers who participated in all studies. The nature of the experimental procedures followed for these and other studies were considered, and some suggestions were offered to explain why the present results are not consistent with many already in the literature. The human visual system is very complex, and the methods employed in the present studies may not be sufficient to tease apart the effects of rod photoreceptor input from those of other anatomical and physiological differences at multiple levels of the visual system.

ACKNOWLEDGEMENTS

I want to gratefully acknowledge help I've received during the many years I've been a graduate student at Colorado State University. First I want to sincerely thank Diane Huber for cleaning my house all these years and helping to consistently restore order to what has been a chaotic home throughout this long process. I want to thank Dr. Kevin Michie who has cheerfully put me back together physically every couple of weeks since 1995. Without your care I never would have made it through graduate school! I want to thank Christine Cherny, C.M.T. for regularly undoing what hours at the computer have done to the muscles in my neck and shoulders. I want to thank Dr. Robert Calhoun for pushing me to get the hell out of Dodge. Each of you, with your expertise and friendship, has helped me to complete this Ph.D., and I thank you from the bottom of my heart for all you've done for me and for my family.

I'd also like to thank my friends, neighbors, and relatives, especially Dr. Miho Toi Scott, who have continued to ask if I've finished school yet, and how much longer it's going to take, for the past decade. These reality checks have always helped me to shift my gaze, even if only for a second, and remember that real life is still going on all around me, and the rest of the world isn't the least bit concerned with the drama taking place in my tiny academic universe. I can't wait to be able to say, "Yes, I'm finished!"

Sincere thanks to Graham Baker Parkinson for serving as experimenter during the collection of my unique blue and binary hue data in the summer of 2009. You were a big help and I appreciate your willingness to sit in the dark basement with your mom and help me finish data collection.

Thanks to Dr. Kathryn Medler for advice, encouragement, and friendship during these graduate school years. And thank you for teaching me how to do RT-PCR and supervising me by phone and email!

I am grateful to Stuart Tobet, who joined the faculty at CSU during my first year in MCIN. I'm pretty sure I would have called it quits years ago if you hadn't been here to talk to S. Thank you for everything you've helped me with, especially the multiple rewrites of my application statement for the Cold Spring Harbor course. The hours I spent discussing science in your lab were truly the highlight of my graduate school years here.

Thank you to the Fates who arranged for Dan Lopez Paniagua and me to arrive in the Psychology Department at the same time and share an office! Thank you Dan for being the best possible officemate and for "learning" me how to work those baffling personal computers. I hope your life's journey goes on and on and on and on and you don't stop believin'!

Thanks to Armando Trujillo, Katie Youngpeter, Vicki Volbrecht and Jan Nerger, the other observers in these experiments. I would never have suspected that these would be my dissertation experiments when we were doing them.

While my path to this Ph.D. has not been direct, all of my detours have brought me closer to an understanding of the human brain and the human mind, and the relationship between them. My matriculations as a graduate student in Clinical Psychology at Hahnemann University, and in Occupational Therapy, Biomedical Sciences, and Psychology at CSU, have all provided valuable learning experiences, as well as many wonderful friendships and relationships, for which I'm grateful. The tragic

deaths of two of my graduate student colleagues, Erik J. Bluhm and Marc V. Richard, gave me pause. Neither had completed his degree before his sudden death, so there was never a chance to celebrate as they graduated and moved on to new challenges. The sudden death of Dave McCabe, a young psychology faculty member, was another painful reminder of how precious and uncertain life is, as was the death of W. Gardner Kissack, my grown up friend since 1971, who looked forward to the news that I'd finally finished this Ph.D. Remembering these sad losses brings me a greater appreciation for my own opportunity to reach my academic goal, which I might otherwise take for granted.

Once again thank you Tony Smith for telling me back in 1981 that everything I was going to learn I was going to teach myself. And now that it seems I will graduate, thanks again Burt Louden for telling me that same year that you didn't think I had what it takes to earn a Ph.D. The memory of that conversation has stayed with me through these decades, and now we can both see that you were wrong.

Thank you Bruce Parkinson for being my mentor and role model, and for showing me how a successful research lab operates. Thank you for being supportive throughout this long foray back into formal education, and most of all thank you for being brave enough to be the father of my children. Separately and together we have accomplished a lot!

Thank you most of all to my wonderful children, Dr. Lily Alanna Baker Parkinson, Graham Dalton Baker Parkinson, and Robin Maxwell Baker Parkinson. You all were still in the elementary grades when I returned to school, and you've all managed to grow, thrive, and find your own interests and passions while I've been a distracted

student all these years. Your teasing and nagging, and the horrible prospect of never hearing the end of it if I didn't finish this dissertation and Ph.D., have kept me moving forward, slowly, and now it appears I will graduate! Choosing to devote my life to being your mom for many years before I returned to graduate school was the best decision of my adult life, and I thank each of you for the joy you've given me.

DEDICATION

To Bettyanne Lavina Lochte Baker (1919-2002)

and Walter Eugene Baker (1919-2002).

TABLE OF CONTENTS

"But he's got nothing on," marveled a little child.

Hans Christian Andersen

I don’t know who I am, but you know life is for learning.

Joni Mitchell

You can’t always get what you want, but if you try sometimes,
you just might find, you get what you need.

Mick Jagger and Keith Richards

CHAPTER 1: INTRODUCTION

This dissertation presents the results of psychophysical color vision studies conducted to examine the contribution of rod photoreceptors to color perception in the peripheral retina, and to compare peripheral color perception to central, or foveal, color perception. The goal of psychophysical studies is always to define the relationship between physical stimuli (e.g., monochromatic spectral lights) and an observer's psychological experience of those stimuli (e.g., color perception). An additional aim of such studies is to relate the pattern of mental processes reported as perceptual data to the neural processes that underlie them (see Stabell & Stabell, 2009, p. 41, for discussion). While there is a substantial empirical literature that reports on the effects of rod photoreceptor contributions to human color perception (see below), there is no general consensus on what these effects are or how they are physiologically determined. Stabell and Stabell, whose research for the past 45 years has examined rod effects on color vision, recently summed up the current state of the field, "…it must be admitted that our understanding of the underlying mechanisms of chromatic rod vision is still in a rudimentary state." (2009, p. 130). The stimuli and experimental methods used in past psychophysical studies vary greatly, as do the results and conclusions offered by the authors.

The present hue scaling study was undertaken in an attempt to extend findings from a previous investigation, which only examined rod effects on short-wavelength stimuli (Nerger, Volbrecht & Haase, 2003), by testing a wider range of stimuli across the visible spectrum. Another aim was to characterize peripheral color perception changes

across the 30 min time course of dark adaptation, after photobleaching of the photoreceptor cells (rods and cones). The unique and binary hue studies were subsequently undertaken to test the predictions suggested by the hue scaling results. Additionally, comparisons were made of observers' foveal and peripheral color perceptions from hue scaling and unique and binary hue judgments.

Historical Background

Trichromatic theory

Much of the theoretical background concerning human color vision comes directly from work conducted late in the 18th century and in the 19th century. As summarized by Kaiser and Boynton (1996), more than 200 years ago it had already been hypothesized that the human eye contained three types of "filaments" or mechanisms which processed light to mediate color vision. The specific activation ratios of these three mechanisms (one for each primary or principal color, red, green, and violet) by various wavelengths of light were proposed as the physiological substrate of color vision. Labeled the Young-Helmholtz trichromatic theory of color vision, acknowledging Thomas Young (1802), who formally articulated these ideas, and Hermann von Helmholtz (1910/1924), who adopted and developed these ideas some 50 years later, this theory was widely accepted in the latter part of the 19th century and early decades of the 20th century.

James Clerk Maxwell (1855), a Scottish contemporary of Helmholtz, conducted experiments in which he rapidly spun disks comprised of various colored papers, and demonstrated that the gamut of spectral colors could all be created by spinning disks

with specific proportions of three primary colored papers. This was the first report of quantitative data related to the ratios of cone photoreceptor activation that underlie our trichromatic color perception.

Physiological support for the trichromatic theory came in the second half of the 20th century with the identification of the short(S)-, middle(M)-, and long(L)-wavelength-sensitive opsins found in primate and human cone photoreceptors. Using microspectrophotometry it was possible to measure the spectral sensitivities of the different opsins in individual photoreceptor cells (Bowmaker & Dartnall, 1980; Marks, Dobelle & MacNichol, 1964; Wald, 1964). The locations of the three human cone opsin genes and their DNA sequences were subsequently reported (Nathans, Thomas & Hogness, 1986).

Opponent-process theory

Ewald Hering, another German physiologist interested in color vision, objected to the trichromatic theory. He argued that this theory was insufficient to explain color perception, and that there were four, rather than three, primary hue mechanisms at work in the human eye, and they were paired in an opponent fashion. Hering proposed the opponent colors theory in 1872, which he cleverly based in part on the phenomenon of colored afterimages (1964). For example, he noted that the afterimage of a red (green) stimulus was green (red), while for a blue (yellow) stimulus the afterimage was yellow (blue). A similar relationship was also observed for black and white stimuli. Hering's theory states that there are six elemental hues of color: blue, green, yellow, red, black, and white. All color perceptions can be described by these six colors. Furthermore, blue and yellow are opponent to each other, i.e., they are mutually

exclusive such that no single color can be described as bluish yellow or yellowish blue. Similarly, red and green are opponent to each other; but black and white are not mutually exclusive, since both black and white are often used to describe various shades of gray.

Jameson and Hurvich (1955) provided the necessary psychophysical evidence from their hue cancellation studies to quantify and support Hering's opponent processes model of color vision. Physiological evidence in support of Hering's theory was also provided in the mid-20th century by electrophysiologists who identified color-opponent neurons in the lateral geniculate nucleus of the thalamus in primates (DeValois, Smith, Kitai & Karoly, 1958).

Opponent-process theory and trichromatic theory were in competition for decades, although Hering himself stated in his *Outlines of a Theory of the Light Sense* (translated by Hurvich and Jameson in 1964) that he believed the two views were not mutually exclusive, and with slight modifications focusing on the distinction between excitation and sensation, both interpretations of color processing could co-exist side by side. It is now generally accepted that each of these two theories explains color processing at a different stage in the visual pathway. Two- and multi-stage models of color processing in the retina and beyond have been proposed (e.g., Hurvich & Jameson, 1957; DeValois & DeValois, 1993), with an initial stage representing the signals from each of the three cone classes, and a second stage in which these signals are combined to represent the three opponent channels: a yellow/blue (Y/B) channel, a red/green (R/G) channel, and an achromatic black/white (Bk/W) luminosity channel, which processes information about light levels or brightness (DeValois & DeValois,

1993). For Y/B opponency, signals from S cones combine antagonistically with the sum of signals of M and L cones, and this is expressed as S-(M+L). R/G opponency is represented as L-M, or sometimes (L+S)-M, the M-cone signals subtracted either from the L cone signals, or from the sum of L and S cone signals. The latter version takes into account the short-wavelength red inputs from S cones, whereas the L-M model only factors in the long-wavelength red input. Buck (2001) subsequently proposed a color processing model that includes rod signals, that combine early in retinal processing with signals from the three cone types, consistent with results of psychophysical data he obtained.

Due to the opponent relationship between blue and yellow and red and green, it is possible that the blue and yellow components of the Y/B channel can completely cancel each other and in effect nullify output from the Y/B channel. In this case, the Y/B channel is said to be in equilibrium. When this occurs, the only hues that can be perceived are red or green. Likewise, when red and green components in the R/G channel completely cancel each other, the only channel able to provide hue information is the Y/B channel. In studies using monochromatic stimuli from the visible spectrum (400 nm-700 nm) it is possible to determine the wavelengths of light at which nullification or equilibrium occurs in the Y/B and R/G channels. This wavelength is called the null point and is perceived to be a unique hue (UH). For example, when the Y/B channel is in equilibrium, with equal but opposite input from the yellow and blue mechanisms, a wavelength in the middle region of the visible spectrum is perceived to be green with no blue and no yellow. The wavelength of light is defined as unique green (UG). The R/G channel has two null points, one at a longer wavelength in the

visible spectrum that appears unique yellow (UY), with no red and no green components, and the other at a shorter wavelength that appears unique blue (UB), with no red and no green components. Unique red (UR) is an exception; there is no wavelength in the visible spectrum that appears uniquely red. Observers require a mixture of short- and long-wavelength red lights in order to perceive a unique red that contains neither blue nor yellow components (Abramov & Gordon, 2005; Larimer, Krantz & Cicerone, 1975).

A related concept is binary hue, which refers to a wavelength in the visible spectrum that is perceived as containing equal components of two hues. Each binary hue results from activation of each chromatic opponent mechanism. For example, a binary hue that appears 50% blue and 50% green (i.e., blue/green) is the result of activation of both the Y/B and R/G opponent processes.

Duplicity Theory

Anatomical information about the substrate of human color vision was provided by another important figure in 19th century vision research, the microscopist Max Schultze (1866), who identified two types of photoreceptors, rods and cones, in the retinae of owls and birds. The proportion of each receptor type correlated with the animals' status as either nocturnal or diurnal. This initial identification of two classes of photoreceptors, along with the observation that human night vision is achromatic, provided the initial basis of the duplicity theory of vision. The German physiologist Johannes von Kries (1905) refined the theory, which stated that mammals have two independent visual systems, a photopic system, mediated by cone photoreceptors for

chromatic daylight vision, and a scotopic system, mediated by rod photoreceptors for achromatic vision in the dark.

In the middle of the 20th century evidence began to accumulate that refuted the independence of the photopic and scotopic systems, particularly under mesopic viewing conditions, when both rods and cones are stimulated. For example, Polyak's histological studies (1941) revealed common retinal pathways used by both rods and cones, which supported the idea of interaction of the photopic and scotopic systems. During psychophysical measurement of dark adaptation curves, measured while observers' photoreceptors adapted to darkness over time, observers reported color perception in short-wavelength stimuli presented to the peripheral retina at light levels below the cone plateau, i.e., stimuli at light levels below cone threshold, that would be detected by rods only, providing evidence that rods are involved in color perception (Hecht, Haig & Chase, 1937). Further support for the claim that rods contribute to chromatic as well as achromatic perception was reported by Lie (1963), who expanded on research reported by Loeser (1904) six decades earlier. Both researchers reported that as dark adaptation proceeds past the cone plateau, changes in color perception of a given wavelength correlate with increasing rod sensitivity. Lie proposed that a mixing of rod and cone signals led to these changes in color perception. Stabell and Stabell (1965) subsequently showed that it is possible to elicit different color sensations using low intensity (scotopic) stimuli after chromatic adaptation with a range of colored filters. From these studies, it emerged that 1) rods contribute an achromatic component to a percept, and thus reduce the chromatic content or saturation of a stimulus (e.g., Lie, 1963), and 2) rods contribute a chromatic signal under certain conditions (e.g., Hecht et

al., 1937; Stabell & Stabell, 1965). It should be noted, however, that none of the color vision models proposed before 2001 (see Buck, 2001) include a rod term, and thus the idea that the photopic and scotopic systems operate independently has lingered in the field of human color vision.

Anatomy and Physiology: The Retina and Beyond

Laminar Organization of the Retina

Vision starts in the retina, a 250 μm thick laminar neural tissue that lines the back of the eye (Chaudhuri, 2011). There are five retinal cell layers, each composed of a single neural cell class. Visual information processing in the retina can follow a straight-through, feed-forward pathway, involving just three of the retinal layers [the photoreceptors, bipolar cells (BCs) and retinal ganglion cells (RGCs)], or there can be horizontal signal modulation in either or both of the inhibitory interneuron-like cell layers, the horizontal cells (HC) and amacrine cells (AC). All visual signals exit the eye carried on the axons of RGCs, which form the optic nerve. **Figure 1.1** provides a simplified representation of the anatomical arrangement of the neural cells of the peripheral human retina, and some of the known patterns of connectivity.

Photoreceptor cells in the outermost layer of the retina express photosensitive pigment molecules (opsin with bound chromophore) capable of capturing photons of light. The transduction of that electromagnetic energy into a neural signal initiates the process of vision. Humans possess two classes of photoreceptors, rods and cones, and the photoreceptor layer in a human with normal color vision is comprised of four cell types: rods, which are a homogeneous class of cells, and three types of cones. Each

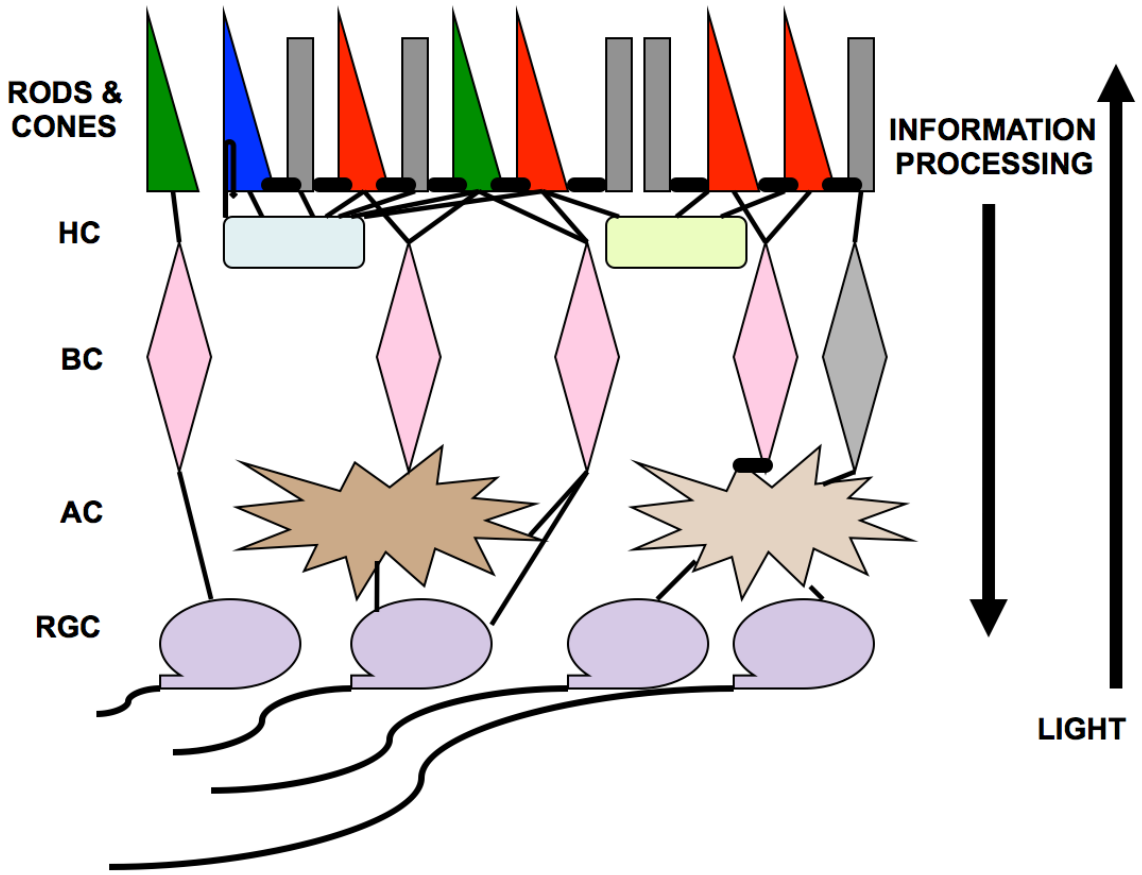

Figure 1.1: Schematic of the peripheral human retina. As indicated on the right, light must pass through all retinal cell layers before photons are captured by opsin molecules in the outer segments of the photoreceptors. Neural signals then travel in the opposite direction. The five neural cell layers, from top to bottom, are the outermost photoreceptor cell layer (rods and cones), horizontal cell layer (HC), bipolar cell layer (BC), amacrine cell layer (AC), and innermost retinal ganglion cell layer (RGC), whose axons form the optic nerves, which exit the back of each eye. Small black cylinders represent gap junctions, a type of electrical synapse that couples some of the retinal cell types. Black lines represent conventional chemical synaptic connections between cells. The connections between the cone, BC and RGC on the left represent the straight through pathway.

human retina contains approximately 120 million rods, but only about six million cones, so the rods constitute 95% of all photoreceptors in each eye (Curcio, Sloan, Kalina & Hendrickson, 1990; Østerberg, 1935). In their outer segments all rods express many molecules of the protein rhodopsin, the product of a gene found on the long arm of

autosome 3 (Sparkes et al.,1986). Bound to each rhodopsin protein is a molecule of the chromophore retinal, and together they comprise the rod photopigment. This photopigment confers an absorption spectrum with a spectral peak near 507 nm to rod photoreceptors (Reeves, 2004).

The outer segments of each cone photoreceptor contain many molecules of a single type of opsin protein, bound to retinal, and the cone photoreceptors are classified into three categories based primarily on the opsin protein they express. The three cone opsins are separate gene products (Nathans et al., 1986). S cones, so called because they express short-wavelength-sensitive opsin, are the least numerous of the cone types, although there is disagreement concerning the exact proportion of S cones in the retina, e.g., Sharpe et al. (1999) report that S cones make up 7% of the cone population, while other authors report they represent approximately 15% (Ahnelt, Kolb & Pflug, 1987; Masland, 2001). The S-opsin molecule, which is genetically encoded on autosome 7, confers an absorbance spectrum centered about 440 nm in the human eye (Sharpe et al, 1999). M cones (expressing middle wavelength-sensitive opsin) and L cones (expressing long-wavelength-sensitive opsin) have been reported to comprise highly variable proportions of the total cone population in observers with normal color vision, i.e., some subjects have 15 times as many L as M cones, while others have twice as many M as L cones (Hofer, Carroll, Neitz, Neitz & Williams, 2005; Roorda & Williams, 1999). The genes for the M-opsin and L-opsin molecules are both encoded on the X chromosome, and it is believed that duplication of an ancestral gene 30 to 40 million years ago led to the emergence of the second opsin gene on the X chromosome (Nathans, 1987).

The amino acid sequence of rhodopsin reveals a 40-45% identity with the sequences of each of the cone opsins, and the S-opsin shares this same identity percentage with the M- or L-opsin sequences. The M- and L-opsins are 96% identical at the amino acid level, in contrast, and have largely overlapping absorbance spectra, with wavelengths of maximum absorbance that differ by only 20 nm: 545 nm for M-opsin and 565 nm for L-opsin (Nathans, Merbs, Sung, Weitz & Wang, 1992).

Present in the photoreceptor cell layer are electrical synapses (gap junctions) between rods and each of the three cone types (Ahnelt, Kerl & Kolb, 1990; Raviola & Gilula, 1975), and between M and L cones (Cook & Becker, 1995). Very little evidence of electrical coupling between S cones and M or L cones has been reported (Ahnelt et al., 1990). There are also feedback inputs from HCs onto the terminals of photoreceptors (Packer, Verweij, Li, Schnapf & Dacey, 2010), so that the initial signals transmitted at the first chemical synapses after photon capture have already undergone mixing that is not yet completely understood.

The horizontal cells (HCs) constitute the next cell layer in the retinal pathway, and are believed to be involved in modulating photoreceptor signals and creating antagonistic input to bipolar cells. While the HCs are post-synaptic to photoreceptors, they are also pre-synaptic, as they show massive feedback connections onto the terminals of photoreceptors. Like photoreceptors, the HCs are also interconnected with their neighbors through gap junctions on the dendrites (Perlman, Kolb & Nelson, 2012). Three HC types have been identified in the human retina: one type is known to synapse with rods and all cone types, the second synapses only with the three types of cones, and it is suspected that the third HC type contacts both rods and M- and L-cones

(Ahnelt & Kolb, 1994). HCs have recently been reported to underlie spectral opponency found in the receptive fields of primate S-cones, due to the lateral inhibitory effects of HCs on signal processing (Packer et al., 2010). Visual signals passing straight through the retina bypass the HC layer and synapse directly on the BCs in the middle layer of the retina.

Kolb et al. (1992) report that the use of Golgi staining has identified eleven anatomically distinct types of bipolar cells (BCs) in the human retina. Ten of these carry cone signals and one type carries rod signals. While it was formerly thought possible that rod signals were segregated from cone signals in the first layers of the retina, the facts that gap junctions couple many rods and cones (Kolb, 2011), and that much of the photoreceptor cell layer inputs are processed in the HC layer (Kolb, 2011), do not support this segregation. Recently published data from mouse retinae indicate that murine cones have a direct input to rod BCs and that rods have direct input to cone BCs, calling into question the accepted model of mammalian retinal circuitry (Pang et al., 2010). It remains to be seen if this pattern of connectivity is also present in the human retina. At this point the data seem to suggest that there is very little separation of rod signals from cone signals in the human retina, and that in general rod and cone signals are combined at the earliest levels of processing. The putative rod BCs are presynaptic to two of the ACs found in the next retinal layer, the AII and A17 amacrines (Kolb et al., 1992).

The second type of retinal inhibitory interneuron-like cells, the ACs, are the next cell layer. ACs are the most diverse class of retinal cells, with 29 different types, classified by morphology, neurotransmitter, and synaptic connections (Masland, 2001).

They are believed to serve a number of functions in visual information processing. As mentioned above, not all visual signals are processed by ACs, since some information is transmitted directly from BCs to retinal ganglion cells (RGCs). Two types of ACs synapse with the putative rod BCs, as mentioned above, and this has previously been thought of as one of the pathways that carry segregated rod signals through the retina.

The innermost cell layer of the retina, RGCs, is also diverse, with 25 different types of RGCs identified in either the human retina or in the macaque monkey, a species that shares much retinal anatomy and physiology with humans (Kolb et al., 1992). RGCs are also classified by size, morphology and connectivity patterns. These are the final output cells of the retina, and the axons of the approximately 1.0 - 1.25 million RGCs bundle together to form the optic nerve of each human eye. The neural signals carried by the RGCs to visual areas of the brain already show the characteristic color-opponent relationship described earlier, with Y/B information carried in the koniocellular pathway and R/G information carried in the parvocellular pathway. Recent electrophysiology data confirm that small, bistratified cells (SBCs), a class of RGC that carry information in the Y/B opponent channel, also carry rod signals that are received via the AII ACs (Field et al., 2009).

Rod Pathways in the Retina

Rods are believed to have evolved more recently than cones, and rod signals combine or “piggyback” onto the cone retinal circuitry that presumably was already in place when rods appeared in the eyes of our ancestors (Masland, 2001). It has been accepted for some time that there are three pathways along which rod signals are transmitted through the retina to the RGCs, whose axons form the final common

pathway for all visual information leaving the eye. As shown in **Figure 1.1**, there are gap junctions that electrically couple rod and cone photoreceptors in the outer retina, and provide a direct connection through which rod signals combine with cone signals (Anhelt et al., 1990; Raviola & Gilula, 1975). Photoreceptor output that is processed by HCs before the signals are sent to BPs is a second step where the rod and cone signals can be combined. Rod BPs are presynaptic to AII and A17 ACs, and this is the third potential site where rod and cone signals might combine in the retina. Recent electrophysiological evidence from murine retinae suggests additional BC routes carrying mixed rod and cone signals. Pang et al. (2010) report findings that suggest that rod BCs receive substantial direct cone input and cone BCs receive substantial direct rod input, which challenges the traditional dogma about the wiring of the mammalian retina and segregation of rod and cone signals. It remains to be seen if this connectivity is also present in the primate retina.

Spatial Organization of the Retina

Retinal topography is defined relative to the fovea, a 1.5 mm diameter dimple located in the center of the retina. The very center of the fovea, the *fovea centralis*, a rod-free region estimated to be between 250 and 750 μm in diameter, contains specialized thin cones in a closely packed arrangement ("Facts and Figures," 2014). These foveal midget cones are wired in a one-to-one arrangement with midget BP cells, which then synapse one-to-one with midget RGCs, such that there is no convergence of cone signals from the central fovea, as illustrated on the left of **Figure 1.1**. Moving eccentrically from the fovea, the interposition of rods between cones increases, and the density of cones falls off sharply as the rod density increases. The cone photoreceptors

found in the peripheral retina are much larger than the foveal cones, with inner segment diameters that are approximately three times those of the cones of the *fovea centralis*. At an eccentricity of 10°, the density of cone photoreceptors differs along the vertical and horizontal meridians. The overall number of cones is greater along the horizontal meridian, in the nasal and temporal retinal regions, than in the superior and inferior retinal locations defined by the vertical meridian (Curcio et al., 1990). At approximately 10° temporal retinal eccentricity, the distribution of cones is stabilized at a low density that remains approximately constant across the surrounding peripheral retina. The density of rods continues to increase out to about 18° eccentricity in the temporal retina, and then declines gradually into the far periphery (Curcio, Sloan, Packer, Hendrickson & Kalina, 1987; Østerberg, 1935). The peripheral retinal location used in the experiments reported here, 10° temporal retinal eccentricity, is characterized by a high rod density and a low cone density, and is therefore an ideal region of the retina upon which to test for rod effects on color perception.

In addition to the changes in photoreceptor distribution as one moves from the fovea out into the peripheral retina, the entire size scale of the retina increases: there are progressive changes in the optics of the eye through which light must pass, increases in the size of the receptive fields of retinal cells, and increases in the degree of neural convergence from photoreceptors to RGCs (Calkins, 2004). Thus, the neural substrate that processes the signals for a stimulus presented to the fovea differs in a number of ways from the neural substrate found in the peripheral retina, with the photoreceptor distribution and neural processing being only two of these differences.

Beyond the Retina

Visual signals from the retina travel along an estimated 20 parallel pathways and are carried to several brain regions, including some which process visual input for non-image forming functions. Optic nerve fibers in the image-forming pathways synapse initially in the lateral geniculate nucleus (LGN) of the dorsal thalamus, in a precisely organized fashion that preserves monocular input, retinotopy, and the segregation of the parvocellular (R/G), koniocellular (Y/B), and additional pathways of visual information. The next synapse occurs in one of the input layers of V1, also called the striate cortex or primary visual cortex, located on the banks of the calcarine sulci of the medial occipital lobes. The retinotopic organization of the visual field is maintained in V1, and an important feature of the processing of visual information here is cortical magnification, defined as progressively smaller areas of cortex processing the visual input from increasingly distal eccentric retinal locations, while visual information from the fovea is processed in a disproportionately large area of cortex. This corresponds to the increase in the size of RGC receptive fields as one moves away from the fovea. Hubel (1988) estimates that magnification for foveal input is 36 times larger than that for peripheral retinal input.

There are at least 30 visually-responsive areas in the cortex of the macaque, receiving inputs along multiple pathways exiting V1 (e.g., Schmolesky, 2000), and recent imaging studies indicate that there are at least 30 separate human visual cortical areas as well (Kulikowski et al., 2009). Each of these separate visual cortical areas contains a map of the entire visual field, with subsequent, secondary cortical areas processing increasingly complex features of the visual world. For decades the literature

has suggested that human extrastriate area V4 is the “color center,” the cortical site where processing of color information occurs, that would be accessible to our conscious perception (e.g., Lueck et al., 1989). A debate arose about the precise cortical location of this color center, with some investigators reporting that V4 is the color center and others insisting that an adjacent or overlapping region of cortex, which they named V8, was in fact the human color center (Hadjikhani, Liu, Dale, Cavanagh & Tootell, 1998; McKeefry & Zeki, 1997). Results of a recent fMRI study confirm that areas V4 and the adjacent VO1 are cortical locations that represent perceptual color space (Brouwer & Heeger, 2009). All of these areas identified as putative color centers are found in the ventral stream or “what” pathway of visual processing areas, a pathway concerned with specific features of visual stimuli, as opposed to the dorsal “where” or “how” pathway, which processes information about the movement or spatial location of visual stimuli. These ventral occipital cortical regions are the most likely processing regions for the color perceptions reported here.

Dark Adaptation

Dark adaptation is the process whereby visual sensitivity recovers in the dark after the eye has been exposed to a bright light, a process called “bleaching” or “photobleaching.” Photon capture during light exposure triggers a conformational change in the opsin molecules found in the outer segments of photoreceptors, and early observations of rhodopsin’s concomitant loss of its purple tint with light exposure is the basis of the term “bleach” (Wald, 1935). Exposing the eye to a bleaching stimulus

causes similar conformational changes in the rod and cone opsin molecules, and dark adaptation, graphically illustrated in **Figure 1.2**, refers to the simultaneous recovery of both the scotopic (rods) and photopic (cones) visual systems along different time courses.

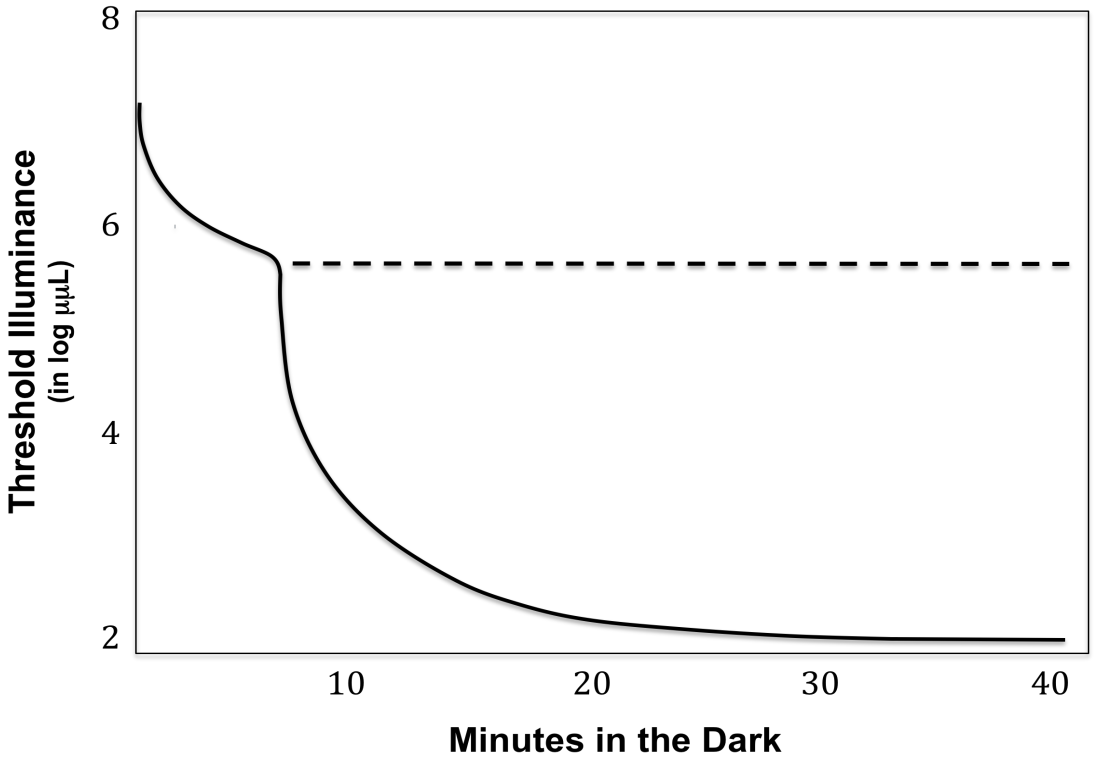

Figure 1.2: Schematic drawing of the classic dark adaptation curve produced when absolute threshold is determined for a test flash of violet light delivered to the peripheral retina. Bleaching occurred at time 0. Solid line represents absolute visual threshold, expressed in log units relative to absolute scotopic threshold. Dashed line represents the "cone plateau," absolute threshold for the photopic visual system. Redrawn after Bartlett (1965).

After exposing the eye to a bleaching stimulus, one's visual threshold is greatly elevated. Psychophysical measurements have identified a predictable pattern of recovery and restoration of maximum visual sensitivity with a time-course of about 10

min for cones and approximately 30-40 min for rods, as illustrated in **Figure 1.2**. It has been known for decades that the recovery of visual sensitivity is associated with the progressive regeneration of visual pigment molecules after photobleaching (Alpern, 1971; Lamb & Pugh, 2004; Rushton & Powell, 1972). Because the time course of cone opsin regeneration is much faster than that of rhodopsin (Rushton, 1957), a "rod bleaching" paradigm (stimulus presentation during the experimental window between 4-9 min post-bleach) can be used, during which cone photoreceptors are functioning exclusively or nearly exclusively at threshold detection levels. After bleaching with a stimulus calculated to isomerize all or nearly all the opsin molecules, the rods will remain saturated for a number of minutes, even in the dark, and thus will not contribute or will contribute minimally to visual perception. A theoretical explanation for this involves the presence of intermediate photoproduct molecules that are thought to remain in the photoreceptors for some time after rhodopsin has been isomerized, that act as "equivalent light" thus "veiling" the rods from incoming light for a period of time (Reeves, 2004). This timing manipulation has been exploited in many studies (e.g., Buck, Knight, Fowler & Hunt, 1998; Nerger et al., 2003), to compare perceptions reported under "bleach" conditions (minimal rod activity) with perceptions reported after complete dark adaptation ("no-bleach" condition), when both rod and cone photopigments have regenerated.

The biochemical pathway followed after photon capture is termed the retinoid cycle. Photon capture by the 11-cis retinal chromophore coupled to each rhodopsin or cone opsin molecule is the initial step in the transduction cascade that leads to vision. This involves the conformational change of the chromophore to an all-trans form, and

the subsequent dissociation of the chromophore from the opsin protein, which has also undergone conformational change. In order to again signal photon capture, the opsin protein must return to a responsive state, and bind to another 11-cis retinal chromophore (Hecht et al., 1937). A canonical pathway through the retinal pigment epithelium (RPE), the cell layer immediately superficial to the photoreceptor layer, is known to be involved in the regeneration of the chromophores which bind to rhodopsin and cone opsins. An additional, faster cone-specific pathway has been suspected to exist, given the rapid timescale of cone recovery after bleaching. Convincing data now suggest that for cone opsin regeneration there is a separate pathway in the retina that recycles all-trans retinol to 11-cis retinal, providing a pool of the chromophore and supporting rapid dark adaptation of cones (Wang & Kefalov, 2009). Rather than passing from the photoreceptors through the RPE, this alternate, fast chromophore pathway involves Müller glia cells of the retina, and evidence supporting the existence of this presumptive alternate pathway contributes to our understanding of the time-course differences between the scotopic and photopic visual systems at the molecular and cellular levels in human dark adaptation.

Review of More Recent Literature

By the 1950s, the ideas that rod and cone signals interact in the retina, and that rods contribute to color perception under mesopic light conditions, were accepted by a number of researchers, although the nature of the contribution conferred by rods was not agreed upon. In an important series of experiments, Lie (1963) asked observers to describe their perceptions of monochromatic stimuli across the time course of dark

adaptation. The same wavelength was simultaneously presented to the fovea and 6° nasal retina of one eye, and a comparison of the saturation (ratio of hue component to hue and achromatic components) of the two stimuli was used as an indication of the effect of rods on peripheral color perception. Results indicated that stimuli in the periphery appeared increasingly desaturated (i.e., more achromatic and less chromatic), as well as brighter, as rod contribution increased. These findings were explained by a model in which cones contribute a chromatic component to hue perception, while rods contribute an achromatic component that increases in strength, during dark adaptation. These studies set a precedent of comparing foveal to peripheral color perception as a technique for examining rod effects (e.g., Abramov, Gordon & Chan, 1991).

In a 1970 article, Trezona reviewed the results of a number of color matching studies that had been conducted in the previous two decades (Trezona, 1970). In these trichromatic color matching studies observers were typically shown two adjacent light fields, a test field of a single wavelength and a comparison field composed of three wavelengths from the blue, green, and red regions of the spectrum, the proportions of which observers were asked to adjust in order to match the test field. While various parameters differed in the studies reviewed, e.g., test and comparison field sizes, retinal locations, wavelengths tested, there were a number of results that indicated that color perception in retinal locations outside the rod-free fovea differed from foveal color perception. Trezona (1970) evaluated whether or not these results were consistent with the assumption that under photopic viewing conditions, rods elicit a blue sensation. This suggestion had been in the literature for at least a decade previous to Trezona's work (and even today is still occasionally implied to be an accepted "fact" about rod

effects on color perception; e.g., see Field et al., 2009). Trezona (1970) concluded that peripheral color perception (in retinal locations where rods are found) differed from foveal (rod-free) color perception, and in many of these studies the difference was a deviation in a blue direction.

In a subsequent study, the effects of rods on peripheral color perception were examined specifically to determine whether rods act as "blue" receptors, by comparing color-matching results obtained on the cone plateau and during dark adaptation (Ambler & Proctor, 1976). Observers were asked to make a color-match to a 500 nm test stimulus presented to the peripheral retina of either a dark-adapted or light-adapted left eye, using a mixture of 470 and 520 nm lights, adjusted by the observer, and viewed by the right eye. Observers required more 470 nm (i.e., short-wavelength) light to match the peripheral test stimulus under the dark adaptation condition than when the same stimulus was presented after light adaptation, consistent with the idea that more blue was perceived when rods were contributing to the perception. The same comparison was made with a foveal presentation of the test stimulus, and no difference in the blue component was needed for the match under the different adaptation conditions, leading the authors to conclude that in their experimental paradigm rods contributed a blue response.

In a series of studies beginning in the 1960s, the prolific Stabells obtained results consistent with the view that rods contribute a chromatic, but not exclusively blue, signal to color perception. Their experiments were carried out using a Wright colorimeter, a device which allows observers to adjust the wavelength components (red, green and blue light) viewed by one eye in order to make a color match to stimuli presented to the

other eye, or between different regions of the retina in the same eye. Their results were then reported as values in the WDW foveal color space (Wright, 1946) that describes the wavelength composition of their color matches. The Stabells' 1975 color matching study examined the effect of superimposing an achromatic scotopic stimulus on a long-wavelength (red) photopic test stimulus, and observing the difference in hue perception that resulted from the addition of a wavelength that stimulated only the rods for dark-adapted observers. Several different wavelengths between 420 nm and 550 nm were presented as the scotopic stimulus, and the wavelength used had no effect on the outcome. When the achromatic light was superimposed over long-wavelength (red) stimuli, this manipulation yielded a perceptual hue shift towards yellow (Stabell & Stabell, 1975). In a second experiment observers made color matches on the cone plateau six minutes after photobleaching, and then 25 minutes later after total dark adaptation, with the assumption that any differences between the two matches were due to the contribution of rods. Stimulus intensity was systematically varied during this experiment. The data showed that middle- and long-wavelengths (yellow-green and orange) shifted "markedly" towards yellow, while shorter wavelengths (violet and blue-green) shifted towards blue, but only when the intensity of the test stimulus was low (Stabell & Stabell, 1975). For the low intensity stimuli observers also reported decreased saturation when stimuli were viewed after dark adaptation, compared to when they were viewed on the cone plateau. As stimulus intensity increased, the difference in saturation at the two time points decreased, until there was no difference in saturation reported when the stimuli were of high intensity. The authors concluded that rods contributed an enhanced blue signal for stimuli in the short-wavelength region of

the spectrum, and an enhanced yellow signal for long-wavelength stimuli, contrary to the assumptions that rods only contribute a blue color quality and/or a desaturating component to color perception.

A subsequent color-matching study in which the peripheral retinal location tested was varied yielded the same conclusions, namely that rod input during dark adaptation produced changes in all hues, and that the blue signal was enhanced for stimuli in the short-wavelength region of the spectrum, while yellow was enhanced for stimuli in the middle- and long-wavelength regions of the spectrum (Stabell & Stabell, 1976). These results were further interpreted to indicate that the rod contribution to peripheral color perception strengthens the Y/B opponent process relative to the R/G process. Results from a later study (Stabell & Stabell, 1979) focused on rod effects for long-wavelength stimuli, that tested three different intensities of both bleaching stimuli and test stimuli, again led the Stabells to conclude that the effect of rods is to alter the perception of long-wavelength stimuli towards yellow, in contrast to the suggestions in the literature that rods only contribute a blue component or an achromatic component. For example, a 620 nm stimulus perceived as red on the cone plateau was subsequently perceived as orange-red under dark adaptation conditions with maximal rod input. The overall conclusion that the Stabells report after many studies is that rods alter perception of all principal hues of the spectrum by strengthening the blue and yellow signals for stimuli of various wavelengths (Stabell & Stabell, 1979).

Since the 1970s Abramov and Gordon have collaborated on a research program that compares peripheral color vision and foveal color vision (e.g., Abramov, Gordon & Chan, 1991; Gordon & Abramov, 1977). Much of their work has been concerned with

perceptive fields, the psychological correlate of receptive fields, which increase in size with greater retinal eccentricity, such that colored stimuli presented to the peripheral retina must be much larger than those presented foveally in order to obtain qualitatively similar hue scaling data (Gordon & Abramov, 1977). Small stimuli viewed in the peripheral retina appeared desaturated and of uncertain hue, except for long wavelength stimuli, that were perceived as saturated and red. These authors suggested that the sparse arrangement of cones in the far periphery (45º nasal retina) requires a larger stimulus diameter to adequately stimulate all four color mechanisms.

An interesting finding from the hue scaling study of Gordon and Abramov (1977) was that observers reported a blue hue component at longer wavelengths for stimuli viewed in the peripheral retina than for those viewed foveally, which the authors suggested might be explained by rod contributions to the blue channel and to a luminosity channel, leading to a desaturated color appearance. However, this early study used a high photopic light level of 1200 phot td (3.1 log td), and thus any rod contribution would likely have been negligible. Observers dark adapted for only 10 min before beginning data collection, so no comparisons under conditions of minimal and maximal rod contribution were reported (Gordon & Abramov, 1977).

In subsequent papers these researchers reported refinements of their hue scaling procedure (Gordon & Abramov, 1988; Gordon, Abramov & Chan, 1994), and it is their method that was followed to collect the hue scaling data reported here. Further investigations of perceptive field sizes in different retinal locations using stimuli equated to 20 td, a mesopic light level that would be expected to stimulate both cones and rods,

indicated that at 10º temporal retina, fovea-like color perceptions were reported for a stimulus with a 2° diameter (Abramov et al., 1991).

Given that colored stimuli in daily life are more likely to be surrounded by bright fields than dark surrounds, Abramov et al. (1992) presented the same 20 td monochromatic hue scaling stimuli used in the studies described above, but this time they were surrounded by a large, 8 td, broadband annulus (i.e., “white” ring of light) instead of the dark background used in previous studies. This experimental condition might be expected to decrease rod contribution, as a large portion of the retina surrounding the test stimulus was in a state of light adaptation throughout the experimental sessions, but these conditions did not maximize or minimize rod activity to the degree that stimulus presentation on the cone and rod plateaus of dark adaptation would predict. When these peripheral hue scaling results were compared to those obtained with the dark background, perceptive field sizes for all hue mechanisms were found to be smaller when the broadband annulus was present, but variable, stimulus size-dependent effects on saturation were also seen. Small stimuli appeared more saturated, while larger stimuli were less saturated under these conditions. Foveally-presented stimuli were perceived as more saturated than the peripheral stimuli. The authors suggest that the white surround reduces rod contributions, which might explain the difference in perceptive field sizes, but does not offer a way to understand the size-dependent saturation changes (Abramov et al., 1992).

Buck and colleagues have studied the effects of rods on color perception for many years, using direct hue scaling and UH measurement methods (e.g., Buck et al.,1998; Knight & Buck, 2002). Results from a hue scaling study (Buck et al., 1998),

which isolated rod effects by comparing color appearance data obtained under cone plateau conditions with data obtained after dark adaptation, showed changes in the perception of all hues when rod contribution was maximal. The spectral distribution of each of the hues shifted when rods contributed to color perception, compared to the range of each hue reported when stimuli were viewed under cone plateau conditions. Though each of the three observers' results showed a shift, the direction and magnitude was not consistent across observers. Also, the percentage of each hue perceived changed in different portions for all observers when rods were active, although again the changes were not uniform increases or decreases of any given hue term in particular portions of the spectrum.

Additional results from these authors indicated that rods influence the perception of short-wavelength stimuli by enhancing the amount of short-wavelength red perceived, while for longer-wavelength stimuli rods contribute an enhanced green signal, thus showing different effects on the same R/G opponent process (Buck & Knight, 1997). There was also an enhancement of blue perception for shorter-wavelength stimuli when rods contributed, indicating that rods influence both the R/G and Y/B opponent mechanisms. Knight and Buck (2002) suggest that rod signals combine with those of S-cones to enhance the perception of short-wavelength red and blue for shorter-wavelength stimuli, whereas the rod signals combine with those from M- or L-cones to enhance the perception of green for longer-wavelength stimuli. It was noted that alterations in wavelength, light level, and stimulus duration all affected the rod influence, and the authors concluded that these "multiple" rod influences also follow different time courses (Knight & Buck, 2002). These time courses were characterized in a

manipulation involving a broadband ("white") scotopic stimulus upon which monochromatic test stimuli were superimposed, either simultaneously, or after either a one sec or five sec time delay (Knight & Buck, 2002). Hue scaling data were obtained with these background conditions following a rod bleach along the time period associated with the cone plateau of the dark adaptation function, or after 30 min of dark adaptation. The authors found that rods appear to enhance a green perception when there is no delay or a one sec delay between the onset of the background stimulus and the test stimulus presentation, but this effect is reduced or eliminated if there is a five sec delay. Enhancements of blue and red only occur when there has been the five sec delay in stimulus timing. These results support the idea that there are multiple pathways through which rod and cone signals interact in the retina and beyond.

Results of UH measurements made under cone plateau and dark adaptation conditions, to assess the influence of rods, were inconclusive and demonstrated a light-level dependence (Buck, Knight & Bechtold, 2000). The authors concluded that, in general, at low light levels that would presumably permit a greater rod influence, the locus of unique blue (UB), unique green (UG), and unique yellow (UY) shifted to longer wavelengths. It should be noted that a large 7.6º test stimulus, centered at 7º eccentricity, was used for the peripheral measurements. Not only is a large area stimulated, but this area of the retina is characterized by rapid changes in receptor populations and distributions.

A more recent study from Buck's lab investigated the effects of stimulus size, duration, and light levels on peripheral UH loci (Buck, Thomas, Connor, Green & Quintana, 2008). The results were inconclusive, showing unexplained variability in

individual observers' data, and no systematic rod effect across conditions. In fact, there was a strong light-level dependence of the rod influence on UB, such that shifts in opposite directions were seen at different light intensities. The authors conclude that generally, at low light levels, rods influence the loci of UHs with a shift to longer wavelengths, but again this was not a consistent finding among observers. Even now these results illustrate the state of our knowledge of rod effects: there is considerable variation in the effects found across studies that seem highly dependent on the experimental method used and on various aspects of the stimuli utilized. A number of rod effects have been proposed, and different experiments may evoke different combinations of these effects, or different strengths of various effects simultaneously (Buck, 2001).

In Lembessis' unpublished doctoral dissertation on the influence of rods on color vision (1997), observers in a hue scaling study perceived decreasing saturation across the time-course of dark adaptation for monochromatic stimuli of short, middle, and long wavelengths. The ratios of all four primary hues perceived changed across the time-course of dark adaptation as well, but the data show much inter-observer variability, so that no consistent pattern of influence emerged.

Nerger and Volbrecht for a number of years have also investigated the effect of rods on peripheral color vision, and the differences between foveal and peripheral color perception (e.g., Nerger, Volbrecht & Ayde, 1995; Nerger, Volbrecht, Ayde & Imhoff, 1998; Nerger et al., 2003; Volbrecht, Nerger, Imhoff & Ayde, 2000). A series of UH studies used stimuli equated to 250 td, an intensity at which rods would not be expected to contribute to hue judgments. Not surprisingly, the results did not show a strong rod

effect on the loci of the UHs. Differences in the locus of UHs measured at the fovea compared to those measured in the periphery (at 8° nasal, 8° superior, or 20º temporal retina) were generally in the direction of the UH locus shifting to a shorter wavelength with greater eccentricity (Nerger et al., 1995; Volbrecht, et al., 2000). Effects of stimulus size on UH shifts were found (Nerger et al., 1995): the loci for UY remained invariant in both the fovea and the peripheral retina with test size, the foveal loci for UB increased with increasing stimulus size up to 1°, then remained invariant with increases in test size, while in the periphery the UB locus increased as test sizes increased up to 2° (or 4° for some observers), then remained invariant with larger test sizes, and the UG loci showed a similar pattern of increases with test size in the fovea up to 0.25° (or 0.5° for some observers), with no changes as larger test sizes were viewed, and in the periphery the UG loci increased with increasing test sizes up to a 2° stimulus size, and then remained invariant with larger stimulus presentations. We now know that many of the stimulus test sizes presented in the periphery were not sufficiently large to fill the perceptive fields of all four elemental hues, i.e., the stimuli may have been too small to completely fill this psychological correlate of the physiological receptive field. In addition, the pattern of results in these studies was not consistent across observers, e.g., the locus of UB in the periphery was longer for some observers and shorter for others when compared to their foveal UH loci. The peripheral locus of UG was shorter for all observers than the foveal locus, with the loci differing between 10-20 nm for different observers, depending on the stimulus size, and overall the UG loci varied greatly among observers (Nerger et al., 1995).

To test for the frequently reported rod enhancement of blue in peripheral color perception, Nerger et al. (2003) designed a hue scaling study to examine the time-course of rod effects on short- and middle-wavelength stimuli. After photobleaching, hue scaling responses were obtained at successive time-points across 30 minutes of dark adaptation, including the cone plateau, intermediate points of increasing rod sensitivity, and complete dark adaptation with maximal rod sensitivity. Stimuli were presented to both the nasal retina and fovea. Observers reported decreased saturation for all peripheral stimuli viewed under maximal rod input conditions after dark adaptation, in addition to hue changes. Interestingly, in the periphery the authors found no change in the percentage of blue detected in short-wavelength stimuli when rod input was maximized after dark adaptation, which contradicts results from earlier studies described above (e.g., Ambler & Proctor, 1976; Trezona, 1970). Observers in this study did report green and yellow hue changes across the course of dark adaptation. Only short- and middle-wavelength stimuli were presented, so no results concerning the perception of long-wavelength red were reported.

When hue scaling data from the fovea were compared to the peripheral data, observers actually reported a larger component of blue in the short wavelengths when they were viewed foveally, which is also inconsistent with results from earlier studies. The 25 td stimulus intensity used in the study should have been sufficiently dim to permit rod participation, but the stimulus size of 1.5º in the periphery was not large enough to fill all perceptive fields, and the authors suggested that a larger stimulus size might minimize differences between the foveal and peripheral hue scaling (Nerger et al., 2003). The hue scaling study reported in this dissertation used a larger, 2.55º

peripheral stimulus size, which completely filled the perceptive fields of all four hues under cone plateau and dark adaptation conditions (Troup, Pitts, Volbrecht & Nerger, 2005).

Thus, at the start of this century, understanding of the nature of rod contributions to color perception remained elusive. In a 2001 review of the literature on rod influences on hue and color pathways, Buck reported that "[t]here are many questions and issues left unanswered…" (Buck, 2001). Parry et al. summarized the literature a few years later, saying, "In general, rod influence appears to lead to a desaturation of colored stimuli as well as to bring about a complex range of changes in perceived hue… their effects appear to be dependent on a variety of stimulus parameters such as intensity and temporal presentation" (Parry, McKeefry & Murray, 2006).

Aims of the Present Studies

Hue Scaling Studies

The hue scaling studies reported here were designed and carried out in an attempt to quantitatively characterize the effects of rods on peripheral saturation and hue perception using a protocol in which rod contribution was isolated as a variable. Monocular stimulus presentation (with the other eye patched) removed any effects of hemispheric differences or communication. To minimize many of the concerns present in previous studies, the peripheral retinal region tested, stimulus wavelengths, intensity, size, and duration were all deliberately defined. In particular, the present studies were conducted to characterize the development of rod influences on perceived hue and saturation across time during the course of dark adaptation when perceptive fields are

filled for the four hue terms, to reveal how the relationship between achromatic and chromatic perception is altered over time.

By convention, and as a control, hue scaling responses for the same stimuli presented to the fovea were also collected, and compared to the descriptions collected from presentation to the peripheral retina under bleach conditions. The longstanding claims that rods contribute a blue component and/or lead to decreased saturation, which has often been described as contributing an achromatic component, were also evaluated.

Hue Loci Studies

The hue loci studies, which measured the loci for three hues, (UB, UG, UY) and also measured the loci for four binary hues (red/blue, blue/green, green/yellow, yellow/red), were carried out to test the predictions of rod influences derived from the hue scaling study results. In addition to the trends present in the hue scaling results, hue scaling functions of the hue percentages reported for the test stimuli at 4 min post-bleach and 28 min post-bleach were used to make predictions about the UH loci obtained by direct measure. The two adaptation conditions tested in the peripheral retina, a cone-only (bleach) condition, and a rod and cone mediated (no bleach) condition, corresponded to the 4 min and 28 min time-points of the hue scaling study. Additionally, for observers LB and VV, these color naming functions were used to make predictions for the binary hue loci perceived under bleach and no-bleach conditions. Again, following convention and as a control, these loci were also measured in the fovea, and the results were compared to the descriptions obtained when the stimuli were presented to the peripheral retina under bleach conditions.

CHAPTER 2: METHODS

Three types of psychophysical data were collected to compare foveal and peripheral color perception, and to investigate the contributions of rod photoreceptors to human peripheral color vision. The first is a data set of hue scaling responses describing monochromatic stimuli presented to the fovea and to the peripheral retina. The peripheral responses were obtained during dark adaptation, at four-minute intervals after observers adapted to a photobleaching stimulus. The second data set includes the wavelengths identified by each observer as the loci of unique blue (UB), unique green (UG), and unique yellow (UY). Unique hue (UH) loci were determined for two retinal locations, the fovea and 10° temporal peripheral retina. In the periphery, stimuli were presented under two adaptation conditions, one that maximizes rod contribution (no bleach) and one that minimizes the contribution of rods to color perception (bleach). The third data set are the wavelengths identified by each observer as the loci of balanced binary hues, wavelengths of light that are perceived as an equal mixture of two non-opponent hue categories, i.e., red/blue (purple), blue/green, green/yellow, and yellow/red (orange). Binary hue loci were also obtained in both the fovea and peripheral retina. As with the UH loci data, the stimuli presented to the peripheral retina were viewed under the bleach and no-bleach conditions. The apparatus used for all studies, and the specific details about observers, stimuli, and the experimental procedures, are described below.

Apparatus

A three-channel Maxwellian-view optical system, shown schematically in **Figure 2.1**, was used for these experiments. A 300 W (5500 K) xenon arc lamp (Oriel, Model 66065) regulated at 290 W by a dc power supply (Oriel, Model 68811) provided illumination for all three channels. Light leaving the two exit ports of the lamp housing passed first through infrared heat absorbing filters, then through collimating lenses. Pairs of lenses were positioned throughout all channels of the optical system to capture as much light as possible, and to provide both collimated beams and focal points needed for the placement of various optical components. All lenses were achromatic doublets and all mirrors were front surfaced.

Light leaving one of the exit ports formed Channel 1 and produced the test stimulus. A focusing lens directed the light onto the entrance slit of a grating monochromator (Instruments SA, Inc., Model H20; 4 nm half-amplitude bandpass). After exiting the monochromator, the light passed through a two log-unit neutral-density wedge (Ealing Electro-Optics), then through a collimating lens. A field stop placed in this collimated portion of Channel 1 defined the diameter of the circular test stimulus (2.55° or 1°). The light was then reflected 90° by a mirror, and passed through neutral density filters held in a filter box. The light was then focused and collimated by a pair of lenses. A shutter controlled by a driver system (Uniblitz, Model T132), placed at the focal point of the lens pair, controlled the exposure duration of the stimulus at 500 msec. The collimated light of Channel 1 was then combined with the light from Channels 2 and 3 via a beam splitter, and all of the light passed through the final lenses.

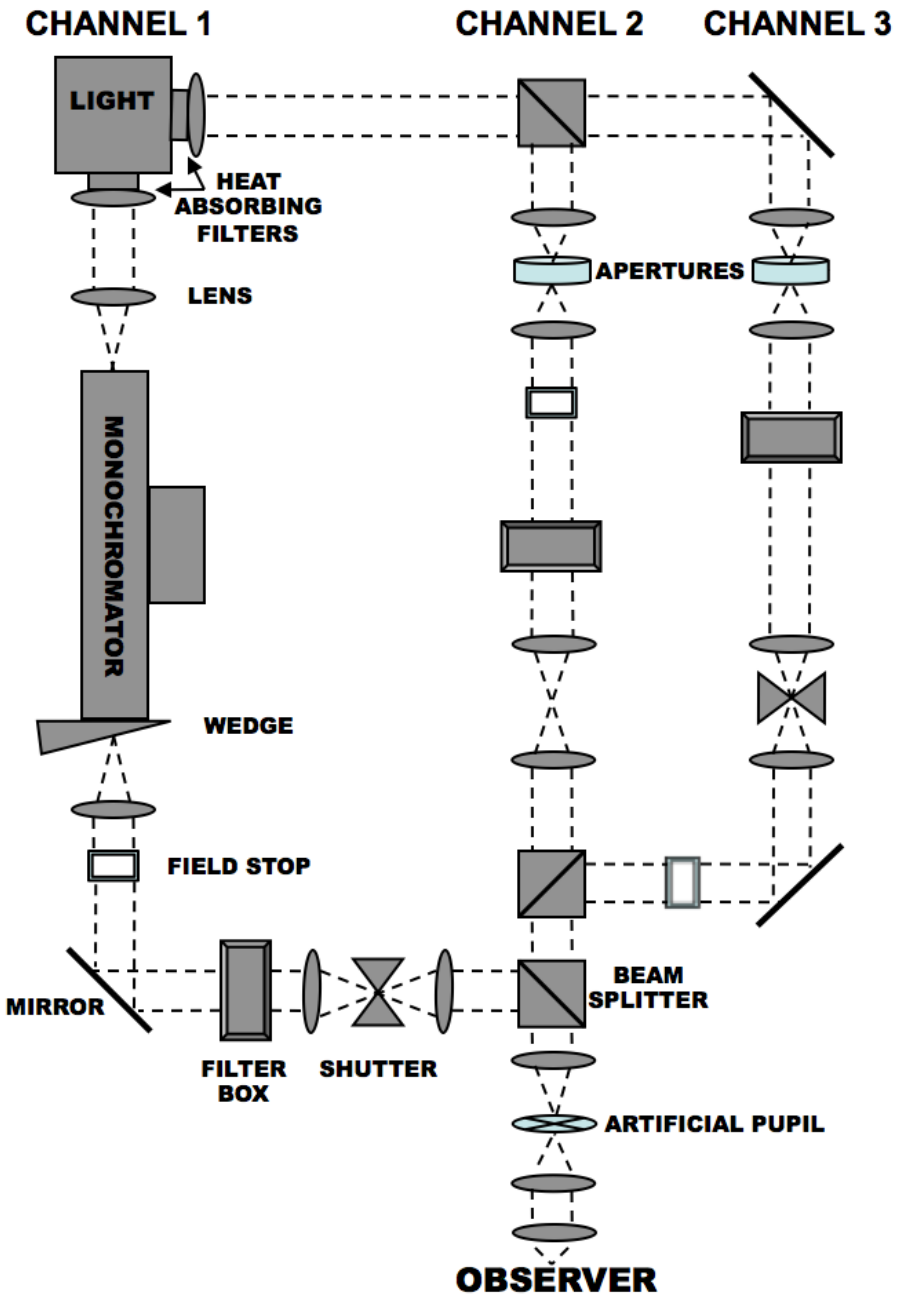

Figure 2.1: Schematic diagram of three-channel Maxwellian view optical system. Each type of component is labeled once. Observer's position is at the lower right, as indicated.

Light leaving the second exit port passed through a beam splitter to create Channels 2 and 3. In Channel 2 light passed through an aperture bracketed by a pair of

lenses, and then through a field stop which produced the fixation array. The light next passed through neutral density filters, held in a filter box, selected by each observer to dim the fixation array until it was just visible during stimulus presentation. The light passed through another pair of lenses, then through two beam splitters, first to recombine with the light from Channel 3, and second to combine the light from all three channels into the final pathway.

The light in Channel 3 was reflected 90° by a mirror and passed through an aperture bracketed by a lens pair, and then through a neutral density filter held in a filter box that determined the intensity of the bleaching stimulus. A second pair of lenses in Channel 3 bracketed a shutter at the focal point, which was controlled by a driver system (Uniblitz, Model T132) to maintain the 10 sec exposure duration of the bleaching stimulus. The collimated light was again reflected 90° by a mirror, then passed through a field stop which defined the 9.62° diameter of the broadband (5500 K) bleaching stimulus. Light then passed through the pair of beam splitters in Channel 2, described above, where light from Channels 2 and 3 was first recombined, and then light from all channels was combined into the final light pathway to the observer's eye. An artificial pupil, positioned at the focal point between the final pair of lenses, defined the 1.8 mm diameter of the Maxwellian image that entered the observer's eye through his or her own larger pupil, ensuring that all of the light from the optical system was indeed entering the observer's eye. A final lens in the light path focused the light from all channels onto the plane of the observer's right eye pupil. The observer was aligned with respect to the optical axis of the system via a dental-impression bite bar assembly that permitted adjustment for depth, height, and lateralization.

Calibrations

Neutral density filters and the neutral density wedge (Ealing Electro-Optics) in Channel 1 were calibrated by taking radiometric measurements (UDT Instruments, Model S370) from 400-700 nm in 10 nm steps. Filters used in Channel 3 for the bleaching (5500 K) stimulus were calibrated with a Minolta Chroma Meter (Model CS-100).

To calculate retinal illuminance for the test stimuli presented in Channel 1, photometric measurements were made at the reference wavelength of 550 nm and the photopic troland (phot td) value was calculated using Westheimer's (1966) method. Phot td values for the other wavelengths were determined with respect to the reference wavelength based on the Vos and Walraven (1971) photopic luminosity function, adjusting for log energy and photopic sensitivity differences.

A photometric measurement of the broadband (5500 K) light from Channel 3 was used to calculate the retinal illuminance of the bleaching field. The calibration of the monochromator was assessed at 632.8 nm with a helium-neon laser (Spectra Physics).

Observers

Two sets of observers participated in the experiments described in this dissertation (see **Table 2.1**). Three females (KY, 21 years; VV, 49 years; LB, 50 years) and one male (AK, 22 years) comprised the first set of observers, who participated in the hue scaling studies and the determinations of unique blue, unique green, and unique yellow loci. Observers KY, AK, and LB had no previous experience with the

psychophysical procedures used in these studies, while observer VV had previous experience with the procedures. All observers also served as experimenters.

Table 2.1: Summary of data sets for each observer. **Periphery** refers to 10° temporal retinal eccentricity, **B** indicates bleach condition, **NB** indicates no-bleach condition, **2.55°** and **1°** refer to the diameter of the stimulus presented to collect a data set.

	Hue Scaling			**Unique Hues**				**2nd Unique Blue**			**Binary Hues**		
Observer	Periphery		Fovea	Periphery		Fovea		Periphery		Fovea	Periphery		Fovea
	B	NB	(2.55°)	B	NB	(2.55°)	(1°)	B	NB	(1°)	B	NB	(1°)
AK	x	x	x	x	x	x	x						
KY	x	x	x	x	x	x	x						
LB	x	x	x	x	x	x	x	x	x	x	x	x	x
VV	x	x	x	x	x	x	x	x	x	x	x	x	x
JN								x	x	x	x	x	x

Three females (JN, 48 years; VV, 51 years; LB, 52 years) comprised the second set of observers, who participated in the determinations of the binary hue loci and the second set of unique blue loci measurements. These three observers had previous experience with the procedures used in these studies.

All observers were assessed for normal trichromatic color vision using anomaloscopic matches (Neitz OT-II Anomaloscope) and three color panel tests (Farnsworth D-15, Farnsworth-Munsell 100 Hue, Lanthony's desaturated 15 Hue). All observers were naïve with respect to their data during these studies. Observer LB had bilateral, colorless acrylic intraocular replacement lenses post-cataract surgery, which had been in place for more than two years at the beginning of data collection.

Stimuli

Test stimuli in all studies were circular, monochromatic spectral lights presented on a dark background with a 500 msec stimulus duration, consistent with previous studies conducted in this and other laboratories (Troup et al., 2005; Abramov et al., 1991). Stimuli presented to the peripheral retina in all studies were 2.55° in diameter, a size known to completely fill the perceptive fields of all four elemental hue mechanisms, i.e., blue, green, yellow, and red, under both bleach and no-bleach conditions (Troup et al., 2005). Stimuli presented to the fovea were of two different diameters, 2.55° and 1°.

Bleaching Stimulus

A circular broadband (5500 K) stimulus, 9.62° in diameter, was viewed in the peripheral hue scaling study, and in the "bleach" trials of the unique hue and binary hue studies. The retinal illuminance of this stimulus was 6.23 log scotopic (scot) tds and the stimulus duration was 10 sec. The bleaching stimulus isomerized approximately 86% of the rhodopsin within the exposed area of the retina, as calculated using the methods of Alpern (1971) and Rushton and Powell (1972). Previous studies conducted in this laboratory have demonstrated that the broadband bleaching field does not differentially adapt any of the cone mechanisms nor alter hue perception (Nerger et al., 1995; Troup et al., 2005).

Hue Scaling Stimuli

Eight stimulus wavelengths ranged from 480 to 620 nm in 20 nm steps, and were equated to 20 phot td, so that all wavelengths equally stimulated the combined M- and L-cones. The S-cones and rods received different levels of stimulation at each stimulus wavelength. A second set of four stimulus wavelengths, ranging from 480 to 540 nm in

20 nm steps, was also presented to two observers in a second set of experimental sessions. The retinal illuminance of the second stimulus set was 100 scot td, such that the rod photoreceptors were stimulated at a constant level by each of these wavelengths, while the three classes of cones received different levels of stimulation.

Unique Hue Stimuli

The range of stimulus wavelengths for each of the UH determinations was as follows: for UB, wavelengths ranged from 430-480 nm in 2 nm steps; for UG, wavelengths ranged from 480-540 nm in 2 nm steps; and for UY, wavelengths ranged from 540-600 nm in 2 nm steps. The stimuli presented to the peripheral retina were 2.55° in diameter. Two sets of UH measurements were obtained in the fovea, one set with a 2.55° stimulus, and another set with a 1° stimulus. All stimuli were equated to 20 phot td.

Binary Hue Stimuli

The range of stimulus wavelengths for each of the binary hue determinations was as follows: for binary red/blue (R/B), wavelengths ranged from 400 to 450 nm in 2 nm steps; for binary blue/green (B/G), wavelengths ranged from 460-520 nm in 2 nm steps; for binary green/yellow (G/Y), wavelengths ranged from 510-570 nm in 2 nm steps; and for binary yellow/red (Y/R), wavelengths ranged from 570 to 620 nm in 2 nm steps. The stimuli presented to the peripheral retina were 2.55° in diameter, and those viewed foveally were 1°. All stimuli were equated to 20 phot td.

Fixation Array

Stimulus position on the retina, for the bleaching stimulus and for all test stimuli, was controlled through the use of a fixation array located in Channel 2. As illustrated in

Figure 2.2, the array consisted of three pinhole-sized points. Bleaching and test stimuli were centered between two vertically displaced pinhole fixation points, while observers fixated on a third fixation point centered and positioned 10° horizontally from the vertically displaced points. The intensity of the fixation points was adjusted to be just visible to the observer in order to minimize any adaptation effects (Jameson & Hurvich, 1967). Stimulus positioning on the retina for foveal viewing was also controlled through the use of a fixation array generated in Channel 2, so that only the two vertically-displaced pinholes of light were visible. These pinholes were aligned to the central axis of the optical system, and the observer fixated at the location midway between the two points, where the test stimuli would appear during stimulus presentation.

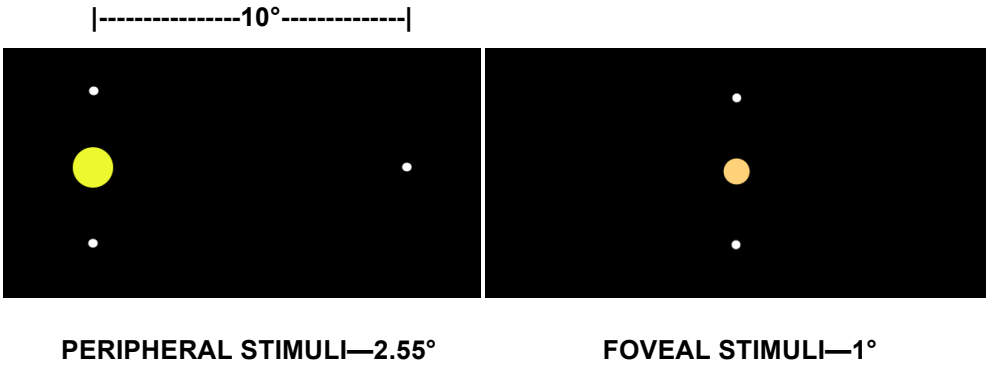

Figure 2.2: Fixation arrays and test stimuli as seen in the Maxwellian-view optical system. Left: with the right eye, observers fixated on the fixaton point at the far right, and the test stimuli appeared between the two vertically displaced pinholes, ensuring that these stimuli were imaged at 10° temporal retinal eccentricity. The bleaching stimulus was centered and superimposed over the two vertically displaced pinholes. Right: For foveal stimulus presentations, observers fixated between two vertically displaced pinholes, and stimuli were centered with respect to the two fixation points.

All procedures adhered to federal regulations and were approved by the Colorado State University Institutional Review Board.

Hue Scaling Procedures

Fovea

Observers aligned to the optical system and then adapted to the dark for 10 min, after which the wavelengths of the 2.55° stimuli were presented in pseudo-random order. Hue scaling responses for each stimulus were recorded using the "4 + 1" technique described by Gordon and Abramov (1988). First observers assigned percentages to one or two of the four elemental hues (blue, green, yellow, red) to describe their total hue experience, which was required to sum to 100%. Then observers assigned a percentage to describe the degree of saturation of the stimulus, ranging from 0% (completely achromatic) to 100% (completely chromatic). On fewer than ten occasions during all data collection sessions, when an observer was unable to make hue and saturation judgments following one presentation of the stimulus, a second presentation of the test stimulus was made within 15 sec.

Test sessions lasted approximately one hr, with observers providing hue scaling responses for four pseudo-randomly ordered sets of the eight test stimuli. In order to avoid fatigue, observers participated in no more than two test sessions in one day. Each observer provided a total of four hue scaling responses for each of the eight test wavelengths presented to the fovea.

Peripheral Retina

Observers aligned to the optical system and then adapted to the dark for 10 min. Next they fixated on the rightmost fixation point in the optical system (see **Figure 2.2**), and the broadband (5500 K) bleaching stimulus was presented for 10 sec between the two vertical fixation points.

When the bleaching light was extinguished, a timer started, and one pseudo-randomly selected stimulus wavelength was presented every four minutes until 28 minutes had elapsed. Hue scaling responses were recorded after the presentation of each stimulus, using the "4 + 1" method. Because of the importance of timing in this portion of the study, if an observer was unable to make hue and saturation judgments following one presentation of the stimulus, he or she could only view the stimulus one more time at that time interval.

Test sessions lasted approximately 1.25 hr with observers adapting to the bleaching stimulus twice and providing hue scaling responses for two pseudo-randomly ordered sets of the test stimuli. In order to avoid fatigue, observers reported on four sets of stimuli at most in one day. Observers provided hue scaling responses for each of the eight test wavelengths a total of three times at each of the seven time increments.

The same procedure was followed for the peripheral presentation of a subset of stimuli (480-540 nm in 20 nm steps) equated to 100 scot td. Observers VV and LB participated in this experiment. Once again a total of three responses were obtained for each wavelength at each time increment from each observer.

Unique Hue Procedures

The three spectral UHs, UB, UG, and UY were measured in the peripheral retina for each observer under the bleach condition and the no-bleach condition. In the fovea, stimuli were presented only under the no-bleach condition.

Each UH locus was obtained using two interleaved staircases of the appropriate wavelengths (see above). Initially, the experimenter presented an anchoring stimulus

from one of the ends of the wavelength range, and the observer's task was to respond with one of two hue terms. For UB and UY determinations, the observer's task was to respond either "red" or "green" to indicate if the stimulus was perceived as reddish-blue or greenish-blue (or reddish- or greenish-yellow). Similarly, for UG determinations, the observer's task was to respond either "blue" or "yellow." The experimenter selected the subsequent anchoring stimulus wavelength from the opposite end of the wavelength range. The first anchor from one of the staircases was a shorter wavelength, while the initial anchor for the second staircase was a longer wavelength. These anchors were chosen so that the observer could easily see the hue component in their judgment (e.g., there was a obvious reddish-blue and an obvious greenish-blue for UB judgments). Once there was a reversal in a hue response (e.g., change from "red" to "green," or "green" to "red"), a new wavelength was selected from the range of possible wavelengths. For example, if 430 nm had been selected as the first wavelength in one of the two staircases, followed by 478 nm, and the observer responded "red" for the 430 nm stimulus and "green" for the 478 nm stimulus, the next wavelength presented would be from the shorter end of the wavelength range, but not as short as the initial anchor wavelength. The experimenter would continue to present longer wavelengths until the observer changed his/her response from "red" to "green." Then, a new wavelength longer than the preceding would start the process all over until a narrow range of wavelengths were identified that zeroed in on the locus of the UH. After each response reversal, the step size between the wavelengths for each stimulus presentation decreased until the smallest step size of 2 nm was reached. As noted above, two staircases were run simultaneously, with the constraint that no more than four

consecutive responses were recorded on a single staircase before the experimenter switched to the other staircase. This constraint reduced the predictability of the stimulus presentation for the observer. A staircase was terminated when there were four response reversals at the smallest step size (2 nm). A mean wavelength was calculated from these four responses, and defined the locus for that UH from that staircase. Overall mean hue loci were calculated from the means from four pairs of staircases for each UH.

Fovea

Observers aligned to the optical system and adapted to the dark for 10 min. Stimuli from the two interleaved staircases were then presented, and responses recorded, until one pair of staircases was completed, after which the observer adapted to the dark for an additional 10 min before completing a second pair of interleaved staircases. Only a no-bleach procedure was conducted for the foveal presentations. Each test session lasted approximately 45 min. A total of four pairs of staircases were completed for each UH with a stimulus size of 2.55°, and four additional pairs of staircases were completed for each UH with a stimulus size of 1°.

For the second set of observers' UB measurements, one UB locus was measured in the fovea under no-bleach conditions, using a 1° stimulus. A total of three pairs of staircases were completed by each of the three observers in this second set of UB measurements.

Peripheral Retina

As in the hue scaling procedure described above, stimuli were presented to the peripheral retina, centered at 10° temporal retinal eccentricity, as determined by the use

of the fixation array. One set of UH loci were determined under bleach conditions, and a second set were determined under no-bleach conditions.

Bleach Condition

Observers aligned to the optical system, then adapted to the dark for 10 min, after which the peripheral retina was adapted to the bleaching stimulus for 10 sec. A timer was started when the bleaching light extinguished, to ensure that stimulus presentations occurred between 4-9 min post-bleach. If the observer had not achieved four response reversals at the smallest step size for each staircase by 9 min post-bleach, then he or she again adapted to the bleaching stimulus, dark adapted for another four min, and then continued to view and respond to the stimuli during the second 4-9 min post-bleach time window until four response reversals for each of the two interleaved staircases were obtained.

Test sessions lasted approximately an hour, with the observer viewing the bleaching stimulus no more than three times per session. Two pairs of staircases, for two different UHs, pseudo-randomly chosen, were presented in a session. A total of four pairs of staircases were completed for each UH under the bleach condition. To avoid fatigue, only one session with the bleaching field was conducted on a given day,

For the second set of observers' UB measurements under the bleach condition, a total of three pairs of staircases were completed by each observer, following the procedure described above.

No-bleach Condition

After aligning to the optical system, the observer dark adapted for 30 min, after which stimuli from two interleaved staircases were presented. Test sessions continued

until two pairs of staircases for two different, pseudo-randomly chosen UHs were completed, with the observer spending an additional 10 min dark adapting after completing the first pair of staircases and before commencing on the second pair. These sessions generally lasted about an hour. A total of four pairs of staircases were completed for each of the UHs under this condition.

For the second set of observers' UB measurements under the no-bleach condition, a total of three pairs of staircases were completed by each observer, following the procedure described above.

Binary Hue Procedures

The procedures followed to obtain binary hue loci were essentially the same as the procedures for UH determinations. The differences in procedure had to do with the fact that observers were identifying the wavelength that they perceived to be composed of equal portions of two primary hues. In the UH determinations, the process led to the identification of a wavelength that was perceived as containing a single hue, while in the binary hue determinations, the goal was to identify a balanced hue containing two hue components, each equally represented in the perception. For example, for the binary Y/R determination, the staircase was used to find the wavelength that appeared equally yellow and red. In a binary hue determination, the observer's task was to report which of the two binary hue components was predominant, e.g., for a B/G determination, did the stimulus appear to contain more blue or more green? For each binary hue determination (Y/R, G/Y, B/G, and R/B) the observer's task after stimulus presentation was to respond with one of the hue terms, for example "yellow" or "red" (for a binary Y/R

determination), to indicate which hue was perceived as contributing a larger percentage of the chromatic content of the stimulus. Initially the experimenter presented an anchoring stimulus from one of the ends of the wavelength range, that was predominantly perceived as (and described by) one of the hue terms of the binary pair (e.g., red for a Y/R determination), followed by a subsequent anchor wavelength which was predominantly perceived as the other hue (e.g., yellow), followed by a wavelength perceived as primarily composed of the other hue (e.g., red), so that the first few determinations on each staircase were easy to make. The step size (in nm) between subsequent wavelengths decreased with each response reversal until reaching the smallest step size of 2 nm. Mean binary hue loci were computed from the means of the last four reversals of each staircase across three experimental sessions.

Fovea

Observers were aligned to the optical system and adapted to the dark for 10 min. Stimuli from the two interleaved staircases were presented, and responses were recorded, until one pair of staircases was completed, after which the observer adapted to the dark for an additional 10 min before completing a second set of interleaved staircases. Only a no-bleach procedure was performed for the foveal condition. Each test session lasted approximately 45 minutes. A total of three pairs of staircases were completed for each binary hue with a stimulus size of 1°.

Peripheral Retina

As in the UH procedure described above, stimuli were presented to the peripheral retina, centered at 10° temporal eccentricity, as determined by the use of the

fixation array. One set of the four binary hue loci was determined under bleach conditions, and a second set was determined under no-bleach adaptation conditions.

Bleach Condition

Observers aligned to the optical system, then adapted to the dark for 10 min, after which the peripheral retina was adapted to the bleaching stimulus for 10 sec. Stimuli were presented between 4-9 min post-bleach. If the observer had not achieved 4 response reversals at the smallest step size for each staircase by 9 min post-bleach, then she again adapted to the bleaching stimulus, dark adapted for another four min, and then continued to view and respond to the staircase stimuli during the second 4-9 min post-bleach time window until the two interleaved staircases were completed. Bleach condition sessions usually alternated with those completed under the no-bleach condition, so that the observer never adapted to the bleaching stimulus more than three times in an experimental session. A total of three pairs of staircases were completed for each of the binary hues under the bleach condition.

No-bleach Condition

After aligning to the optical system, the observer adapted to the dark for 30 min, after which stimuli from two interleaved staircases were presented. Test sessions continued until two pairs of staircases for two different, pseudo-randomly chosen, binary hues were completed, with the observer spending an additional 10 min adapting to the dark between completion of the first pair of staircases and commencing on the second pair. These sessions generally lasted about an hour. A total of three pairs of staircases were completed for each of the binary hues under the no-bleach condition.

CHAPTER 3: HUE SCALING RESULTS

Percentage data, such as the hue and saturation values reported by observers during the hue scaling sessions, tend to become compressed at the ends of the scale, and variances may thus be artificially reduced near the extremes of 0% and 100%. Applying an arcsine transformation to percentage data reduces the effects of unequal variance (Abramov et al., 1991). All percentage values reported in this chapter were transformed using the following equation:

$$\text{transformed \%} = 100 \times \frac{2 \times \arcsin(\sqrt{\%\ \text{hue}/100})}{\pi}$$

The effect of this transformation is illustrated in **Figure 3.1**. Observer VV's hue and saturation percentages for the 580 nm stimulus are plotted in panels a (before the arcsine transformation) and b (after the arcsine transformation). While the percentage values change after the transformation is applied, the basic data trends are maintained. In panel b the difference in the variance among data points has been reduced when compared to the variance shown in panel a.

All of the hue scaling data presented in this chapter represent the arcsine transformed mean percent values of the responses each individual observer provided for each stimulus. Observers viewed each wavelength four times in the foveal condition. In the peripheral retina each wavelength was viewed three times at each of the post-bleach times. The transformed mean percent values for hue and saturation, and the standard deviations, are reported in Appendix A.

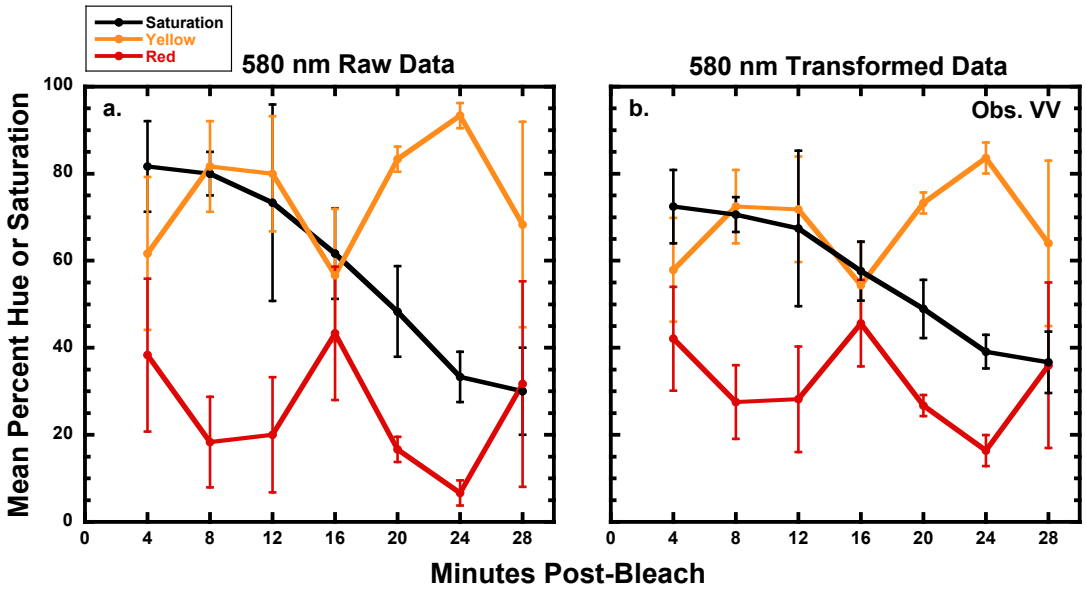

Figure 3.1: Observer VV's mean saturation and hue percentages for the 580 nm stimulus are plotted as a function of minutes post-bleach. **a.** Mean hue and saturation percentages before the arcsine transformation, **b.** Mean hue and saturation percentages after the arcsine transformation. Error bars represent ±1 standard deviation (SD).

Saturation Results

Fovea

Mean saturation percentages obtained from the foveal condition are shown in **Figure 3.2**, as a function of wavelength. Data from each of the four observers is presented in a separate panel. Error bars denote ±1 standard deviation (SD). Because a previous study conducted in this laboratory (Nerger et al., 2003) showed that hue and saturation perceptions do not change with increasing time in the dark for stimuli presented to the fovea, the foveal data reported here were collected at only one time point, i.e., after 10 min of dark adaptation.

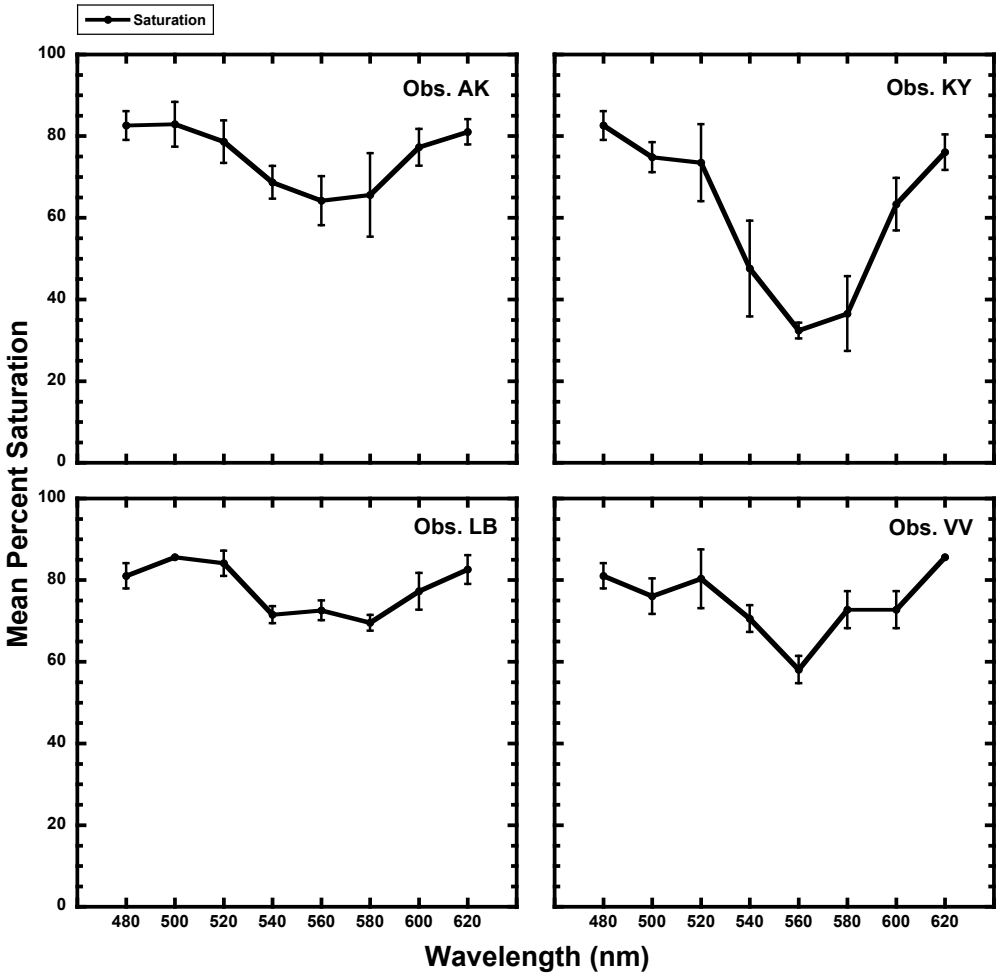

Figure 3.2: Mean saturation percentages (±1 SD) for eight wavelengths presented to the fovea are plotted for each observer in a separate panel.

As shown in **Figure 3.2**, all observers perceived the middle-wavelength stimuli (540, 560, 580 nm) as less saturated than the short- or long-wavelength stimuli. Observer KY reported the greatest decrease in perceived saturation for the middle wavelengths. This pattern is consistent with the literature (e.g., Gordon et al., 1994).

Peripheral Retina

Saturation results obtained across the dark adaptation time in the peripheral retina for each stimulus wavelength are shown in **Figures 3.3-3.10**. Each figure presents data for a different wavelength. Means and SDs from the three responses given for each stimulus at each post-bleach time are presented in a separate panel for each observer.

Figure 3.3 illustrates observers' reported saturation percentages for the 480 nm stimulus at the seven post-bleach times. All observers perceived this stimulus as relatively saturated, with a mean transformed saturation at all time-points of at least 70%. Increasing time in the dark was not associated with a change in saturation for any of the observers.

For each wavelength, each observer's mean saturation values from the 4 min post-bleach and 28 min post-bleach time-points can be compared as an indication of increasing contribution of rods to peripheral color perception. At the 4 min post-bleach time-point, many cone photoreceptors have recovered and are functioning normally, but rod photoreceptors are relatively inactive, or active above cone threshold, as a result of the photobleaching stimulus. The 4 min time-point thus represents cone-dominant peripheral color perception. It might be argued that cone function would be more stable at 8 min post-bleach, and that this time-point might be a good choice to represent cone-dominant peripheral color perception. However, because the photobleaching stimulus used in these experiments isomerized only 86% of the rhodopsin molecules, at 8 min post-bleach there could be enough regenerated rhodopsin photopigment, above and beyond the 14% of photoreceptors expected to be still active after the bleaching

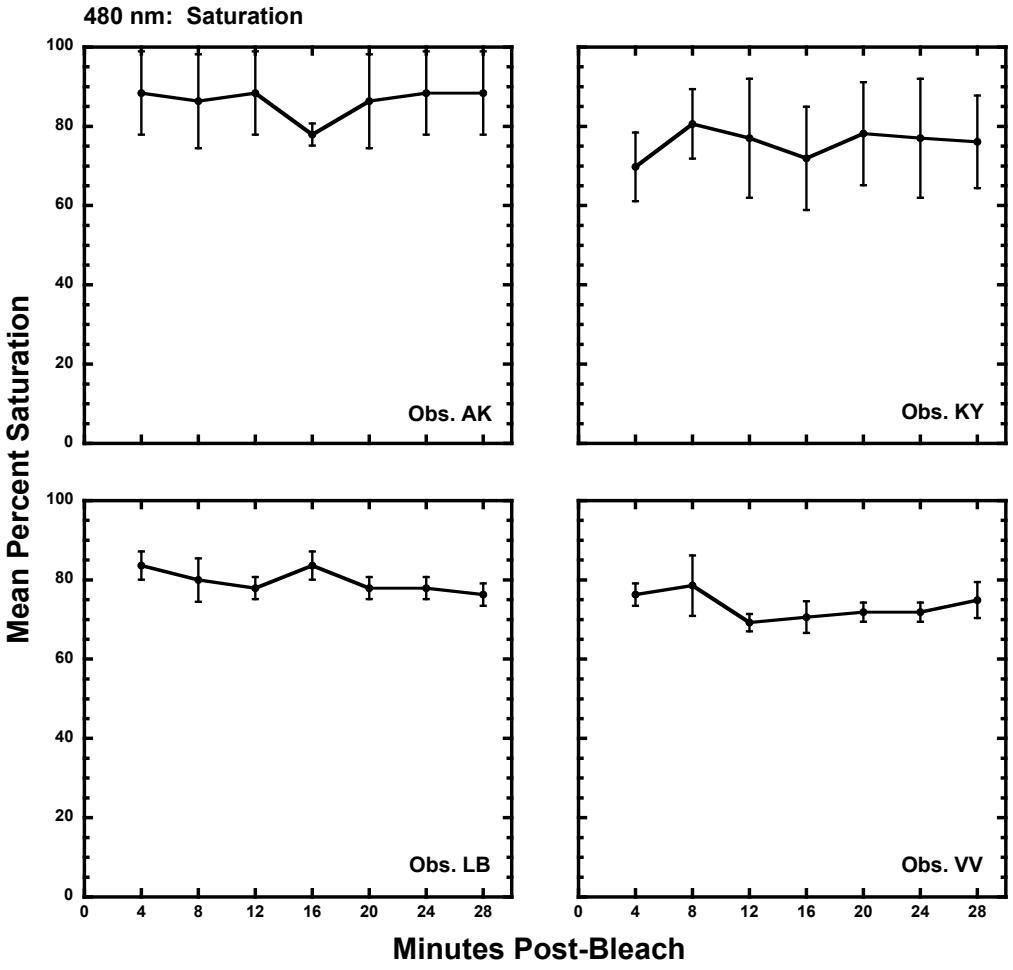

Figure 3.3: Mean saturation percentages (±1 SD) reported by four observers for the 480 nm stimulus presented to the peripheral retina at seven post-bleach times.

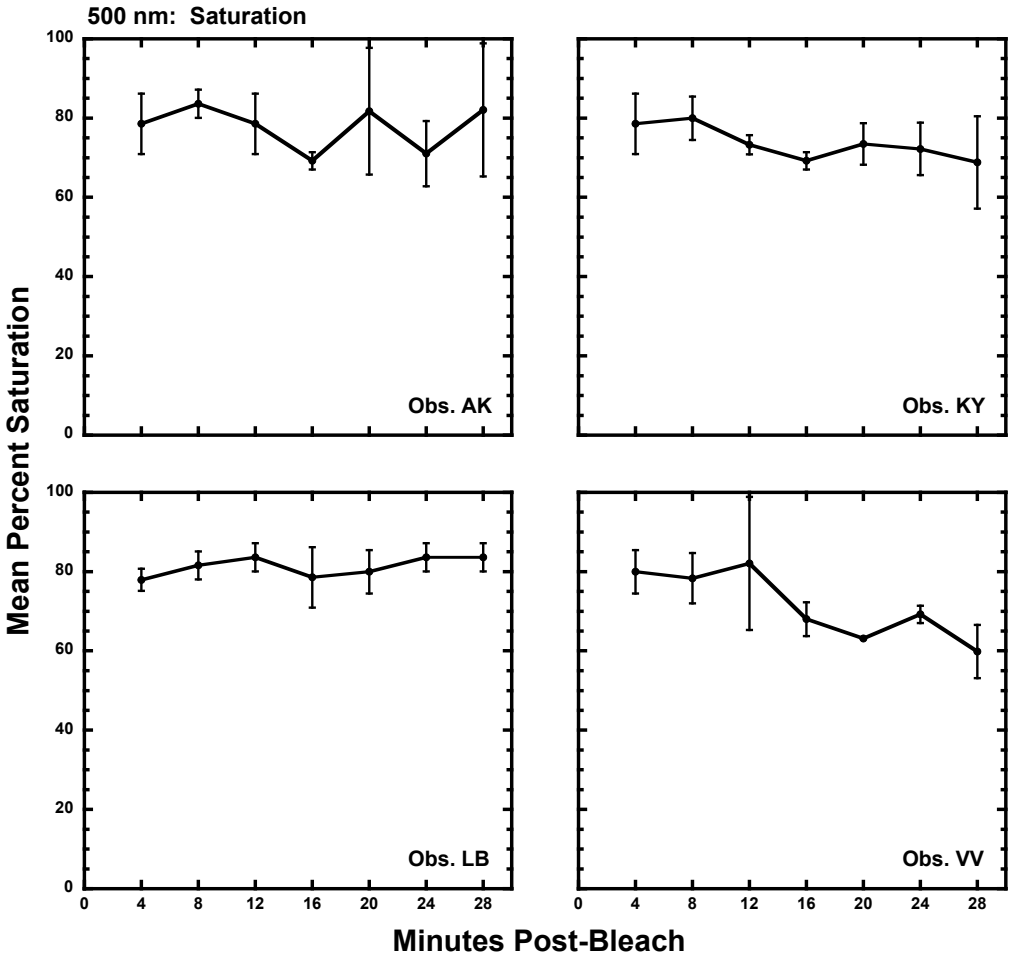

Figure 3.4: Same as **Figure 3.3** except for the 500 nm stimulus.

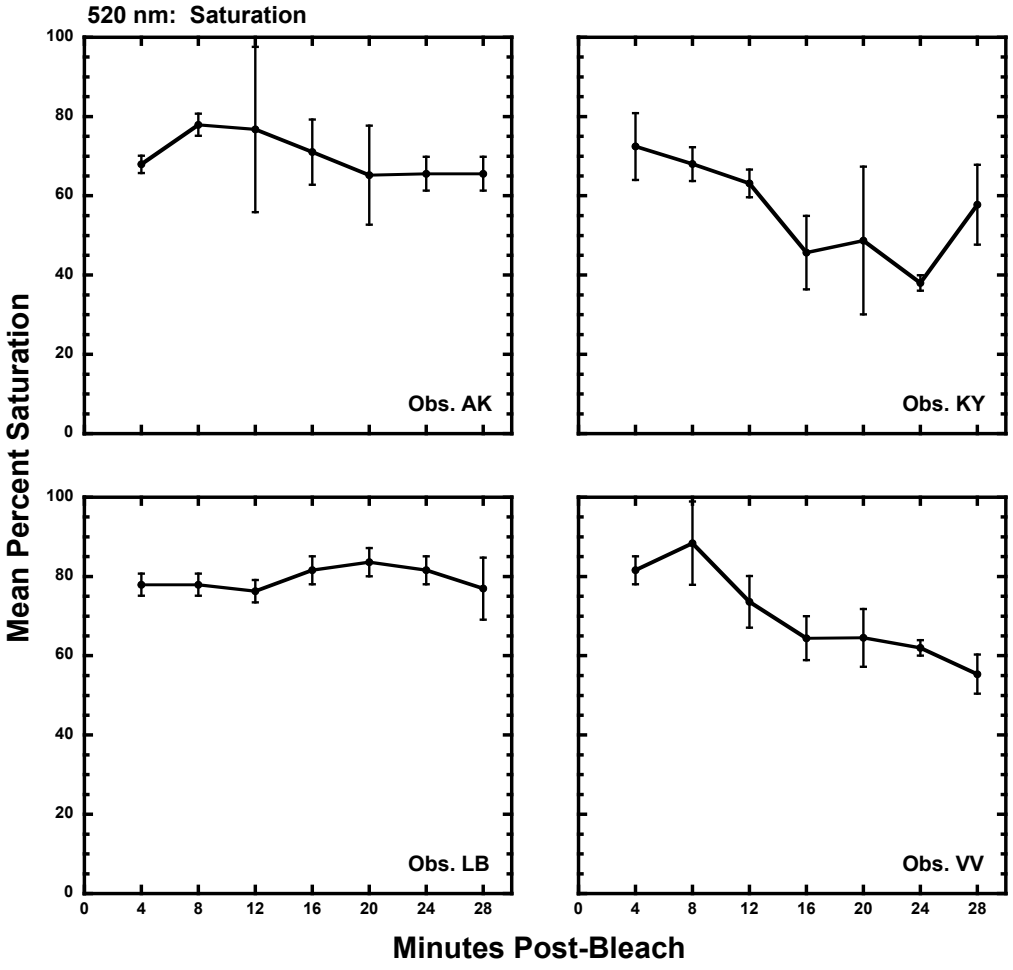

Figure 3.5: Same as **Figure 3.3** except for the 520 nm stimulus.

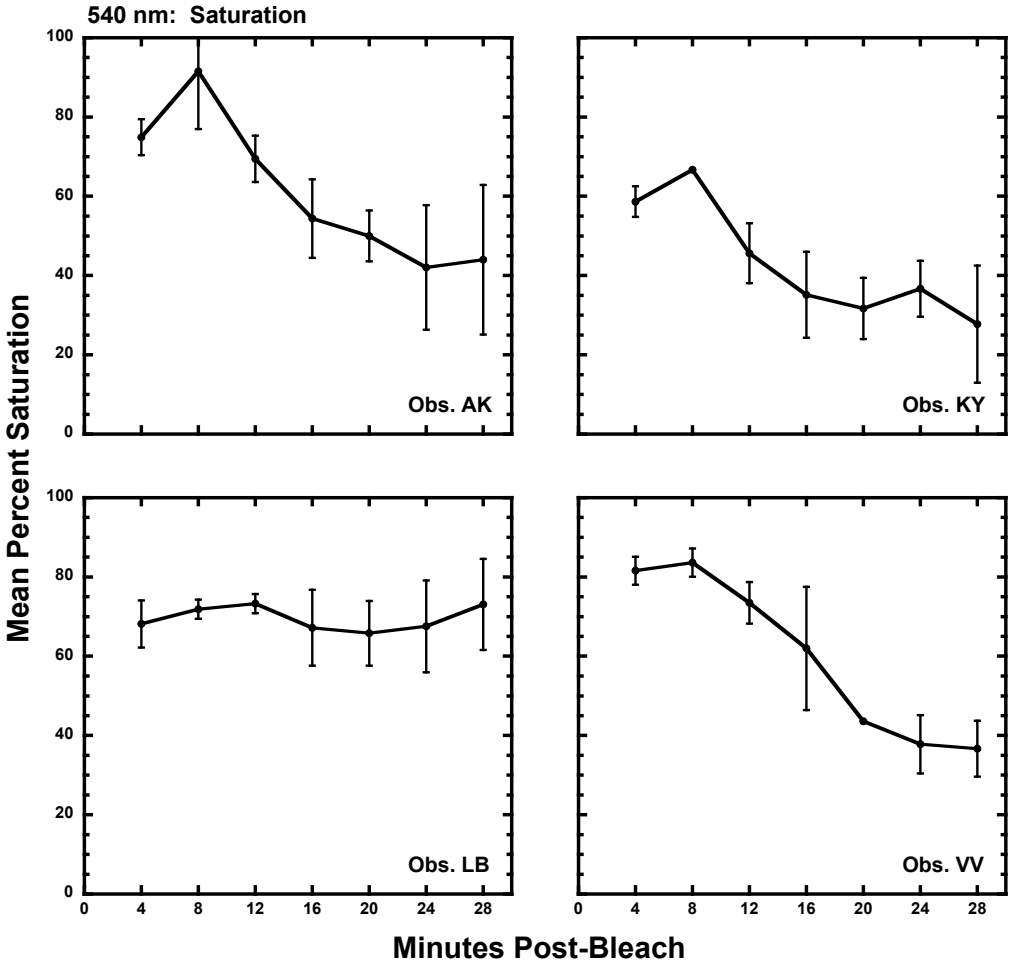

Figure 3.6: Same as **Figure 3.3** except for the 540 nm stimulus.

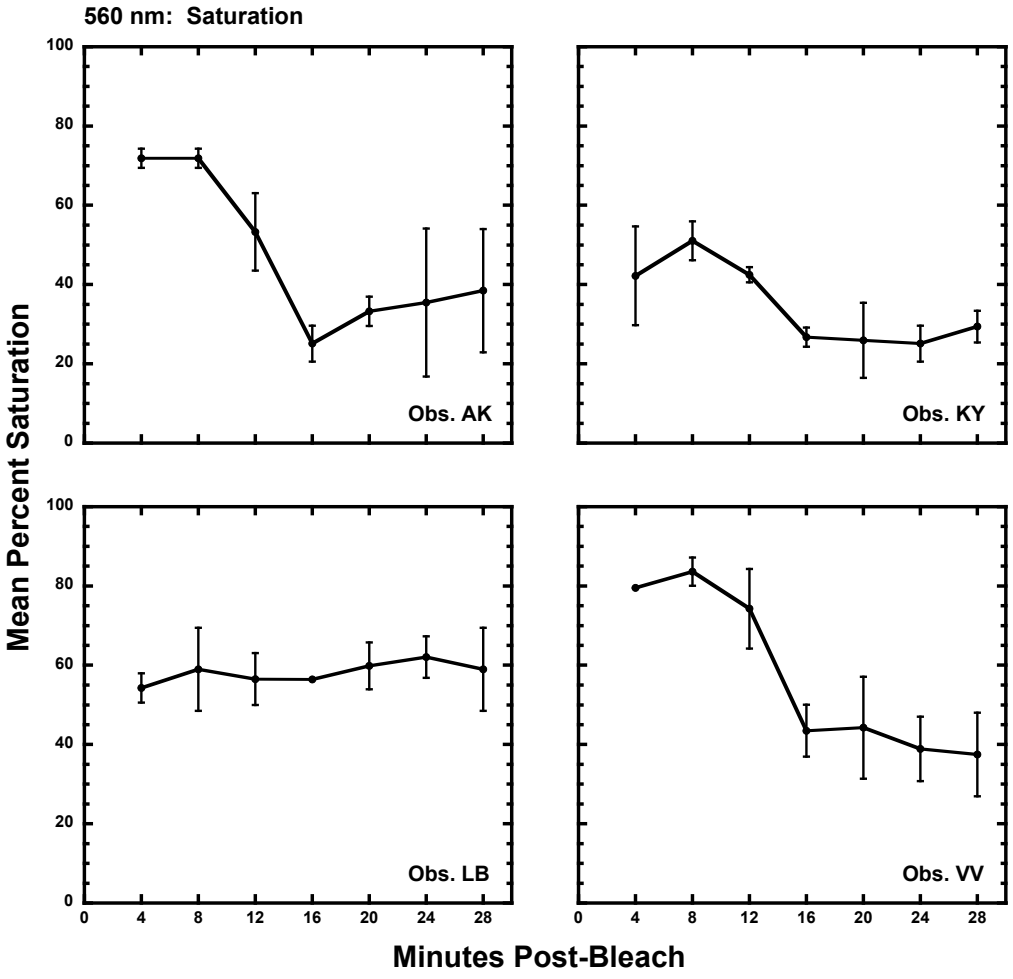

Figure 3.7: Same as **Figure 3.3** except for the 560 nm stimulus.

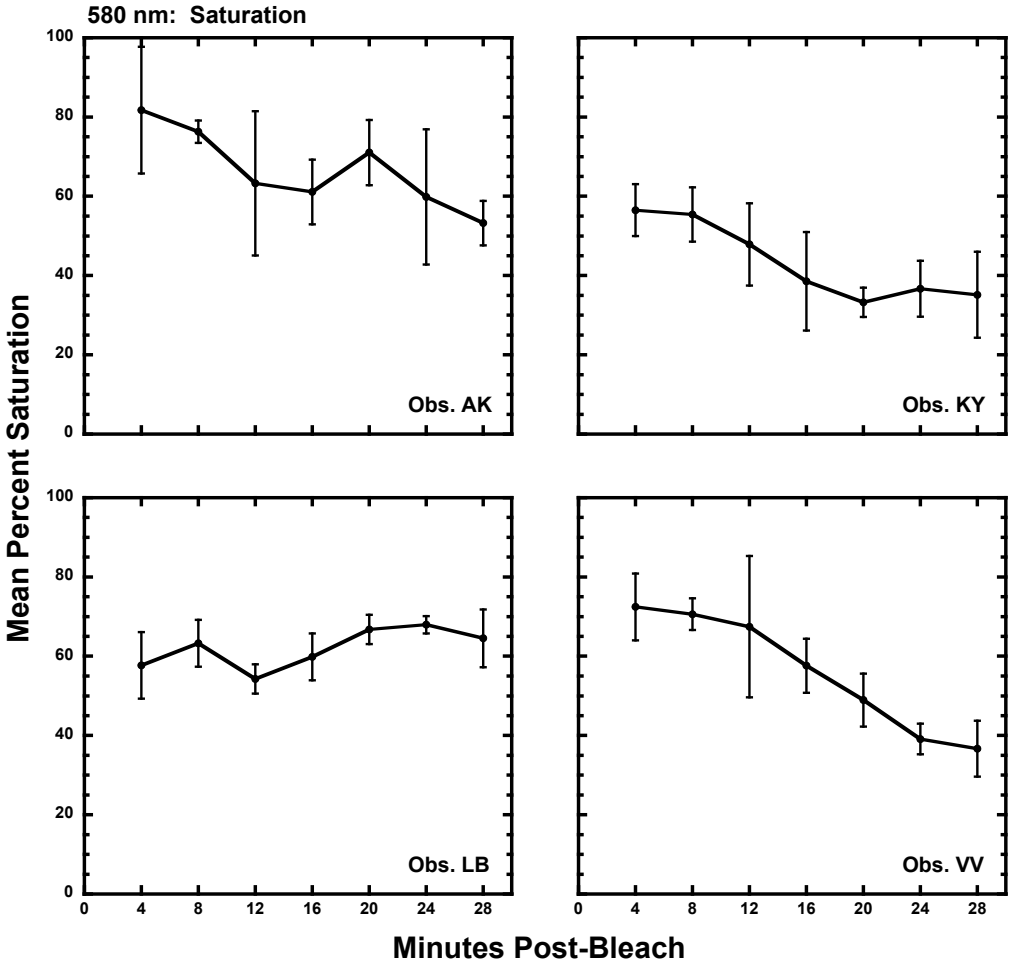

Figure 3.8: Same as **Figure 3.3** except for the 580 nm stimulus.

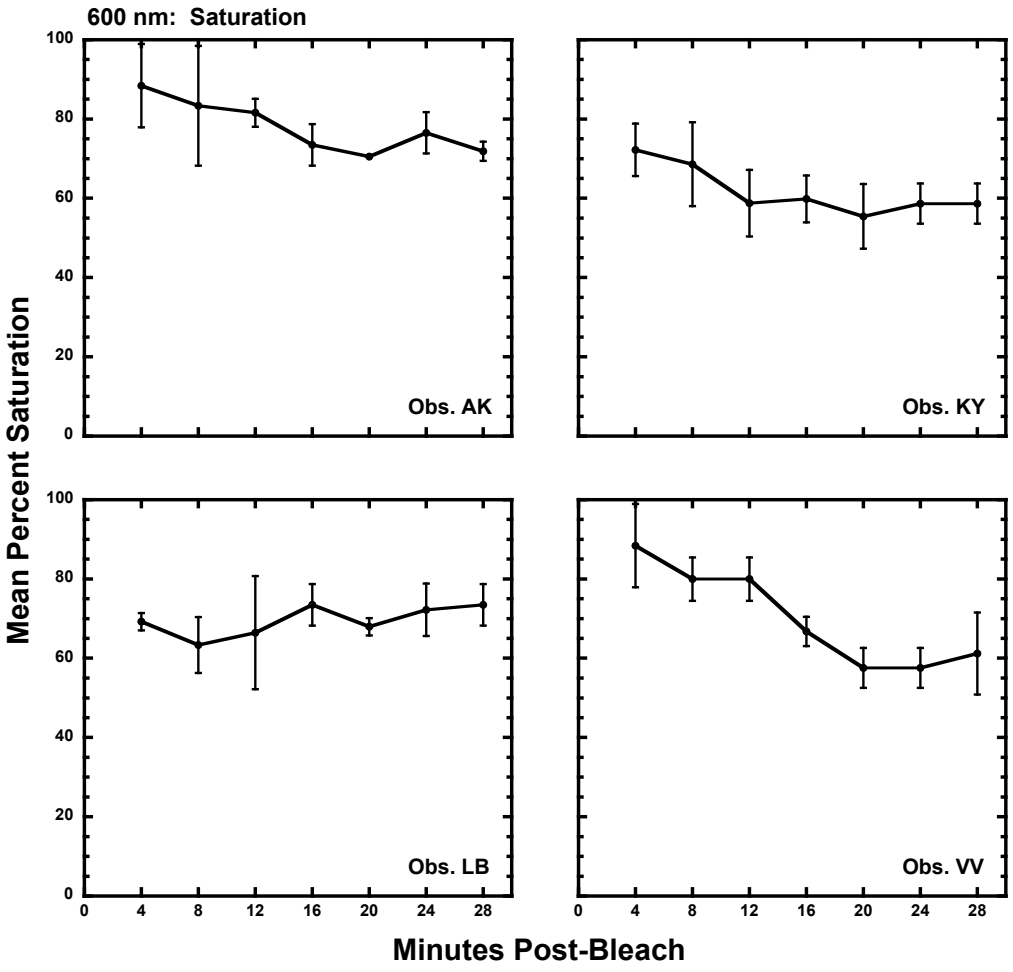

Figure 3.9: Same as **Figure 3.3** except for the 600 nm stimulus.

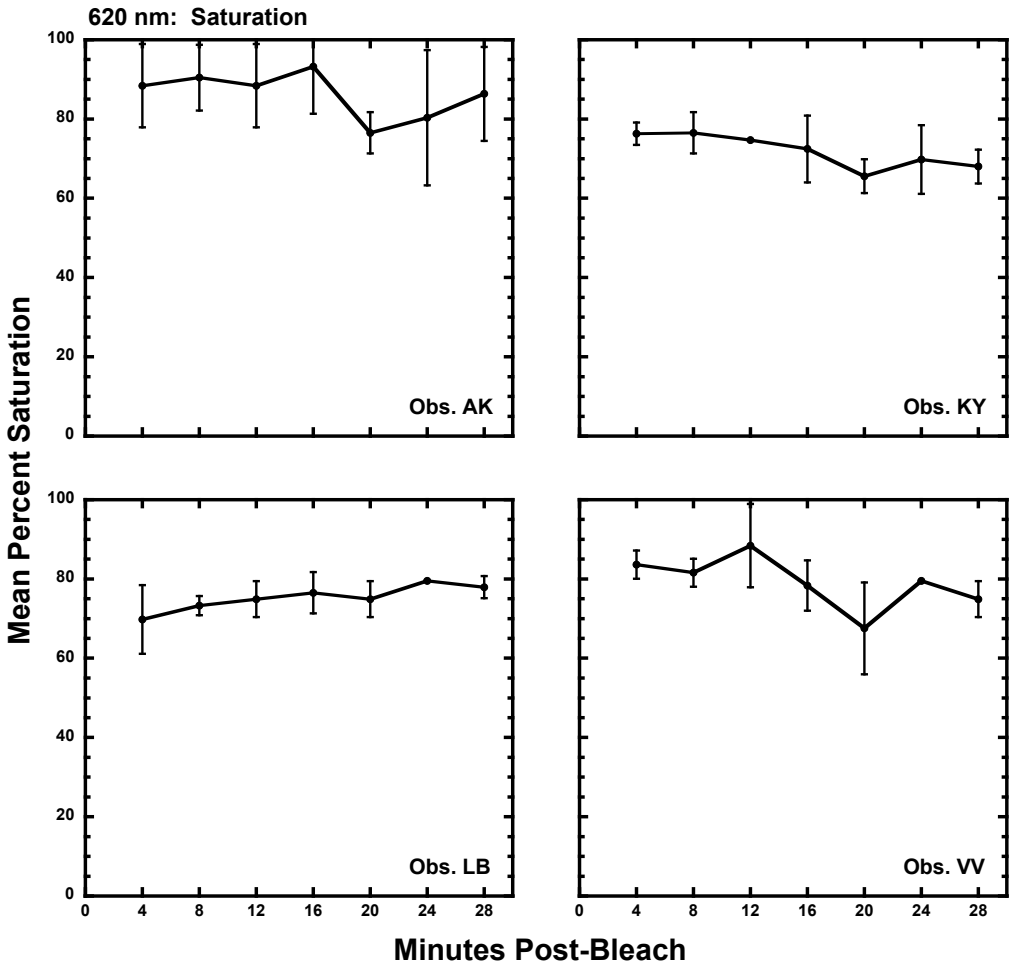

Figure 3.10: Same as **Figure 3.3** except for the 620 nm stimulus.

stimulus exposure, to influence observers' perceptions (Lamb & Pugh, 2006). Thus, data reported at the 4 min time-point were compared to those reported at 28 min post-bleach, when both cones and rods were actively functioning, the time-point that best represents rod-influenced peripheral color perception. If rods contribute a desaturating effect, one might expect to see a reduction in saturation with increasing time in the dark.

For the 480 nm stimulus, there was no difference in saturation reported under the cone-dominant condition (4 min post-bleach) and the rod- and cone-mediated condition (28 min post-bleach).

Figure 3.4 illustrates observers' saturation percentages of the 500 nm stimulus at the seven post-bleach times. All observers perceived this stimulus as relatively saturated (60% and above) at all post-bleach times, with the exception of observer VV at 28 min post-bleach. Three observers' percent saturation did not change across time, while observer VV's data showed a decrease in saturation during the last four time-points, when rods were contributing to color perception.

When the 4 min and 28 min mean saturation values reported by VV are compared, there is about a 20% decrease in perceived saturation across time. This was the only evidence from the saturation percentages reported for the 500 nm stimulus that support a change in saturation associated with rod input.

Figure 3.5 illustrates observers' saturation percentages of the 520 nm stimulus at the seven post-bleach times. Observers KY and VV perceived this stimulus as less saturated as post-bleach time (and rod input) increased, while observers AK and LB reported no changes in saturation across time for the 520 nm stimulus.

Only observer VV's responses provide clear support for the idea that rod influence leads to desaturation for this 520 nm stimulus. When VV's 4 min post-bleach mean saturation value is compared to the 28 min percentage, there is a decrease of about 20% across time, which is similar to the results for the 500 nm stimulus. Observer KY's data also show a trend in this direction, but there the variability at the 28 min time-point does not provide strong support for a desaturating effect of rod input.

Figure 3.6 illustrates observers' saturation percentages of the 540 nm stimulus at the seven post-bleach times. Three observers (AK, KY, VV) reported a decrease in perceived saturation with increasing time in the dark, while observer LB's responses showed increased variability in saturation perception with increased rod contribution, but no net change.

Comparisons of the mean 4 min and 28 min post-bleach percentages for three observers provide support for a desaturating influence of rods on peripheral color perception of the 540 nm stimulus. Observers AK and KY both reported mean saturation perception decreases of about 30% across time, and observer VV's mean saturation percentages decreased 40% across the time course of dark adaptation.

Figure 3.7 illustrates observers' saturation percentages of the 560 nm stimulus at the seven time-points examined. All observers perceived this as the least saturated of the test stimuli. As with the 540 nm stimulus, three observers reported decreasing saturation with increasing time in the dark, while observer LB reported no change in saturation across time. It is interesting to note that for three observers, at the 16 min time-point saturation had reached a low point, and the saturation reported at the later time-points was essentially unchanged. This pattern suggests that by 16 min post-bleach the desaturating effect of rod input was complete for this stimulus.

Comparisons of the 4 min and 28 min mean saturation percentages reported by observers AK and VV show a dramatic decrease in saturation perception across time of at least 30% for AK and 40% for VV. The decrease in mean saturation reported by observer KY across time is about 10%.

Figure 3.8 illustrates observers' saturation percentages of the 580 nm stimulus for the seven post-bleach times. Consistent with the pattern seen for 540 nm and 560 nm, three observers showed mean percent saturation decreasing with increasing time in the dark, while observer LB reported no change in saturation across time.

Comparison of the 4 min and 28 min post-bleach data for three observers support the idea that rods contribute to a desaturated appearance of monochromatic stimuli in the peripheral retina. Observers AK and KY reported a decrease in mean saturation of about 20% across the time course of dark adaptation, while observer VV reported a decrease of about 30%.

Figure 3.9 illustrates observers' saturation percentages of the 600 nm stimulus at the seven time-points examined. While the saturation percentages reported were quite variable across observers, the data of all observers showed that this stimulus was more saturated than the 580 nm stimulus at all time-points.

Three observers' data showed a pattern of decreasing saturation with increasing time in the dark, although the mean difference in saturation percent between the 4 min and 28 min data was less than the decreases reported for the middle wavelengths (i.e., 540 nm and 560 nm). Comparison of the 4 min and 28 min mean saturation percentages reported by AK (KY, VV) showed a decrease of nearly 20% (10%, 30%).

Figure 3.10 illustrates observers' saturation perceptions of the 620 nm stimulus at the seven time-points tested. All observers reported that this stimulus was relatively saturated at all time-points, and increasing time in the dark was not associated with a change in saturation for observers LB and AK. KY and VV did show a small decrease

(<10%) with increasing time in the dark, but the variability among data points suggests this is a relatively weak effect.

In summary, it is interesting to note that all four observers in this study perceived the 540, 560 and 580 nm stimuli as the least saturated wavelengths when they were presented to the fovea and when they were viewed in the peripheral retina; the rods are not most sensitive to these wavelengths of light (recall peak sensitivity is 507 nm). Three observers reported decreases in perceived saturation of these stimuli as post-bleach time increased, suggesting that perception of wavelengths in this range of the visible spectrum, which are described as greenish-yellow, yellow, and orange, is more influenced by rod input than perception of shorter- and longer-wavelength stimuli. The pattern of results for the shorter- and longer-wavelength stimuli viewed in the periphery was similar in that overall, observers assigned greater saturation percentages to the wavelengths perceived as blue and red, with less change across time, compared to the saturation percentages reported for the middle wavelengths. The only stimulus which elicited an unchanging pattern of saturation perception across all four observers was the 480 nm stimulus, which was perceived as equally saturated at all time points by all observers.

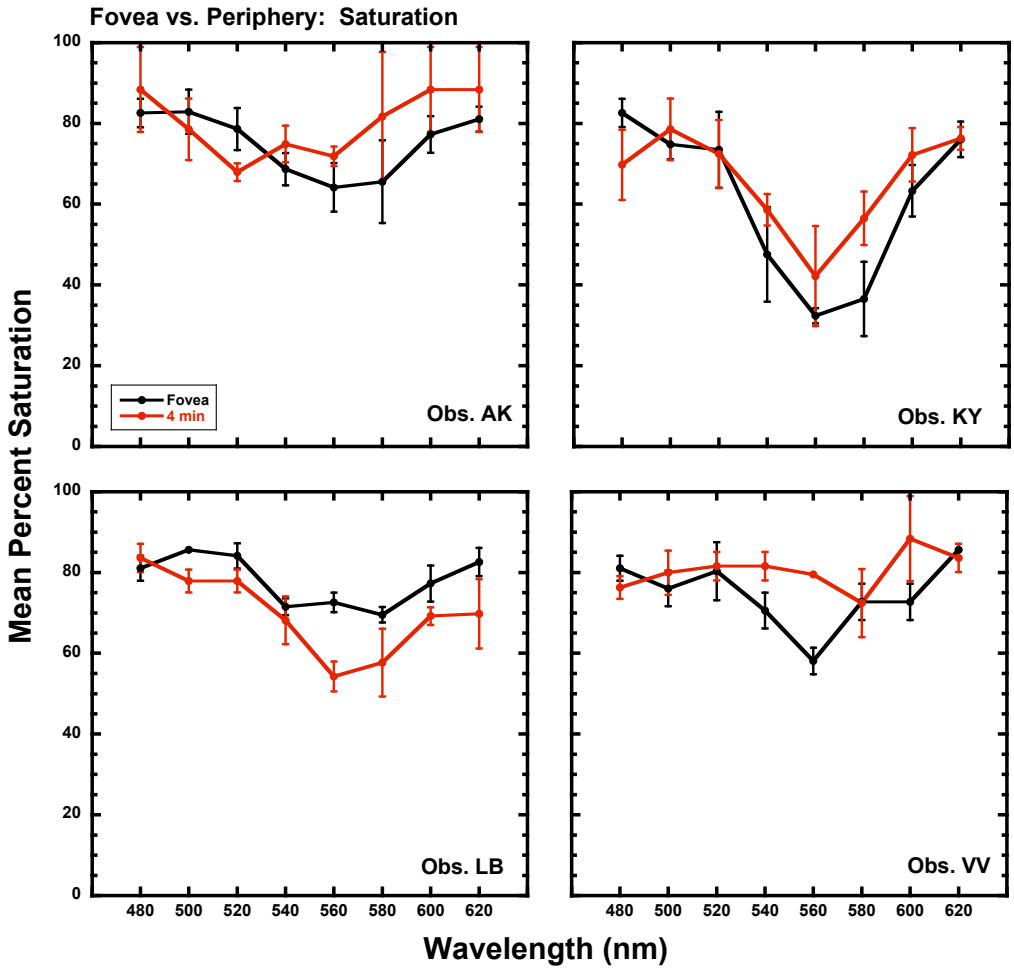

Figure 3.11: Mean percent saturation reported for each wavelength in the fovea (black line) and in the peripheral retina at 4 min post-bleach (red line) for each observer. Error bars represent ±1 standard deviation (SD).

Each panel in **Figure 3.11** displays mean saturation values for one observer at each stimulus wavelength presented in the fovea and in the peripheral retina at the 4 min post-bleach time. The 4 min post-bleach time represents one of the peripheral conditions with minimal rod contribution. There is considerable inter-observer variation in this comparison of saturation percentages, but the overall pattern within each observer is rather similar for the two viewing conditions.

Observer AK's mean saturation percentages differ only for the 520 nm stimulus, which was reported to be about 10% less saturated when viewed in the periphery. The error bars (representing the SDs) for the foveal and 4 min peripheral data overlap for all other wavelengths, so that overall AK's saturation perceptions were similar between the fovea and the periphery on the cone plateau.

Mean saturation percentages for the 480 nm and 580 nm stimuli differed for observer KY, with the error bars for the other six wavelengths overlapping. Interestingly, the 480 nm stimulus was reported to be about 10% less saturated when viewed in the periphery, but the 580 nm stimulus was perceived as more saturated in the periphery, with about a 20% difference between the mean percentages.

Mean saturation percentages for observer VV from the two retinal locations differed for three wavelengths: 540 nm, 560 nm and 600 nm. The mean percentages for the 560 nm stimulus differed by about 20%, which is the largest difference found between the saturation values in these two retinal locations for any observer at any wavelength. The mean saturation values for the 600 nm stimulus also differed by nearly 20%, but the SDs for these values were much larger, so that the error bars nearly touch. About a 10% difference separated the mean values for the 540 nm stimulus. It is interesting to note that these wavelengths where saturation values differed were all reported to be more saturated when viewed in the peripheral retina, which is the opposite of what we might expect, given the decreased density of the peripheral cone mosaic, compared to the tightly-packed foveal cone arrangement.

Differences between the mean foveal and peripheral saturation values reported by observer LB are noted for all wavelengths except 480 nm and 540 nm. Saturation

was reported to be less when these stimuli were viewed in the periphery compared to the fovea. Most stimuli were reported to be about 10% less saturated by observer LB when viewed in the periphery compared to the fovea, except the 560 nm stimulus, which was, in general, the least saturated stimulus for all observers under all conditions, that differed by about 20%. This is consistent with previous research (e.g., Abramov et al., 1992) that suggested that saturation declines in the peripheral retina when compared to the fovea.

Hue Results

Fovea

Mean arcsine transformed hue percentages for each observer are shown in **Figure 3.12.** These data represent the mean percentages from four presentations of each wavelength, and the different colored lines represent the four hue terms. It should be noted that on a given trial no observer ever used more than two hue terms to describe a stimulus. However, the hue terms used to describe a given stimulus may have differed from trial to trial. For example, on one trial a 500 nm stimulus may have been described using the hue terms “blue” and “green,” but on the subsequent viewing the observer may have used the terms “green” and “yellow” to describe the stimulus. Thus, for each observer in **Figure 3.12**, there are some wavelengths for which percentages are plotted for three hue components at a given wavelength. Overall, all four observers showed the same pattern of results, and these were consistent with foveal hue scaling results reported in the literature (e.g., Gordon & Abramov, 1988).

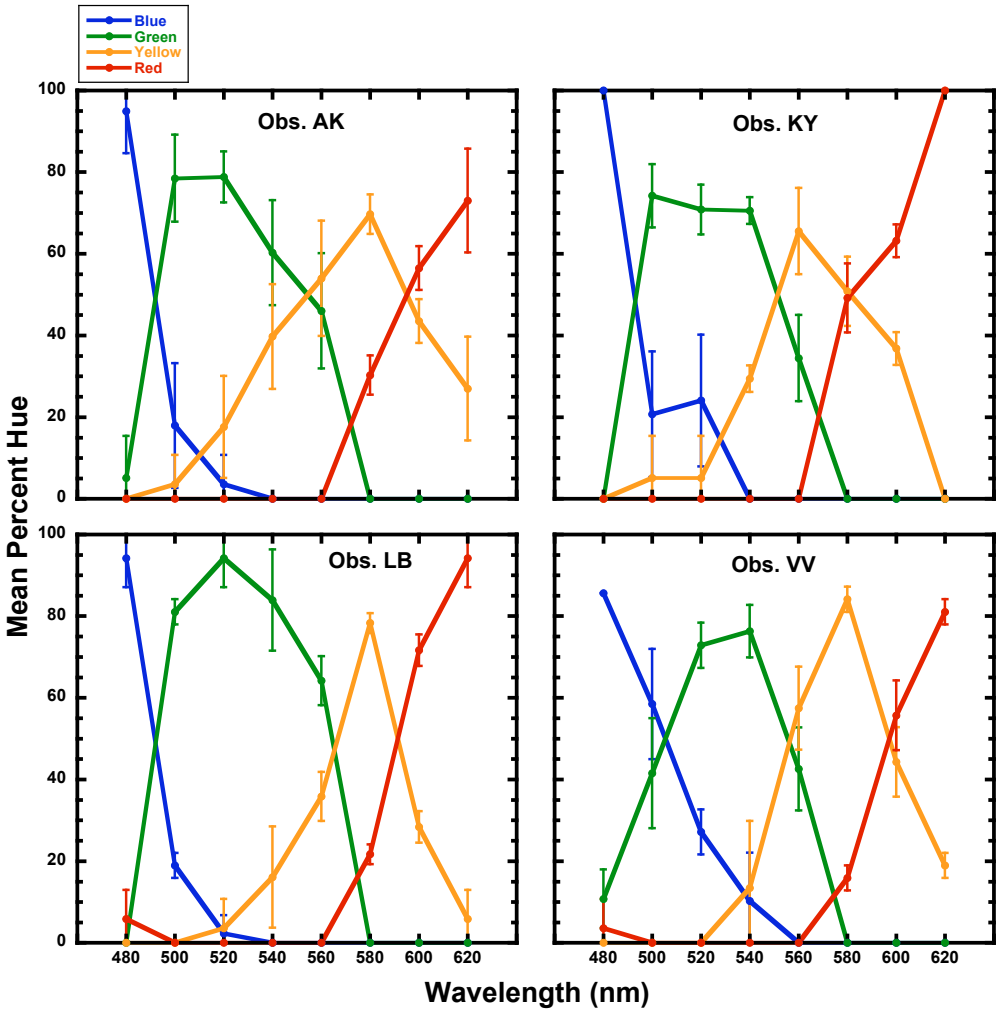

Figure 3.12: Mean hue percentages for eight wavelengths presented to the fovea are plotted for each observer in a separate panel. Error bars represent ±1 standard deviation (SD). The colored lines denote the four different hue terms.

Peripheral Retina

Mean hue percentages obtained across the time course of dark adaptation in the peripheral retina for each stimulus wavelength are shown in **Figures 3.13-3.20**. Each figure presents data for a different wavelength. Means and SDs from the three responses given for each stimulus at each post-bleach time are presented in a separate

panel for each observer. Note that the abscissa in each of these figures represents minutes post-bleach, differing from the abscissa units in **Figure 3.12**.

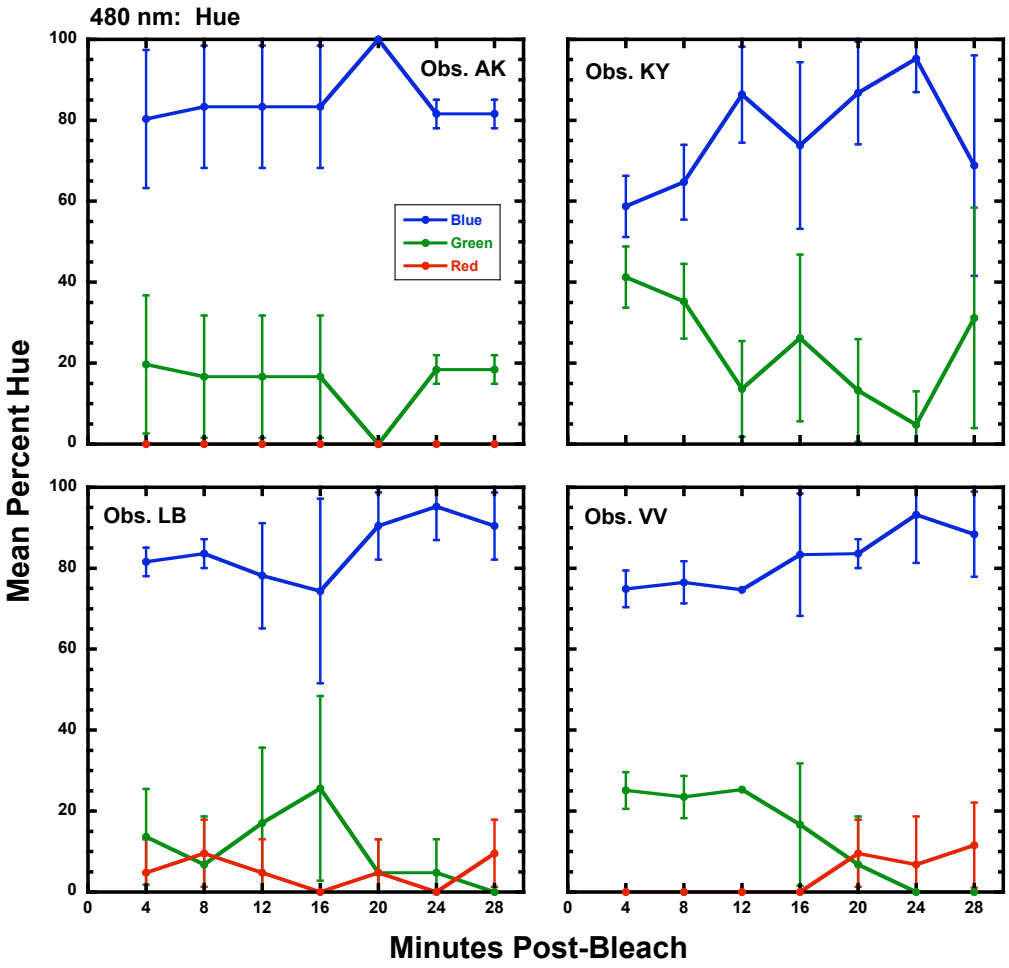

Figure 3.13: Mean hue percentages (±1 SD) reported by four observers for the 480 nm stimulus presented to the peripheral retina at seven post-bleach times. The colored lines denote the different hue terms.

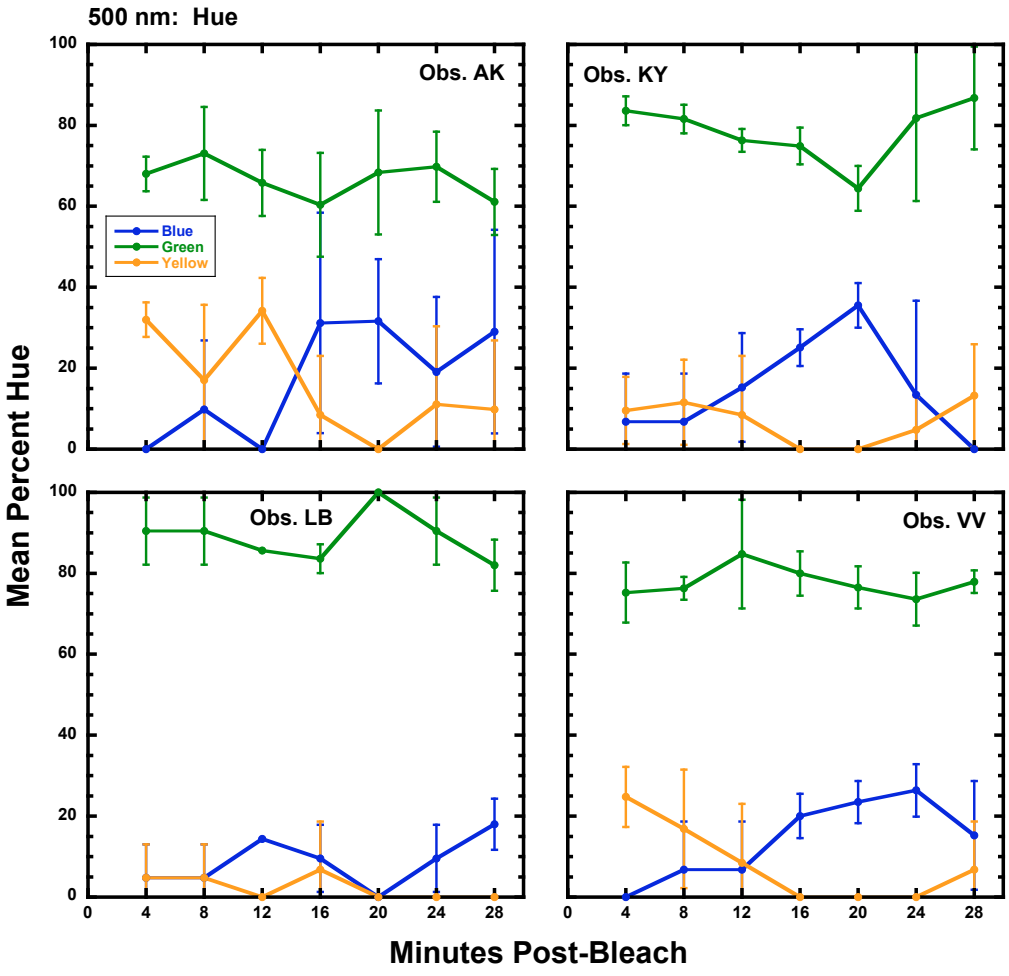

Figure 3.14: Same as **Figure 3.13** except for the 500 nm stimulus.

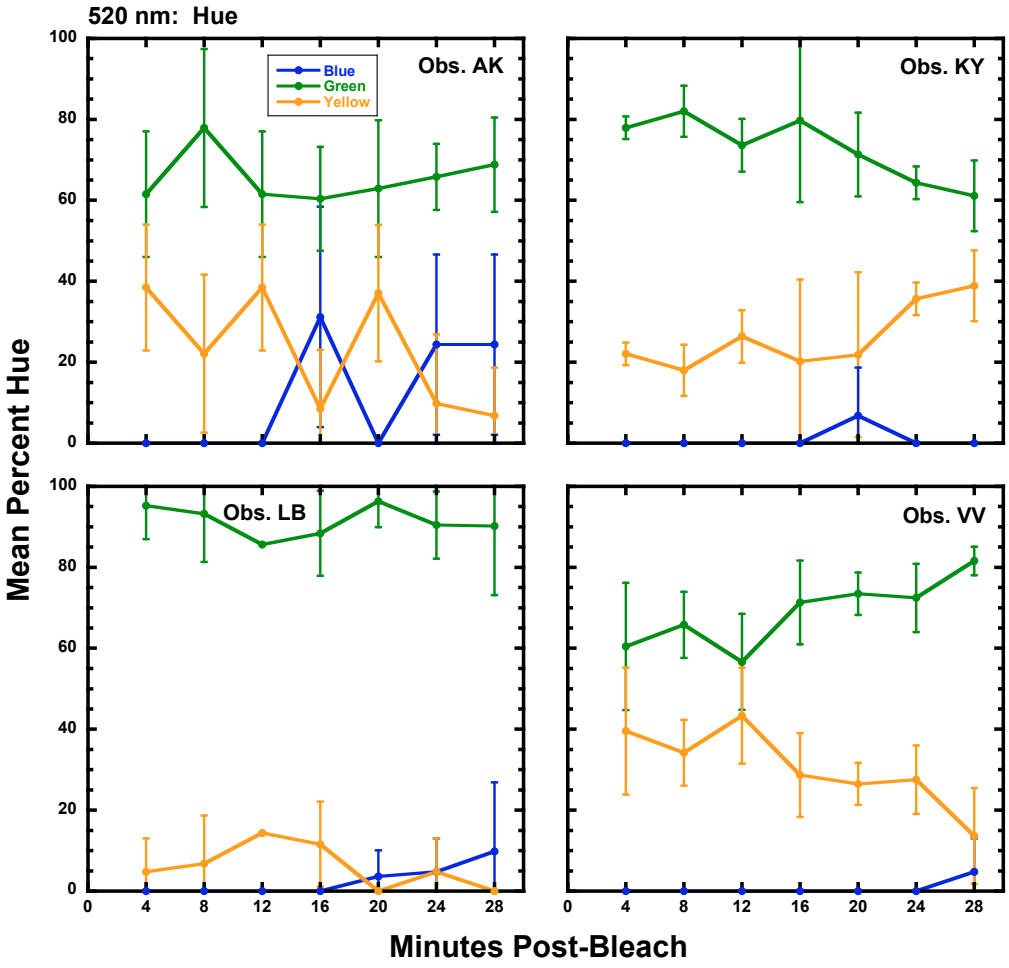

Figure 3.15: Same as **Figure 3.13** except for the 520 nm stimulus.

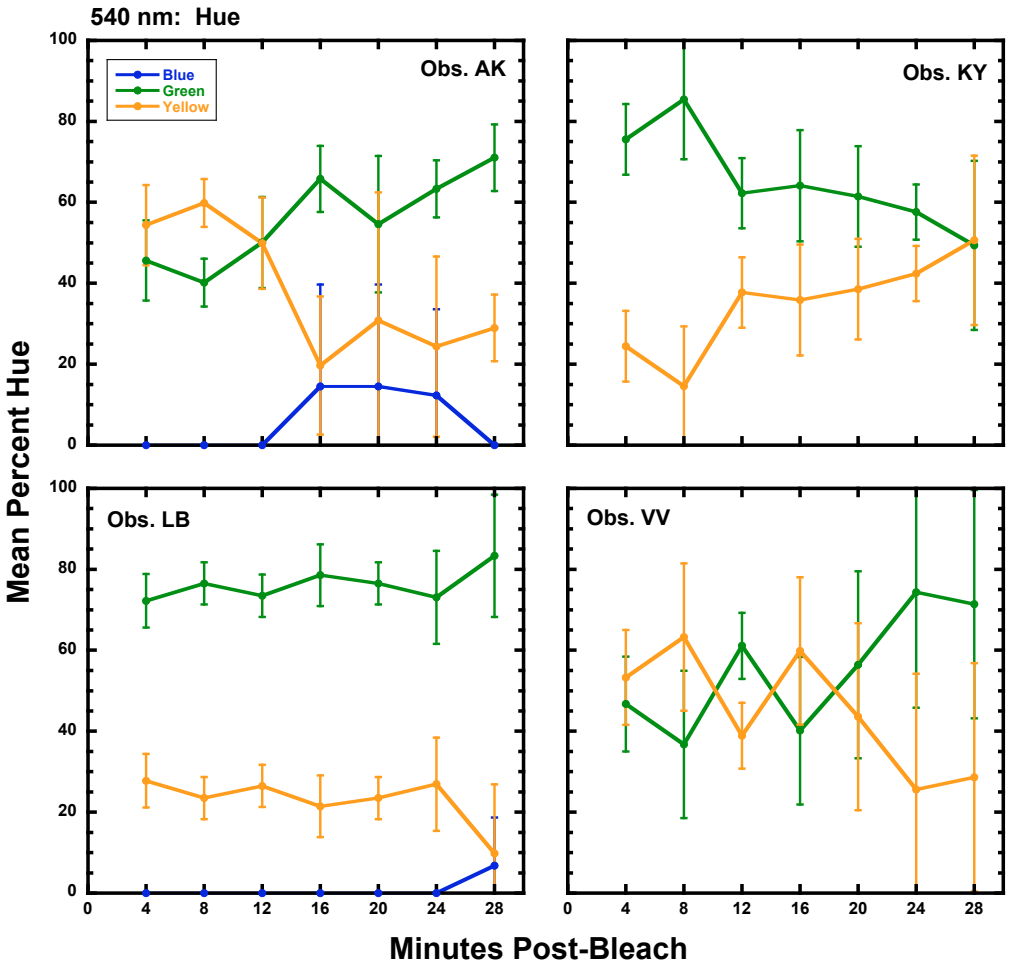

Figure 3.16: Same as **Figure 3.13** except for the 540 nm stimulus.

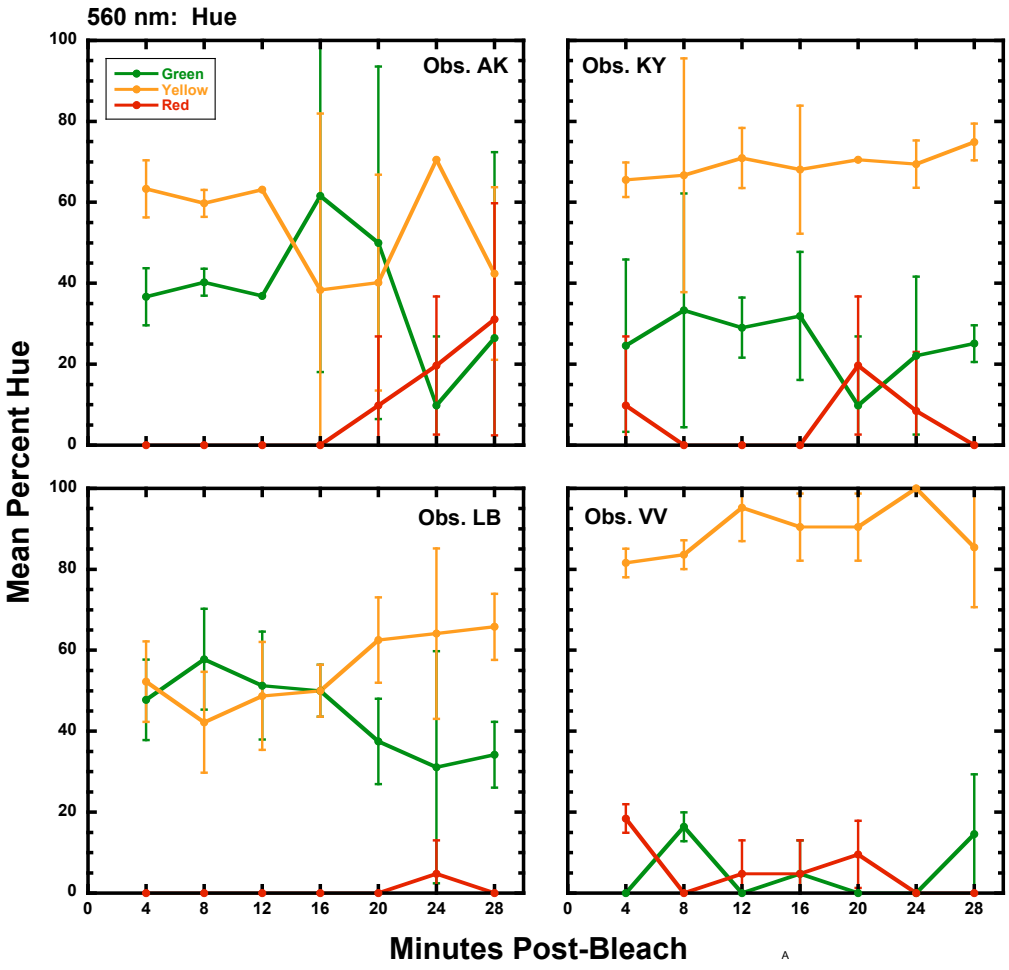

Figure 3.17: Same as **Figure 3.13** except for the 560 nm stimulus.

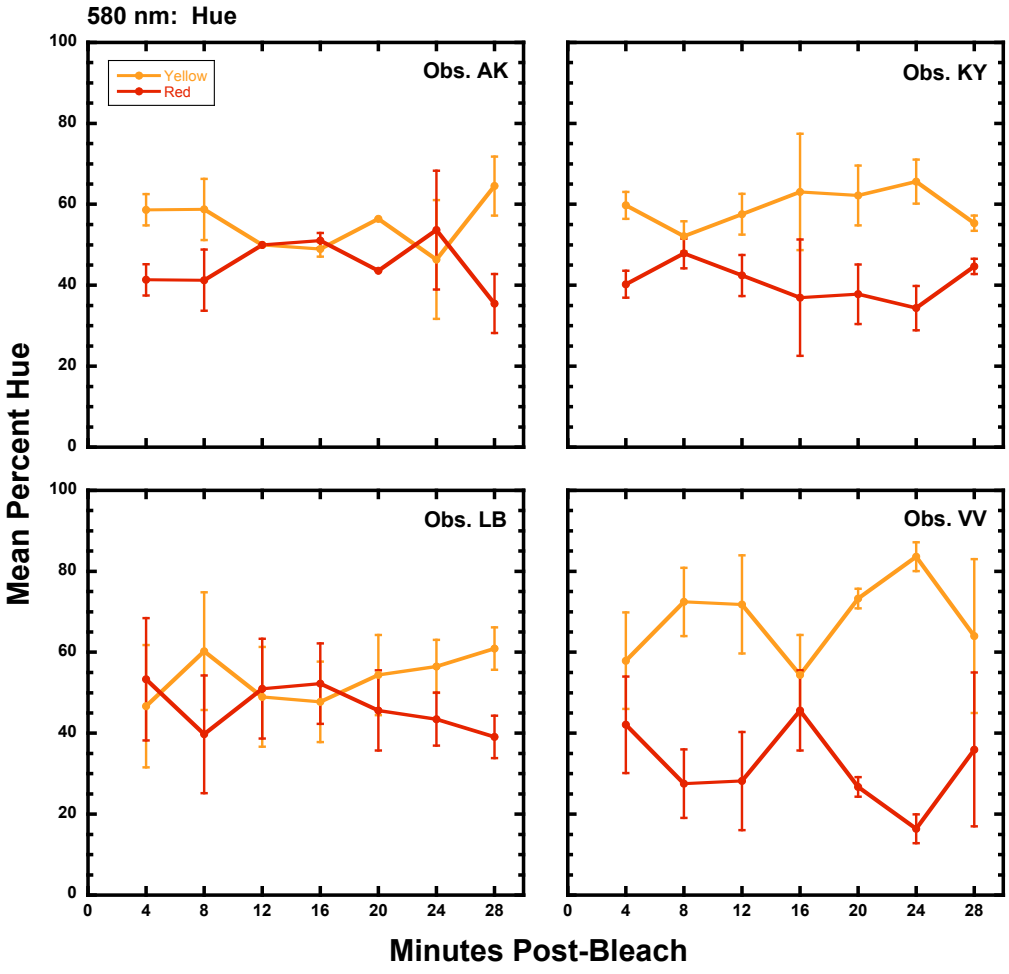

Figure 3.18: Same as **Figure 3.13** except for the 580 nm stimulus.

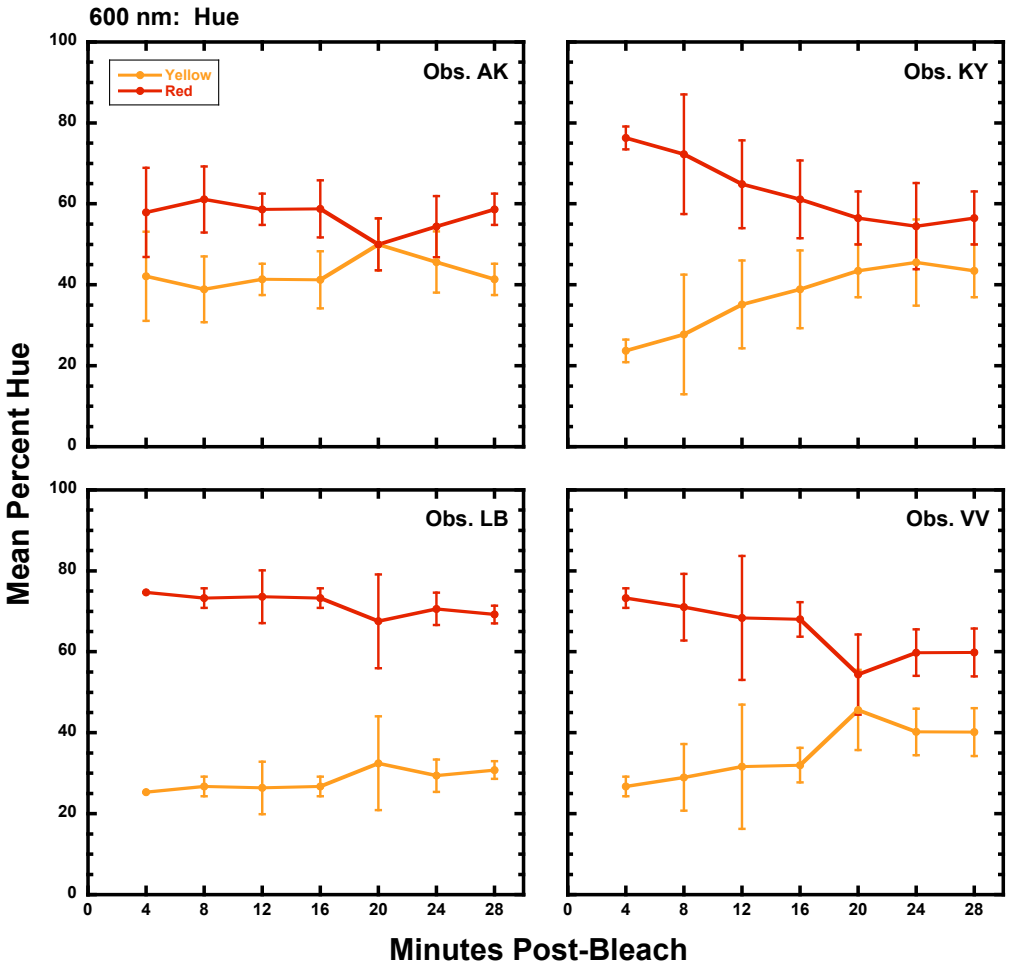

Figure 3.19: Same as **Figure 3.13** except for the 600 nm stimulus.

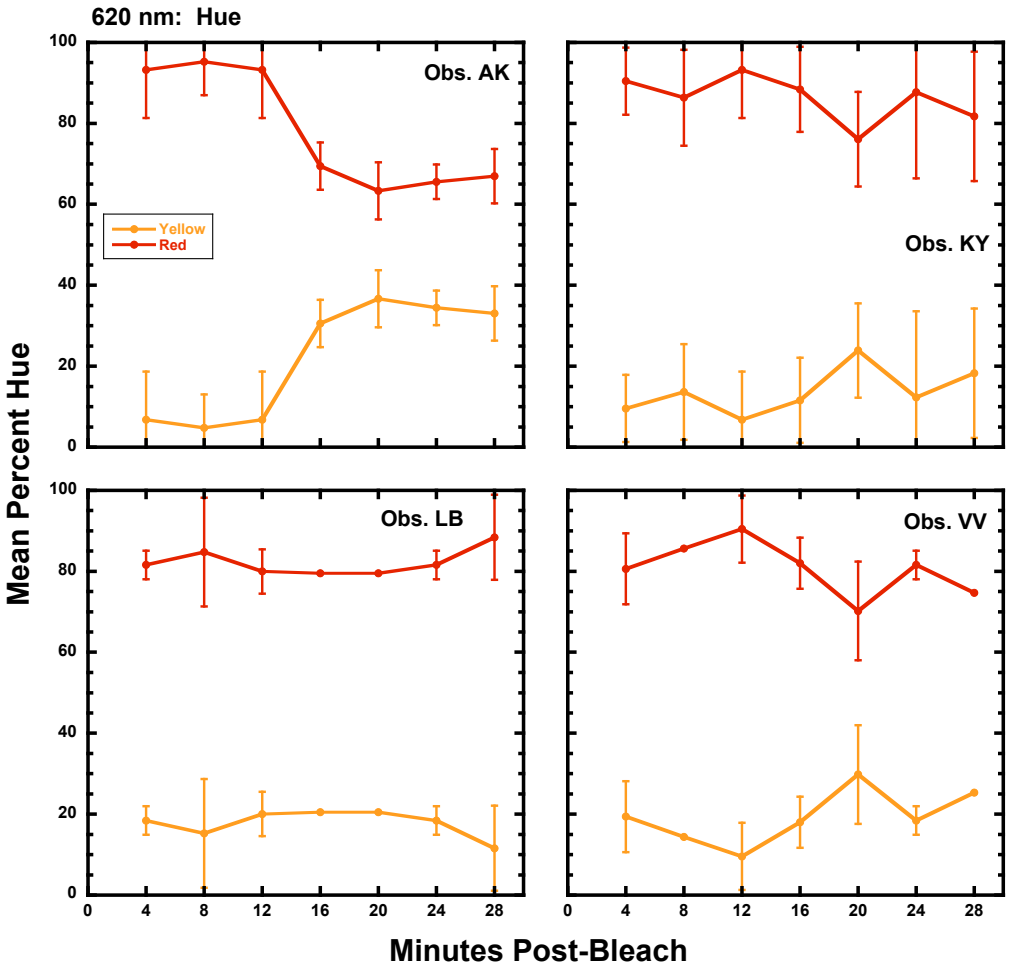

Figure 3.20: Same as **Figure 3.13** except for the 620 nm stimulus.

Figure 3.13 presents the hue percentages of the 480 nm stimulus for each observer at the seven post-bleach times examined. Observer KY perceived this stimulus as greenish-blue at all post-bleach times, while observer AK reported that the stimulus was greenish-blue at all post-bleach times except 20 min, when the stimulus was described as 100% blue on all three trials. This suggests that AK may identify a wavelength near 480 nm as UB. LB and VV sometimes perceived the stimulus as

greenish-blue, and other times as reddish-blue, also an indicator that 480 nm is their unique blue loci. For all observers the 480 nm stimulus appeared close to 100% blue on many trials, but observers reported the presence of a small percentage of either green or red on different trials, thus explaining percent values for three hue terms. For example, at the 8 min post-bleach time, LB reported that the stimulus appeared 95% blue and 5% red on two trials, and 90% blue and 10% green on a third trial. Given similar data, other authors (Abramov, Gordon & Chan, 2009; Volbrecht, Nerger, Baker, Trujillo & Youngpeter, 2010) have chosen to reapportion hue scaling data such as these. If a stimulus was described with three hue terms across multiple trials, the smallest hue percentage was reapportioned into the other two hue terms, thus eliminating one of the three hue percentages while retaining the same ratio of those hue terms. In the present study, the data were not reapportioned, so that the between-session variability was not lost, and no information about any of the hue terms that observers reported was lost.

It is interesting to note that while the percent blue reported by all four observers did not change across time (determined by overlapping of the error bars), the two observers (LB and VV) who perceived this wavelength as reddish-blue on some trials both perceived the stimulus as exclusively reddish-blue at the 28-min time. VV also perceived reddish-blue on all trials at 24 min post-bleach. This is suggestive of a decrease in the perception of green and/or an increase in the perception of short-wavelength red with rod contribution for two observers. Another way to describe this is that at 28 min post-bleach this stimulus appeared to be a shorter wavelength than it did when presented at earlier post-bleach times. If one begins by viewing a short

wavelength of light that appears purple, or reddish-blue, then views progressively longer wavelengths of light, color perception will be described with increasing percentages of blue and decreasing percentages of red until a wavelength of light is viewed which is perceived as 100% blue, or UB. Increasing the stimulus wavelength will lead to greenish-blue being perceived. The hue percentages reported for this 480 nm stimulus can thus be thought of as changing from a perceptually longer wavelength (described as greenish-blue) to a perceptually shorter wavelength (described as reddish-blue).

Figure 3.14 shows hue percentages for the 500 nm stimulus for the seven post-bleach times and four observers. All observers perceived this stimulus as predominantly green, although sometimes it was described as bluish-green and at other times as yellowish-green by all observers. Observer LB reported that this wavelength appeared 100% green on all three trials at the 20 min post-bleach time, suggesting that a wavelength near 500 nm might be identified as unique green by this observer at this point in dark adaptation. Interestingly, the mean percent green reported by all observers remained virtually unchanged across time.

The trend for observers AK, LB and VV was to perceive this stimulus as containing more blue (or less yellow) as time in the dark (and rod input) increased. KY reported a blue hue component on all trials at 16 and 20 min post-bleach, but reported only yellow and green at 28 min post-bleach. Therefore, a comparison of the 4 min and 28 min hue scaling percentages show an increase in perceived blue for only three observers.

In **Figure 3.15** the hue percentages for the 520 nm stimulus are presented for the seven post-bleach times and four observers. All observers perceived this stimulus

as predominantly green. It was described as yellowish-green during the first three time-points by all observers, and then all observers reported a blue hue component at least once during the second half of the time-course, at or after 16 min post-bleach, when rods would have been influencing color perception. For two observers (AK and LB) the percent green did not change across time. Observer KY perceived less green and more yellow across time, while observer VV perceived the opposite changes of more green and a trend towards less yellow as time in the dark increased. Comparing the 4 min and 28 min hue percentages does not provide a consistent pattern of change; only AK's percentages show a clear increase in blue in this comparison. But it is interesting to note that all four observers reported a blue component in this stimulus on some trials, but only at 16 min post-bleach and later, which is suggestive of rods contributing increased blueness to color perception, and may warrant further study.

Figure 3.16 presents hue percentages for the 540 nm stimulus at the seven post-bleach times and four observers. Observer LB described this stimulus as predominantly green at all time-points, observer KY described it as predominantly green at all post-bleach times before 28 min, at which time it appeared to contain equal amounts of green and yellow hue components. The other two observers sometimes described this wavelength as yellowish-green, and at other times as greenish-yellow. Two observers reported a blue hue component in this stimulus on some trials during the second half of the time-course, when rods were contributing to color perception. Overall the variability in observers' hue perceptions for this wavelength was great, and, as shown in **Figure 3.6**, three of the four observers reported that this stimulus was less than 50% saturated during the later time-points, so that overall hue perception was

minimal and thus difficult to specify. Observer AK's hue percentages show an increase in green and a trend towards an increase in blue until 24 min, as well as a decrease in yellow across time. Observer KY shows the opposite trend of decreasing green and increasing yellow across time. Observer LB's hue descriptions did not change across time until 28 min, when a blue hue component was reported for one of the three viewing trials. Observer VV's hue descriptions all contain green and yellow hue components, but there is great variability across time and within the three trials at most post-bleach times.

Figure 3.17 illustrates the observers' hue percentages for the 560 nm stimulus at the seven post-bleach times. Hue perceptions of this stimulus were highly variable. For observers AK and LB the hue data reported for the first three post-bleach intervals appeared relatively stable, and quite different from the data reported for the last four time-points, when rods were contributing to color perception. All observers perceived a red hue component in this stimulus, but for observers AK and LB the red component was reported only during the second half of the time-course. Like the 540 nm stimulus, this wavelength was described as desaturated and hue perception was minimal and not easily described. Observers KY and VV described this wavelength as predominantly yellow at all post-bleach times, while observers AK and LB perceived the stimulus as containing more green at earlier post-bleach times than later post-bleach times. Observer VV's hue scaling percentages suggest that she will likely identify a wavelength near 560 nm as the locus of unique yellow. No clear change in hue perception can be detected when the 4 min and 28 min post-bleach percentages are compared.

The hue percentages for the 580 nm stimulus are shown in **Figure 3.18**. All observers described this wavelength as yellow and red across time, either with yellow as the dominant hue component, or with an approximately equal combination of yellow and red hue components. Hue perception remained generally unchanged across time for all observers for this stimulus, and a comparison of the 4 min and 28 min hue percentages suggests no clear influence of rods on hue perception of this wavelength.

Figure 3.19 presents observers' hue percentages for the 600 nm stimulus as a function of post-bleach time. All observers perceived this stimulus as yellowish-red across time, and each observer's hue perceptions were relatively unchanged with increasing time in the dark, though observers KY and VV did report a mean decrease in red and accompanying increase in yellow across time for this wavelength. This is consistent with the perceptual shift towards yellow that the Stabells reported for long-wavelength stimuli in their color matching studies (Stabell & Stabell, 1975; Stabell & Stabell, 1976).

The hue scaling results for the 620 nm stimulus are given in **Figure 3.20**. All observers perceived this stimulus as predominantly reddish with a smaller yellow hue component, and three observers' hue descriptions did not change with time post-bleach. Observer AK's hue descriptions during the last four time-points, when rods were contributing to color perception, showed a decrease in red and an increase in yellow hue components, which is again consistent with the Stabells' reports from their color matching studies (Stabell & Stabell, 1975; Stabell & Stabell, 1976).

In summary, for these eight wavelengths, the pattern of results for the hue scaling values reported across time provided limited support for the claim that rod

participation in peripheral color perception is associated simply with an increase in perception of blue. For the 480 nm stimulus, the "bluest" stimulus viewed, there was no change in the percentage of blue reported by any of the observers across the time-course of the study. Three observers' data showed a trend of more blue being perceived in the 500 nm stimulus with increasing rod participation.

Results from the 600 nm and 620 nm stimuli provide limited support for a perceptual shift towards yellow associated with rod contribution, as reported by the Stabells (Stabell & Stabell, 1975; Stabell & Stabell, 1976) for long-wavelength stimuli. Two observers' data showed this pattern for the 600 nm stimulus, and one observer showed this pattern for the 620 nm stimulus.

For seven of the eight stimuli, at least one observer, but usually two or three observers, reported that the stimulus appeared perceptually a shorter wavelength when viewed at 28 min post-bleach compared to how it appeared when it was viewed at 4 min post-bleach.

Fovea vs. Peripheral Retina

Comparisons of the mean hue percentages reported for each stimulus viewed in the fovea and in the peripheral retina at the 4 min post-bleach time, when rod contribution is presumed to be minimal, are presented in **Figures 3.21-3.28.** Each figure presents data for a different wavelength. As discussed above, this comparison represents color perception mediated predominantly by cones in the two different regions of the retina.

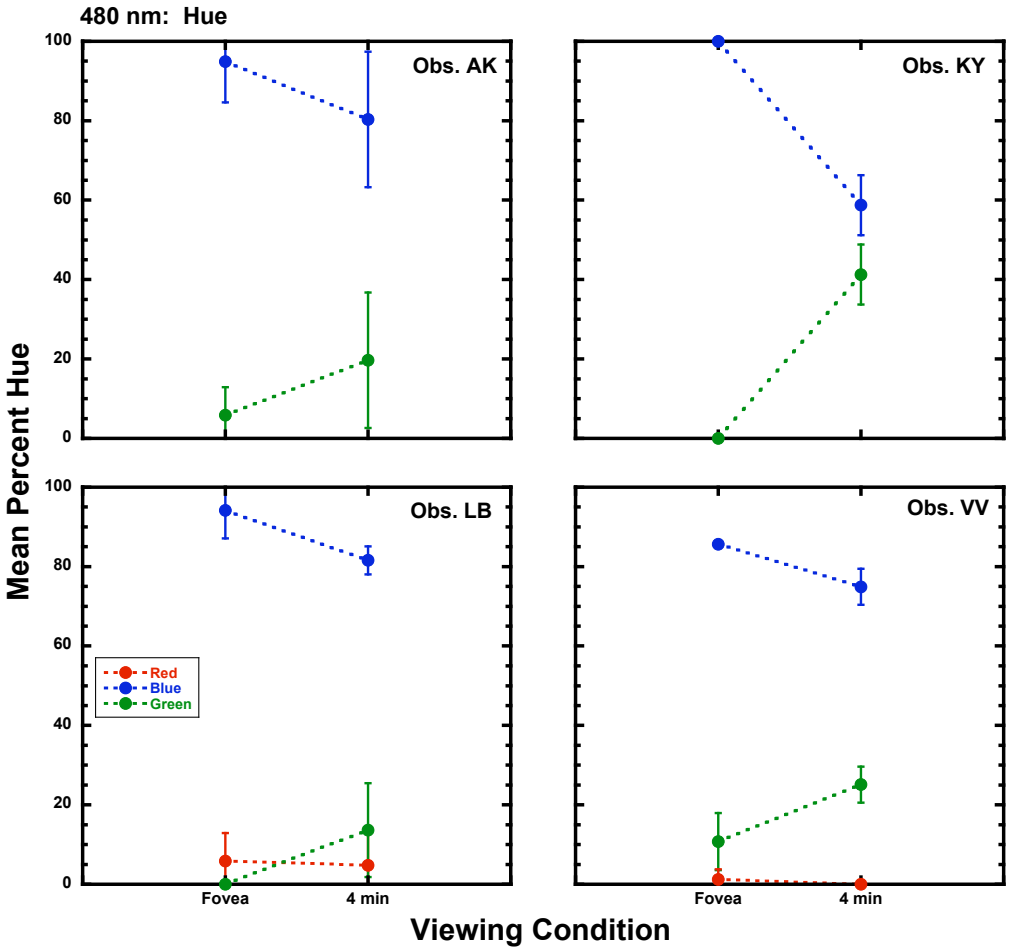

Figure 3.21: Comparison of the mean hue percentages (±1 SD) reported by each observer for the 480 nm stimulus when viewed in the fovea and in the periphery at the 4 min post-bleach time. Colored lines denote the different hue terms.

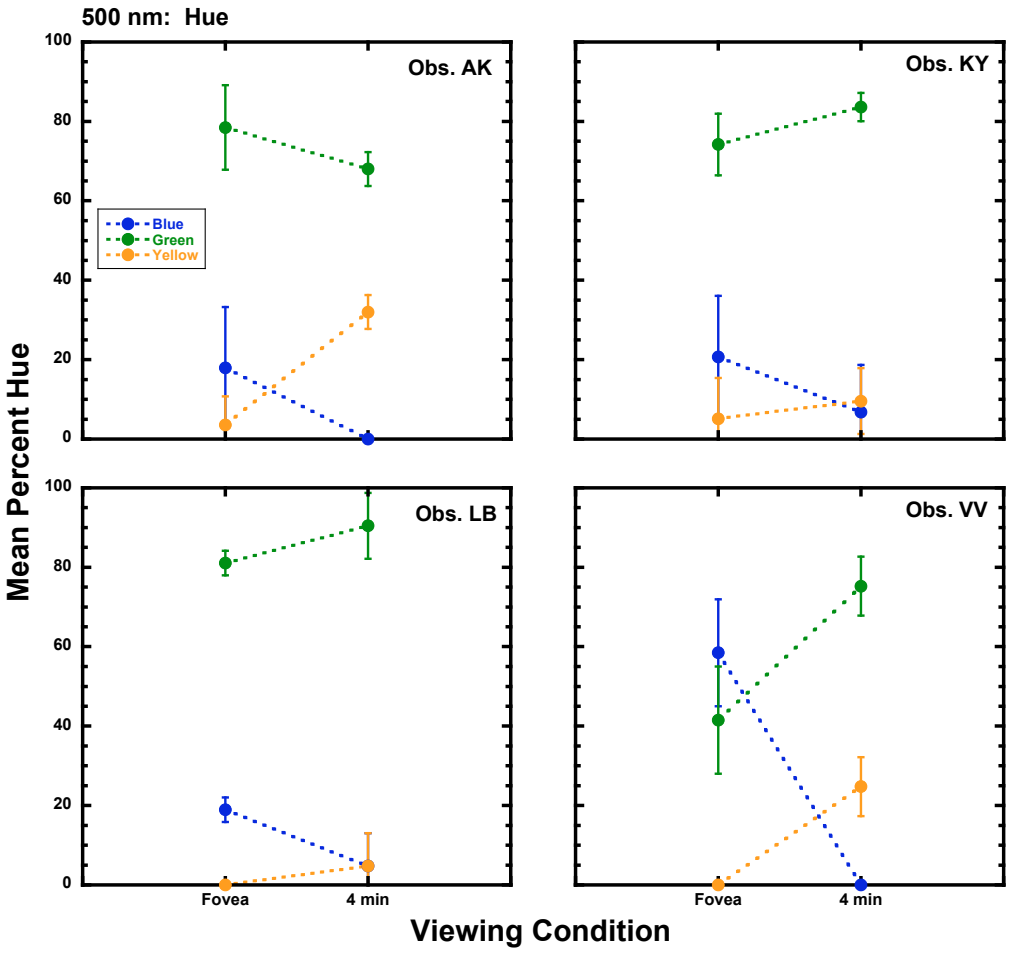

Figure 3.22: Same as **Figure 3.21** except for the 500 nm stimulus.

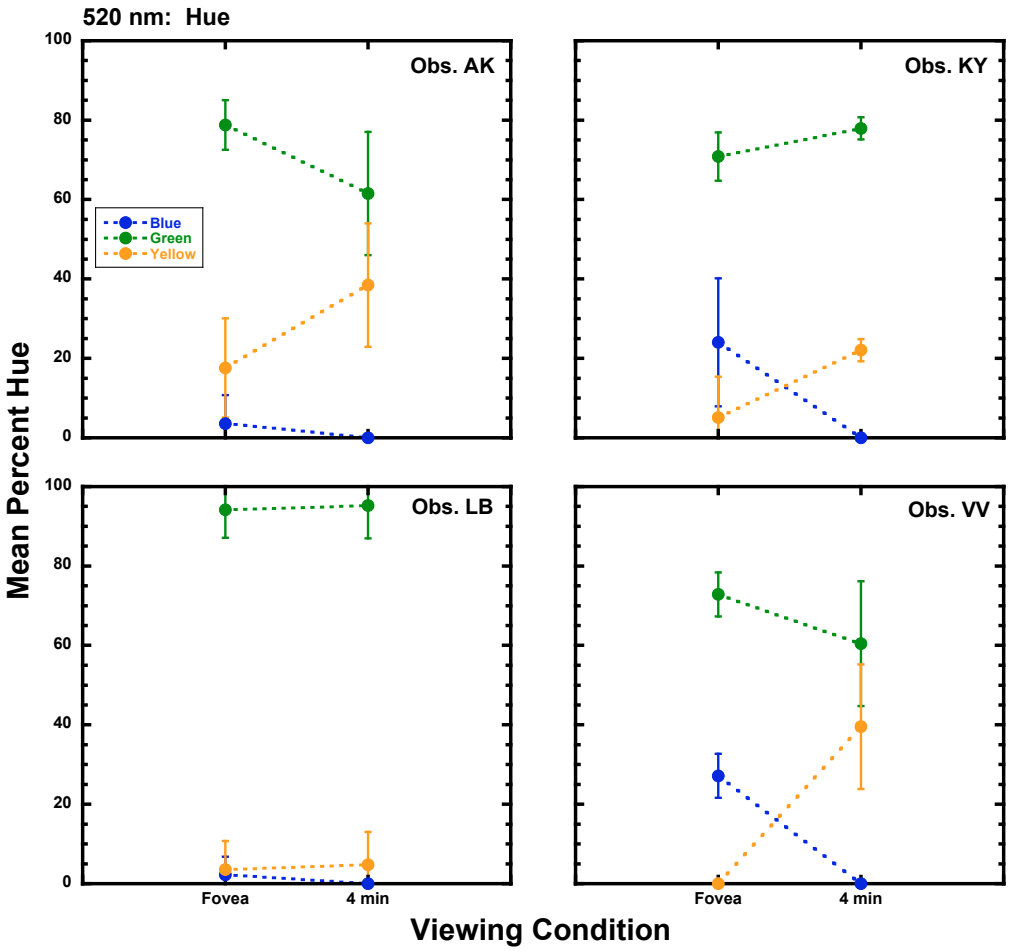

Figure 3.23: Same as **Figure 3.21** except for the 520 nm stimulus.

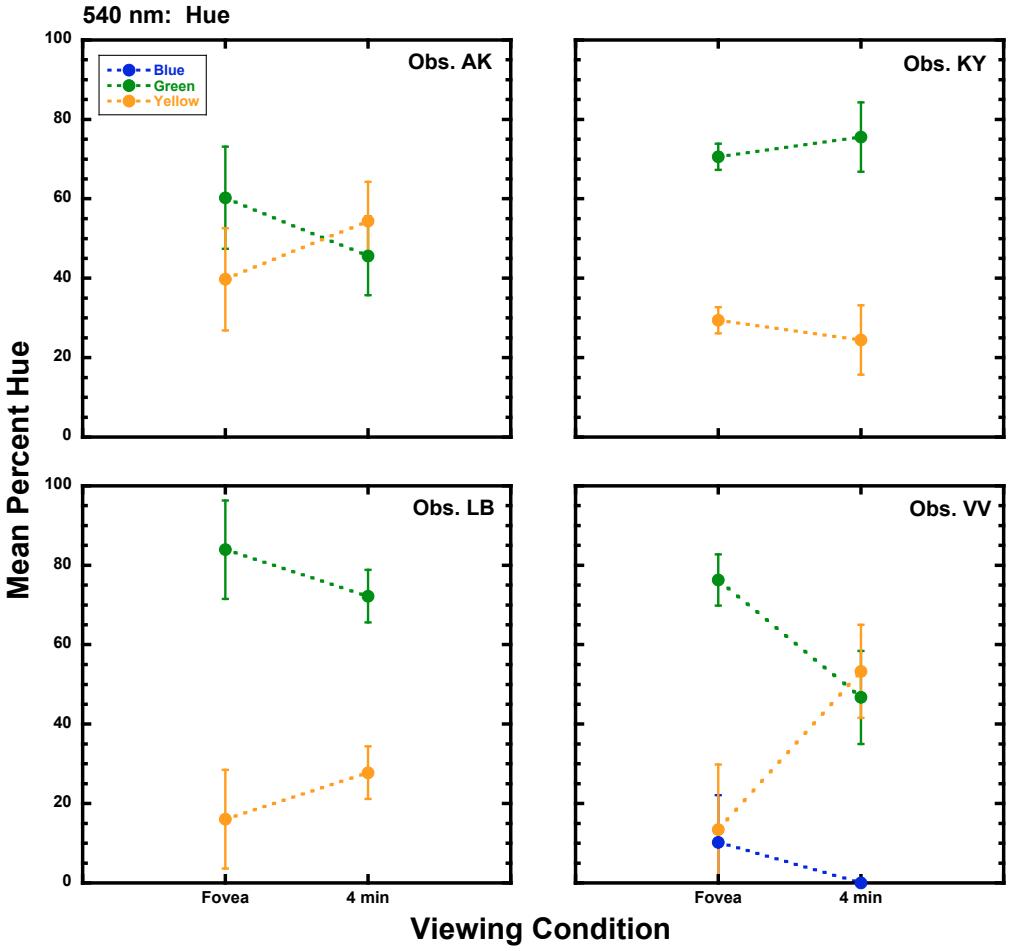

Figure 3.24: Same as **Figure 3.21** except for the 540 nm stimulus.

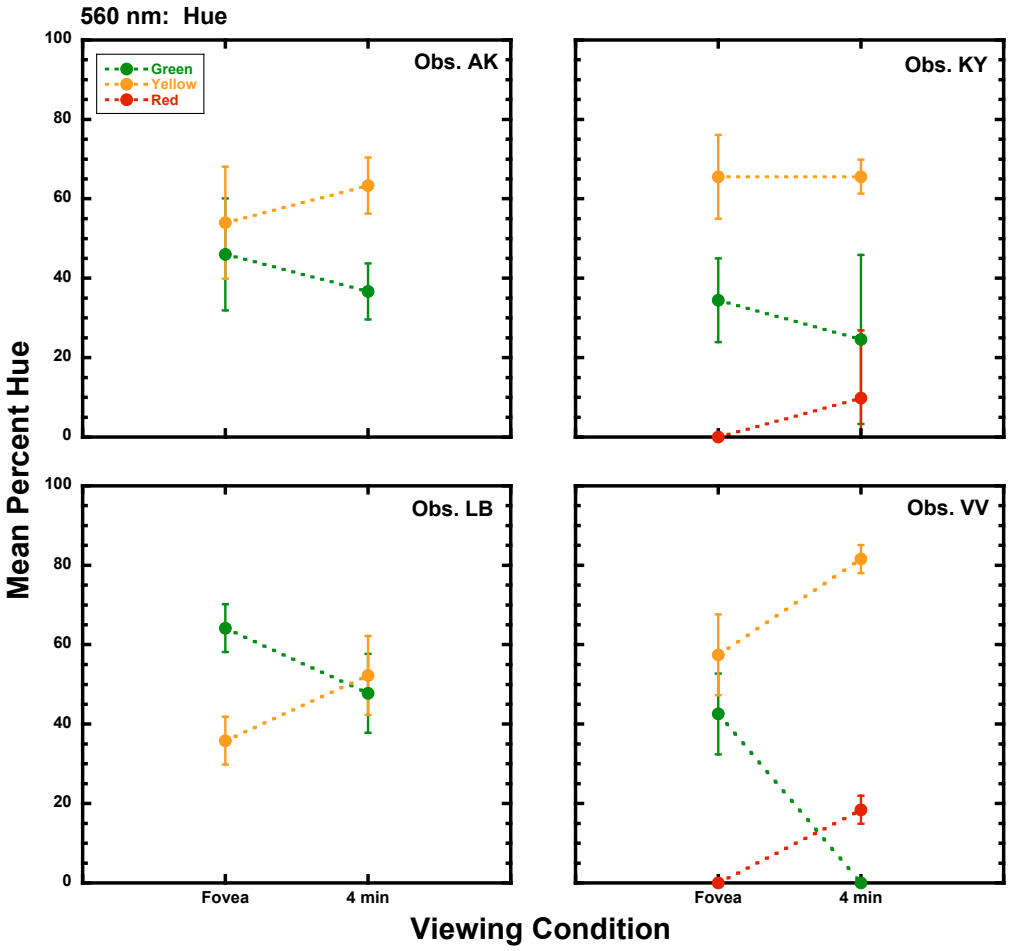

Figure 3.25: Same as **Figure 3.21** except for the 560 nm stimulus.

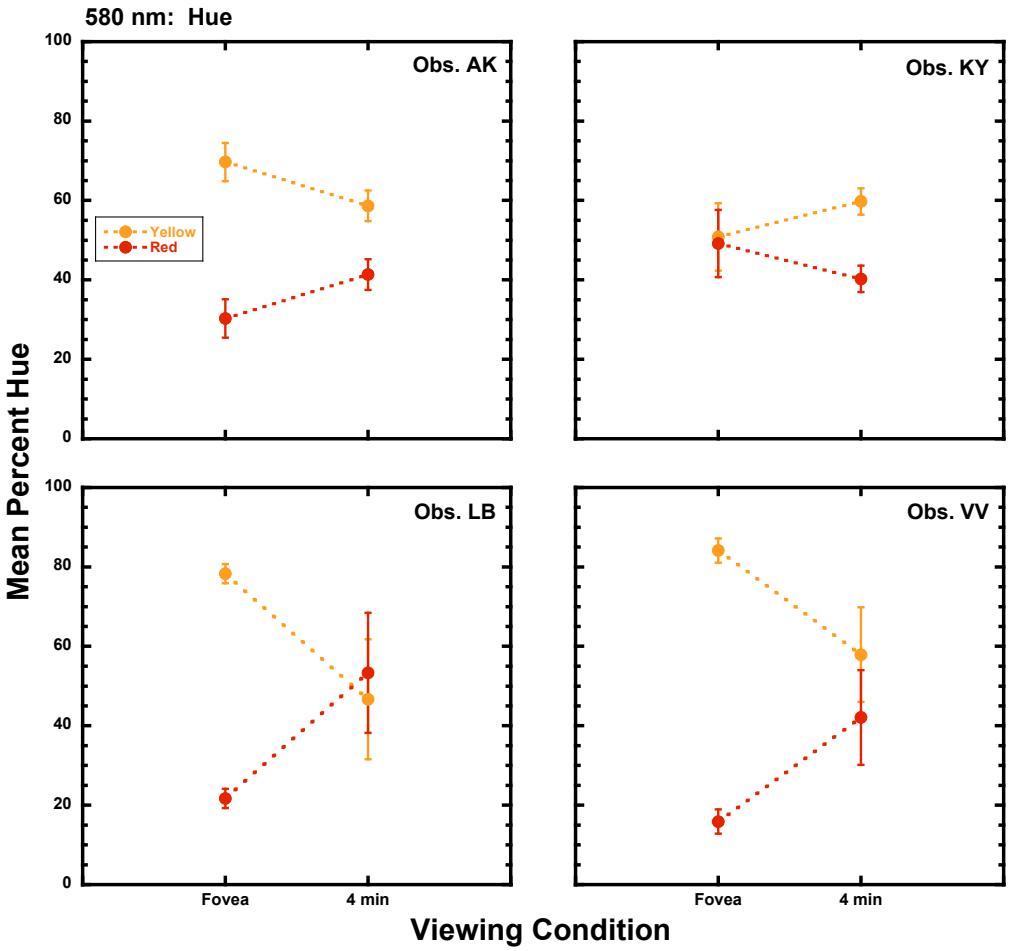

Figure 3.26: Same as **Figure 3.21** except for the 580 nm stimulus.

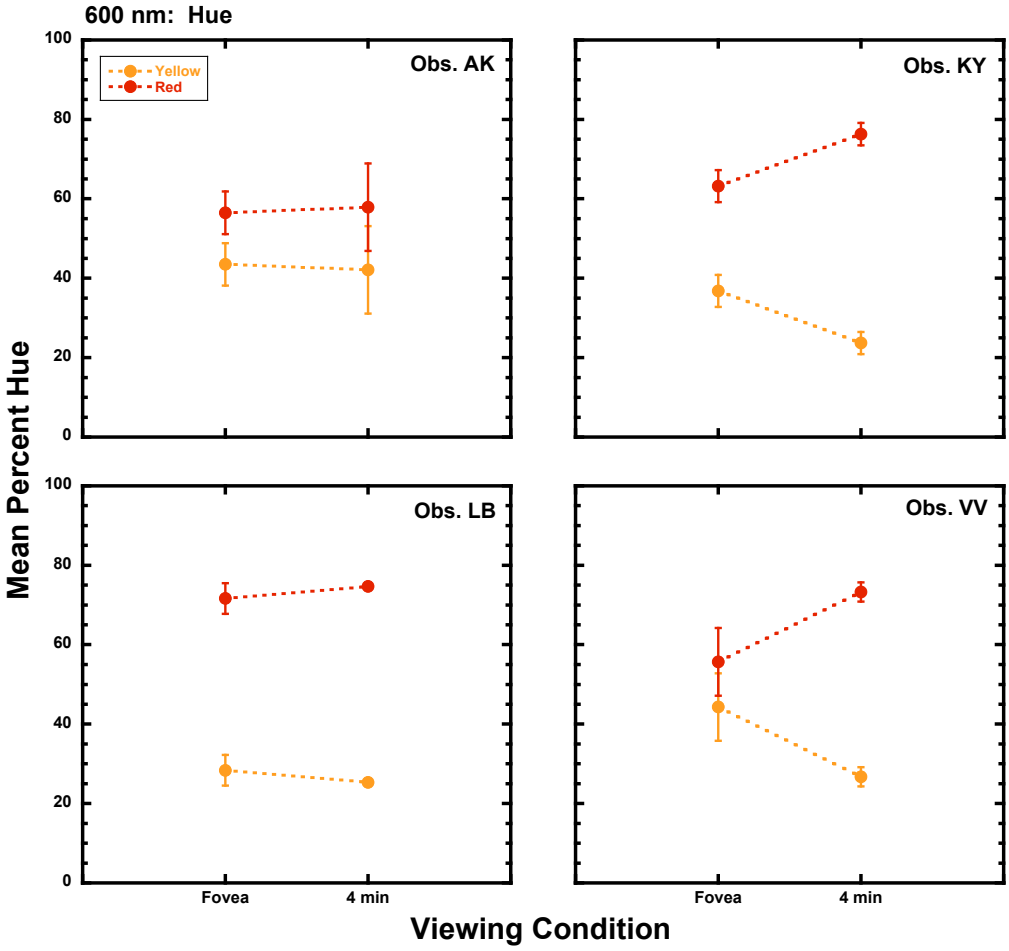

Figure 3.27: Same as **Figure 3.21** except for the 600 nm stimulus.

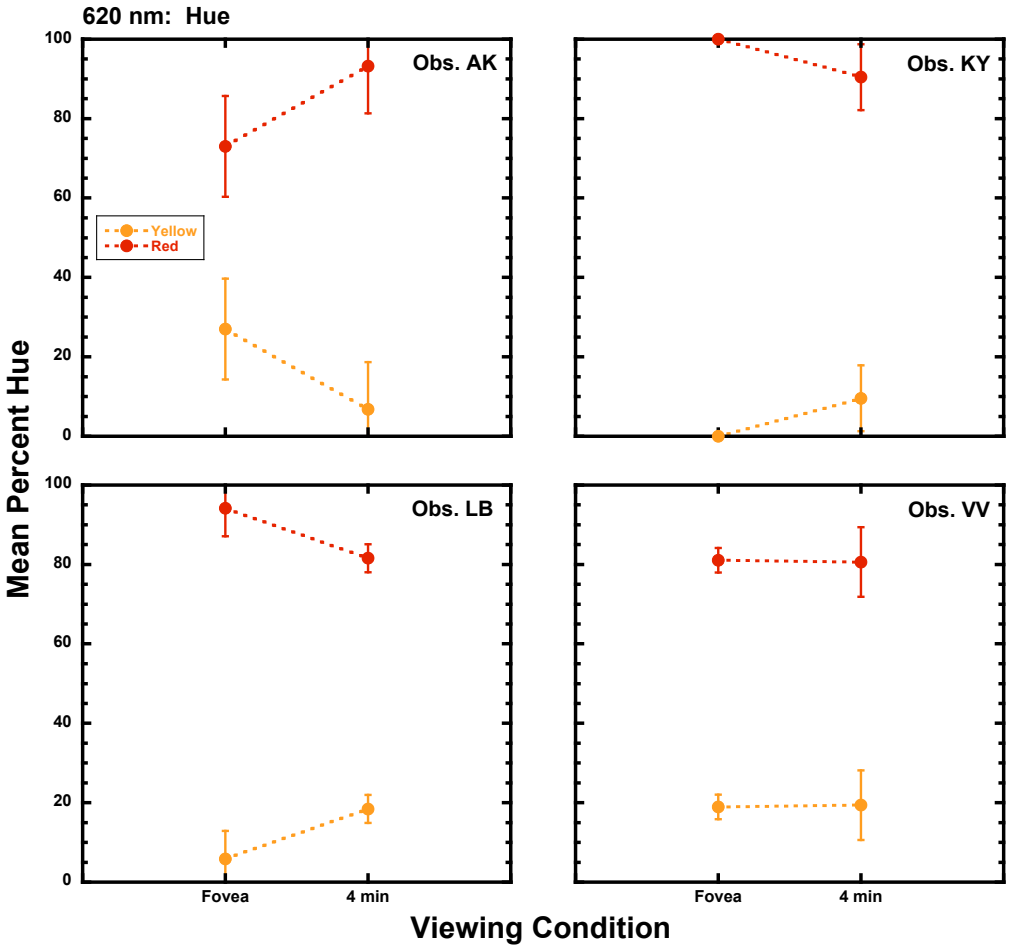

Figure 3.28: Same as **Figure 3.21** except for the 620 nm stimulus.

As shown in **Figure 3.21**, all observers perceived the peripheral 480 nm stimulus as less blue and more green when compared to the fovea. Perceptually, this is equivalent to the 480 nm wavelength being perceived as a longer wavelength in the peripheral retina than in the fovea.

As shown in **Figure 3.22**, three observers reported a larger mean green component for the 500 nm stimulus when this wavelength was viewed in the peripheral

retina, and all observers reported more yellow when viewing this stimulus in the peripheral retina. Consistent with the results for 480 nm, perceptually all observers described the peripheral 500 nm stimulus as a longer wavelength than the foveal stimulus.

As depicted in **Figure 3.23**, three of four observers reported an increase in the perception of yellow in the peripheral retina, thereby increasing the Y:G ratio with retinal eccentricity. Thus this wavelength appeared to be a shorter wavelength in the periphery compared to the fovea. For observer LB there was no real difference in the hue components reported in the fovea and periphery.

As shown in **Figure 3.24**, three observers always perceived the 540 nm stimulus as yellowish-green when it was viewed in the fovea, while observer VV perceived this stimulus to be bluish-green on half the trials and yellowish-green on the other half of the foveal trials, which might be indicative that this wavelength is near her locus for unique green. For three observers the percent yellow was larger in the periphery than in the fovea, and for observers AK and VV this stimulus appeared to be comprised of nearly equal amounts of yellow and green. It is worth noting that the hue percentages reported here have not been scaled to the saturation values, and this wavelength was perceived as desaturated under all conditions, so the actual hue experience for this stimulus was minimal. However, the trend is again for this wavelength to be described as a longer wavelength when viewed peripherally for observers AK, LB and VV, while there is no real difference in the hue components reported by KY in the two viewing conditions.

Figure 3.25 presents responses for the 560 nm stimulus. It should be noted that this wavelength was the least saturated of all the stimuli for all observers under all

conditions, so perceptually the overall hue experiences were minimal. For three of four observers the 560 nm stimulus, presented in the peripheral retina, appeared to have a larger yellow component than when it was viewed in the fovea. Again, this stimulus appeared as a longer wavelength when viewed in the peripheral retina, compared to the fovea.

As seen in **Figure 3.26**, three observers described the 580 nm stimulus as predominantly yellow, with a smaller red component, when this wavelength was viewed in the fovea, while observer KY reported approximately equal amounts of yellow and red under this condition. After 4 min of post-bleach dark adaptation, the peripheral stimulus appeared redder for three observers. Perceptually, KY described this stimulus as a shorter wavelength when viewed in the peripheral retina, compared to the fovea, while for the other three observers, the hue ratios reported for the peripheral stimulus appeared more like a longer wavelength compared to the fovea.

Figure 3.27 shows the mean percentages for yellow and red were essentially the same in both viewing conditions for observers AK and LB for the 600 nm stimulus, a predominantly red light with a smaller yellow hue component. For observers KY and VV, the stimulus also appeared red with a smaller yellow hue component when viewed foveally, but when viewed in the periphery after 4 min of post-bleach dark adaptation, the percentage of red reported increased while the percentage of yellow decreased. The hue ratios for the peripherally viewed stimulus are more similar to a longer wavelength stimulus viewed in the periphery.

Figure 3.28 represents the mean hue scaling data for the 620 nm stimulus. Observer KY described this stimulus as 100% red when viewed in the fovea, while the

other three observers' descriptions indicated a predominantly red stimulus with a smaller yellow hue component. At the 4 min time-point in the periphery, observers' descriptions showed three different trends. Observer VV reported no mean difference in hue perception between the two viewing conditions. Observer AK reported more red and less yellow in this stimulus when it was viewed in the periphery, corresponding to a perceptually longer wavelength in the periphery. Observers LB and KY described this stimulus as containing less red and more yellow when it was viewed in the periphery, which corresponds to a perceptually shorter wavelength in the periphery. The differences in the hue percentages reported by three observers between the two conditions were on the order of 10-20%, not drastically different.

In summary, these comparisons of mean hue scaling responses for these wavelengths in the foveal and 4 min peripheral conditions show a pattern of the hue ratios between hue terms reported in the periphery resembling longer wavelengths. For six of the eight wavelengths, at least three observers' data are consistent with this pattern. For the 600 nm and 620 nm stimuli the pattern does not hold, as only two observers (600 nm) and one observer (620 nm) provided responses consistent with this pattern. The other observers' descriptions indicated no hue change or, for the 620 nm stimulus, two observers reported hue ratios for the stimulus viewed in the periphery that describe a shorter wavelength. Given that the two viewing conditions being compared approximate cone-only color perception, it is surprising that there is a consistent difference in hue perception in these two regions of the retina, as no difference would have necessarily been predicted or expected. Anatomical and physiological differences between the cones found in the fovea and in the peripheral retina, discussed in Chapter

1, as well as the cortical magnification that characterizes the processing of foveal visual information higher in the visual pathway, may be responsible for the difference in color perception in these two retinal areas.

Scotopically Equated Stimuli

To address possible effects attributed to the retinal illuminance level in this study (20 phot tds), which did not equate rod activity across the visible spectrum, two observers repeated the hue scaling study with 480, 500, 520, and 540 nm stimuli equated to 100 scot td. These stimuli are near the peak spectral sensitivity of rod photoreceptors. As noted in Chapter 2, when stimuli were equated to 20 phot td, the M and L cones received a constant level of stimulation with the presentation of each wavelength, while the S cones and rods received stimulation at varying levels, dependent on wavelength. In this second set of presentations, the stimuli were equated to 100 scot td, which means that the rod photoreceptors received a constant level of stimulation for each wavelength, while the three cone photoreceptor types all received varying levels of stimulation for each wavelength. In both cases the S cones never received a constant level of stimulation, but were always stimulated at differing levels for each wavelength. Saturation and hue results from the scotopically equated stimuli are presented in **Figures 3.29-3.36** (dashed lines), with the relevant data from the photopically equated stimuli from **Figures 3.3-3.6** and **3.13-3.16** also included in each figure (solid lines) for comparison. The conversion between 100 scot tds and the corresponding level of phot tds is given in each figure caption.

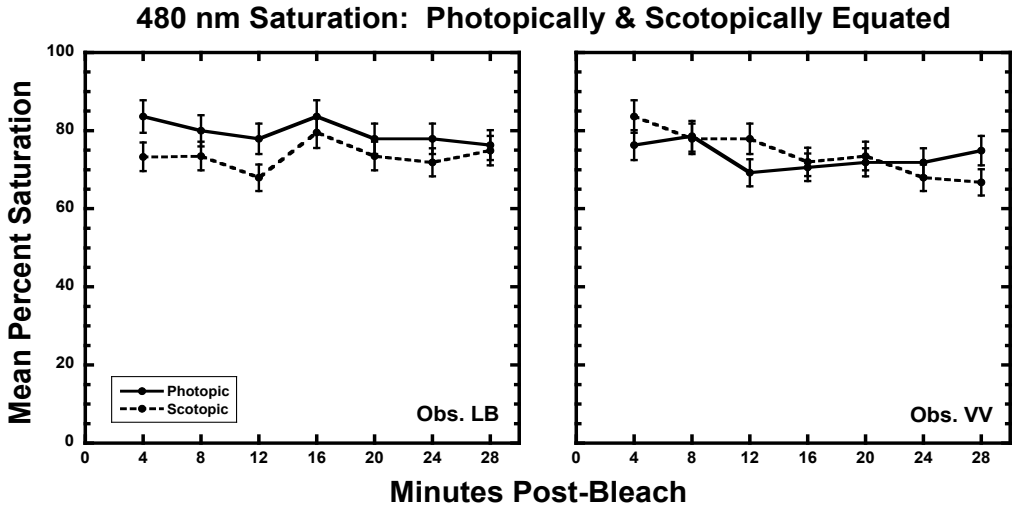

Figure 3.29: Mean percent saturation (+ 1 SD) for two observers is plotted as a function of minutes post-bleach for the 480 nm stimulus. Dashed lines are data from stimuli equated to 100 scot tds (284 phot tds equivalent), and solid lines are data from stimuli equated to 20 phot tds (7 scot tds equivalent). Each panel denotes a different observer.

Figure 3.29 illustrates observers LB and VV's mean saturation percentages for the 480 nm stimulus at the seven post-bleach times examined, under both retinal illuminance conditions. Observer LB reported mean saturation values that were about 10% lower for the first three time-points when this stimulus was scotopically equated, compared to the percentages reported for those time intervals when the stimulus was photopically equated, but overall there was no other difference between the saturation percentages for this wavelength under the two retinal illuminance conditions. There was no change in saturation level across time reported for the scotopically equated stimulus, and a very slight (<10%) decrease between the 4 min and 28 min means when the stimulus was equated photopically. For observer VV, the mean values for the 4 min and 12 min time-points, when the stimulus was scotopically equated, were about 10% higher than those reported when the stimulus was photopically equated. There

was a consistent decrease in the mean saturation percentages across time for the scotopically equated stimulus, so that the 4 min mean is about 15% higher than the mean for 28 min. VV reported no change across time when the stimulus was photopically equated. Thus, the pattern of results differs slightly between the two observers on this comparison, but there are no notable within-observer differences in perceived saturation, even though the levels of rod stimulation (100 scot tds vs. 7 scot tds) and M and L cone stimulation (284 phot tds vs. 20 phot tds) are quite different with the two different retinal illuminance levels.

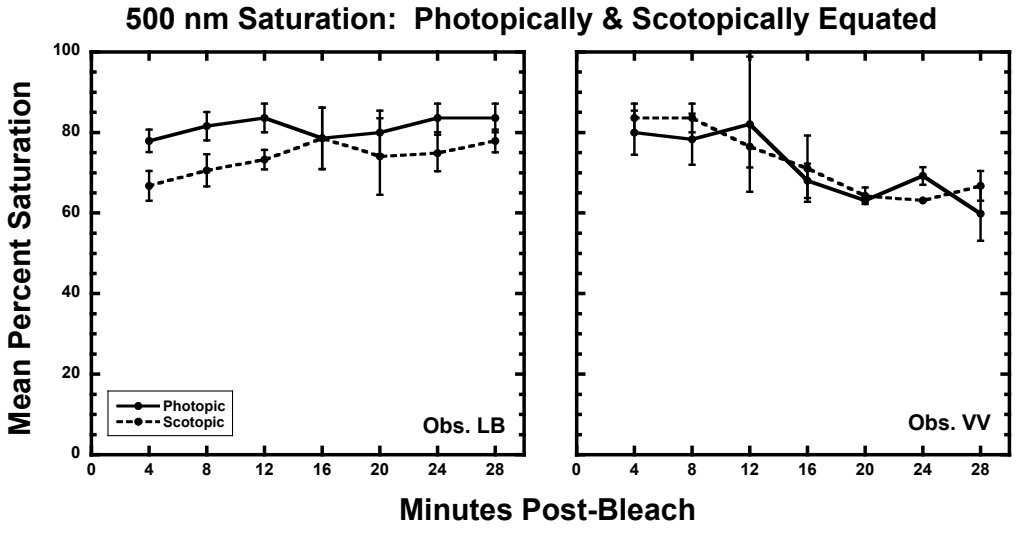

Figure 3.30: Mean percent saturation (± 1 SD) for two observers is plotted as a function of minutes post-bleach for the 500 nm stimulus. Dashed lines are data from stimuli equated to 100 scot tds (151 phot tds equivalent), and solid lines are data from stimuli equated to 20 phot tds (13 scot tds equivalent). Each panel denotes a different observer.

Figure 3.30 presents the mean saturation percentages reported by LB and VV for the 500 nm stimulus at the seven time-points examined, under both retinal illuminance conditions. When equated scotopically, LB described this wavelength as less saturated than when it was equated photopically, during the first three and the last

two time-points. The values from the scotopic condition also show a slight increase with post-bleach time, with a mean difference of more than 10% between the 4 min and 28 min data. In contrast, there was no change across time for this observer when the stimulus was photopically equated. Observer VV's saturation percentages showed a different pattern. There was no difference between the percentages reported in the two retinal illuminance conditions, but the pattern was of decreasing saturation across time under both conditions. The 4 min and 28 min mean saturation percentages differed by about 15-20% in both conditions, again illustrating a different pattern of results between observers, but no notable within-observer differences in saturation perception between retinal illuminance conditions. These data are very similar to those reported for the 480 nm stimulus, and again it is interesting to note that the levels of rod stimulation (100 scot tds vs.13 scot tds) and M and L cone stimulation (151 phot tds vs. 20 phot tds) are very different, yet the reported saturation percentages show no substantial differences.

Figure 3.31 illustrates observers' mean saturation percentages for the 520 nm stimulus at the seven post-bleach times for both retinal illuminance conditions. Observer LB described this wavelength as about 10% more saturated at all times when it was photopically equated, but there was no difference in saturation across time under either condition. For observer VV, the mean saturation percentages were nearly identical under both retinal illuminance conditions, and in both conditions there was a decrease in saturation across time, with the 4 min and 28 min mean saturation values differing by about 20%. Again, the pattern of results reported by the two observers differs for this stimulus, but only LB shows a within-observer difference in saturation perception between the two retinal illuminance conditions, but not what is expected if

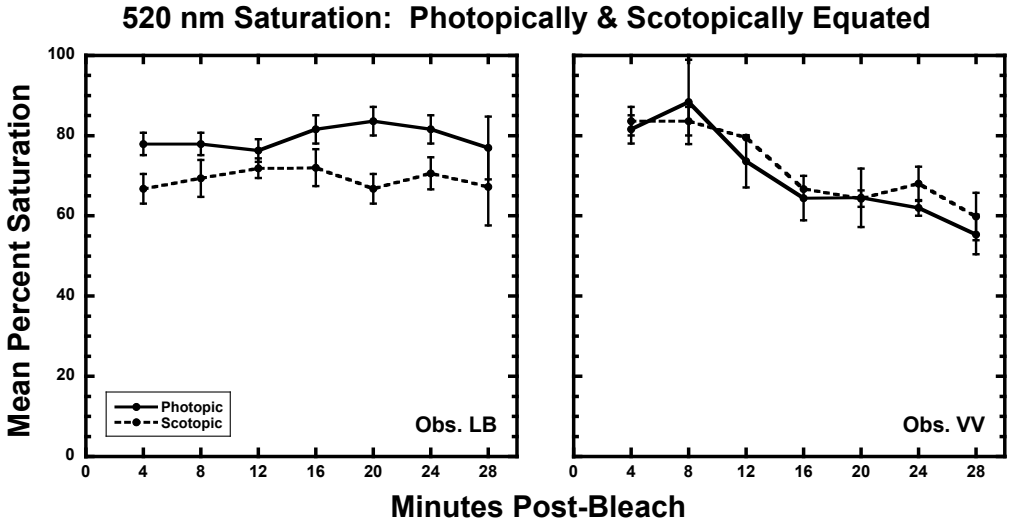

Figure 3.31: Mean percent saturation (+ 1 SD) for two observers is plotted as a function of minutes post-bleach for the 520 nm stimulus. Dashed lines are data from stimuli equated to 100 scot tds (65 phot tds equivalent), and solid lines are data from stimuli equated to 20 phot tds (30.5 scot tds equivalent). Each panel denotes a different observer.

rod input is crucial to saturation perception. First, there is no change in saturation reported across time, as rod input increases. Secondly, the level of rod stimulation in the photopic condition (30.5 scot tds) is only a fraction of the amount of stimulation rods received during the scotopic condition (100 scot tds), yet this observer perceived the stimulus as more saturated at every time point under the photopic condition.

Figure 3.32 illustrates observers' mean saturation percentages for the 540 nm stimulus at the seven time-points examined, under both illuminance conditions. Observer LB's mean saturation percentages were about 5% greater at all time-points in the photopic condition, consistent with the data for the other short-wavelength stimuli. Across time the saturation percentages showed a slight increase under both conditions, with the 28 min mean percentages about 10% greater than the means reported at 4 min. For observer VV, mean percentages reported during the first three time intervals in

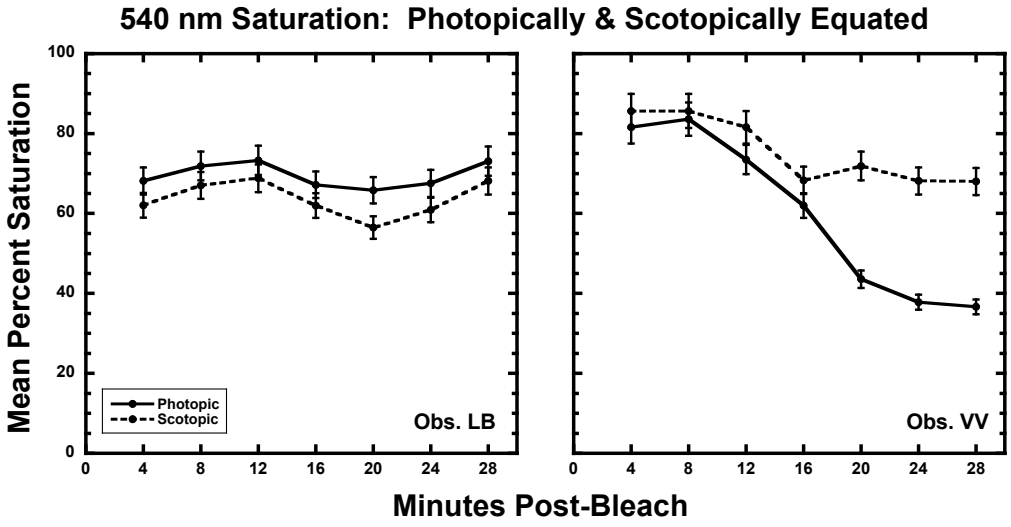

Figure 3.32: Mean percent saturation (± 1 SD) for two observers is plotted as a function of minutes post-bleach for the 540 nm stimulus. Dashed lines are data from stimuli equated to 100 scot tds (34 phot tds equivalent), and solid lines are data from stimuli equated to 20 phot tds (59 scot tds equivalent). Each panel denotes a different observer.

both conditions were about the same, but in the photopic condition there was a more dramatic decrease in the saturation values during the last four time-points than in the scotopic condition. VV's pattern of results was of decreasing saturation across time, but the difference between the 4 min and 28 min values in the scotopic condition was about 15%, while in the photopic condition, the difference was on the order of 40%. It is curious that while this saturation comparison is the only one that showed a notable difference within an observer's data, the relative levels of rod and cone stimulation here are the least disparate of all four comparisons (i.e., 100 vs. 59 scot tds, and 34 vs. 20 phot tds).

In summary, the main conclusion that can be drawn from the comparisons in the preceding four figures is that there were some inter-observer differences, but only one notable intra-observer difference in saturation percentages for the two conditions.

Overall observer LB described the stimuli as less saturated when they were scotopically equated, but in general the pattern of results with post-bleach times was the same across the two conditions. For observer VV, the mean saturation percentages were very similar across conditions, with a tendency for the stimuli to appear more saturated when they were scotopically equated. VV's pattern of results was of decreasing saturation across time, and the magnitude of the decrease was greatest for the 540 nm stimulus when photopically equated. Overall, holding the level of rod illuminance constant while cone stimulation levels varied did not appear to correlate with a clear difference in the mean saturation values for these wavelengths.

Hue

Figure 3.33 illustrates observers LB and VV's mean hue percentages assigned to the 480 nm stimulus at the seven post-bleach times, for both retinal illuminance conditions. Only observer LB shows a difference between the photopically and scotopically equated stimulus across time. For example, LB reported a green hue component at six of the seven time-points when the stimulus was equated photopically, but under the scotopic condition a green hue component was only reported at 4 min post-bleach. In the scotopic condition the hue percentages showed no change across time from 8 min to 28 min, while in the photopic condition there was more variability in reports of red and green hues. LB described this stimulus as reddish-blue on all trials when it was equated scotopically, but as both reddish-blue and greenish-blue on various trials across the time-course when it was equated photopically. Observer VV reported lower blue and higher green hue percentages (about 15%) during the first three time intervals when viewing the photopically equated stimulus, but at 28 min the

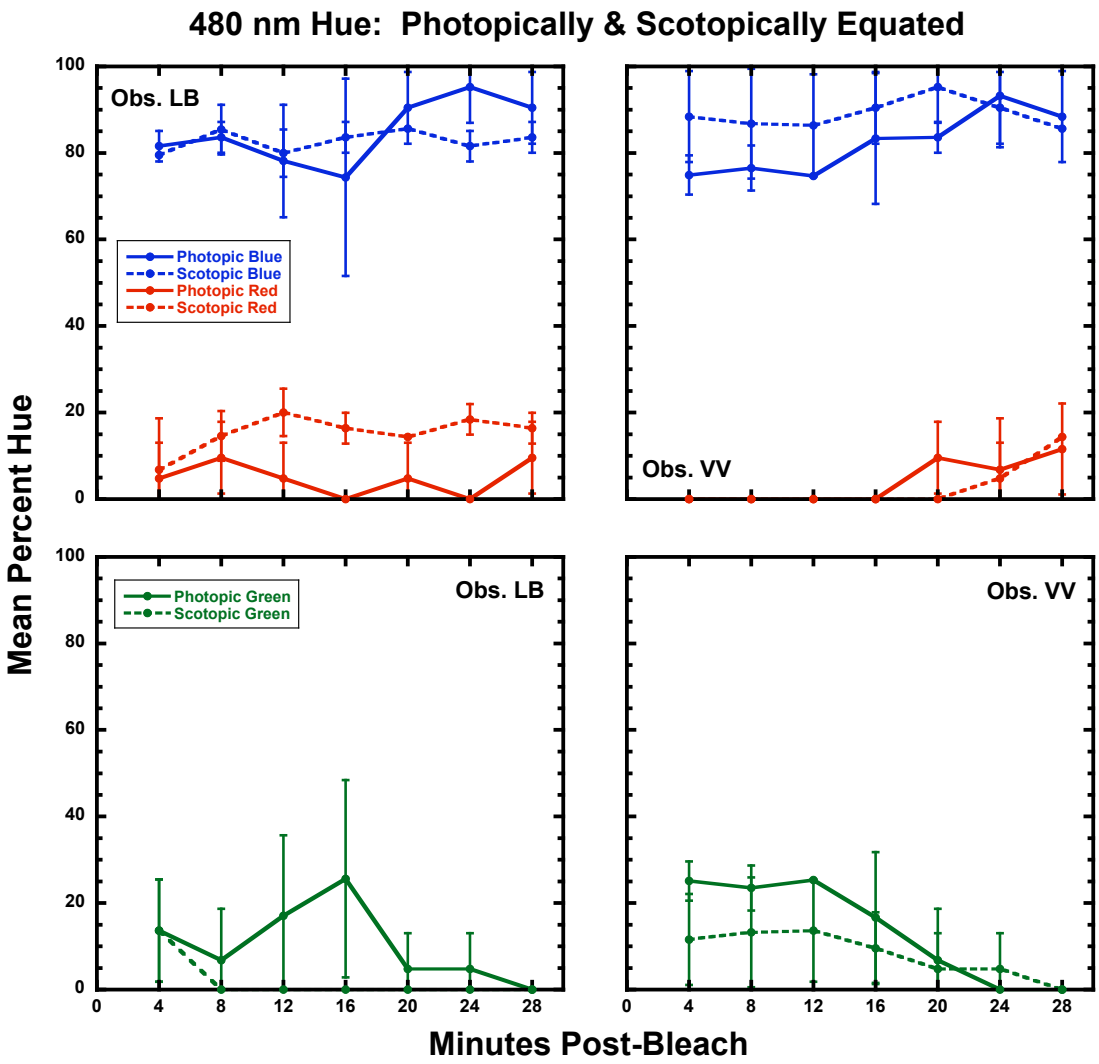

Figure 3.33: Mean percent hue (± 1 SD) for two observers is plotted as a function of minutes post-bleach for the 480 nm stimulus. Dashed lines are data from stimuli equated to 100 scot tds (284 phot tds equivalent), and solid lines are data from stimuli equated to 20 phot tds (7 scot tds equivalent). Each column of panels denotes a different observer.

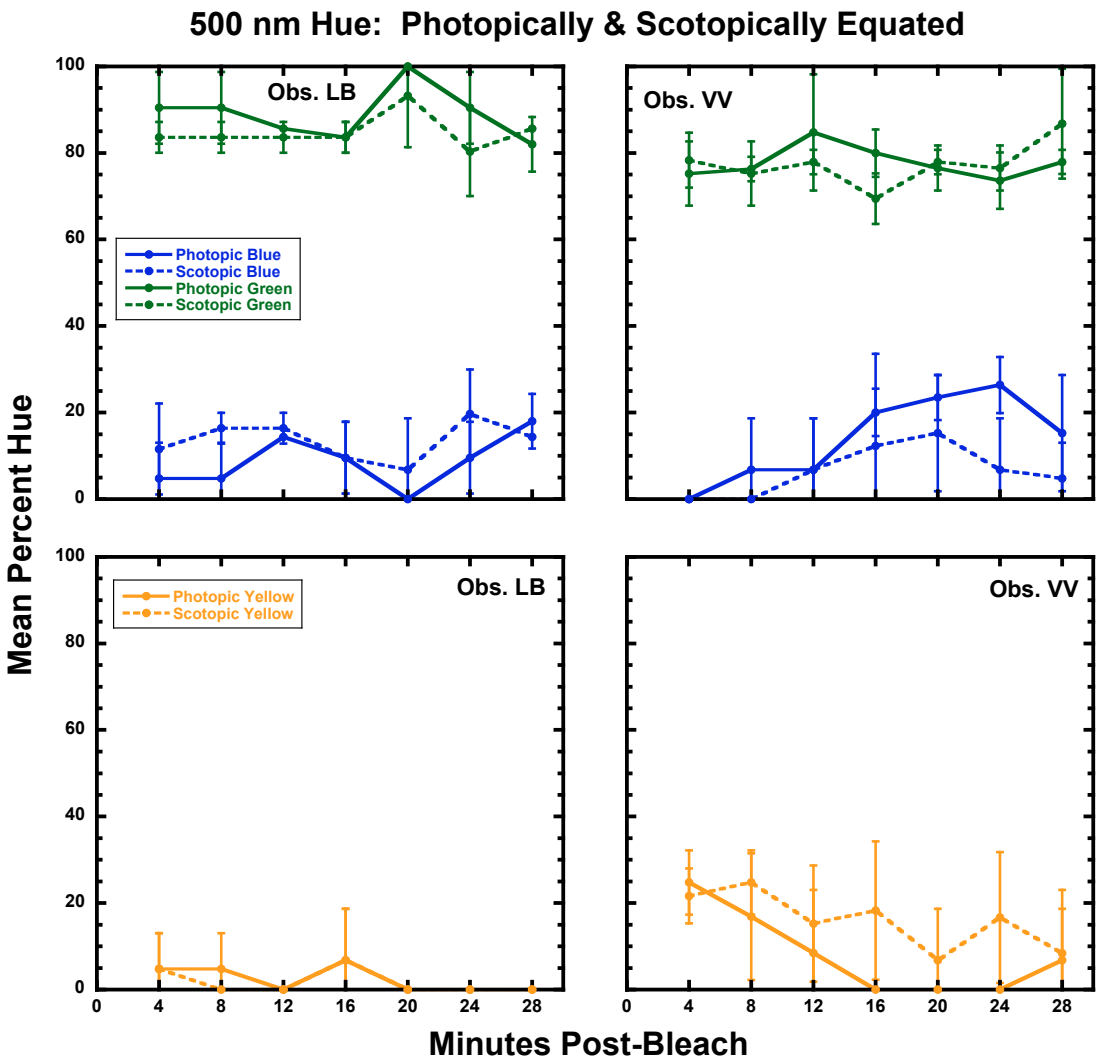

Figure 3.34: Mean percent hue (± 1 SD) for two observers is plotted as a function of minutes post-bleach for the 500 nm stimulus. Dashed lines are data from stimuli equated to 100 scot tds (151 phot tds equivalent), and solid lines are data from stimuli equated to 20 phot tds (13 scot tds equivalent). Each column of panels denotes a different observer.

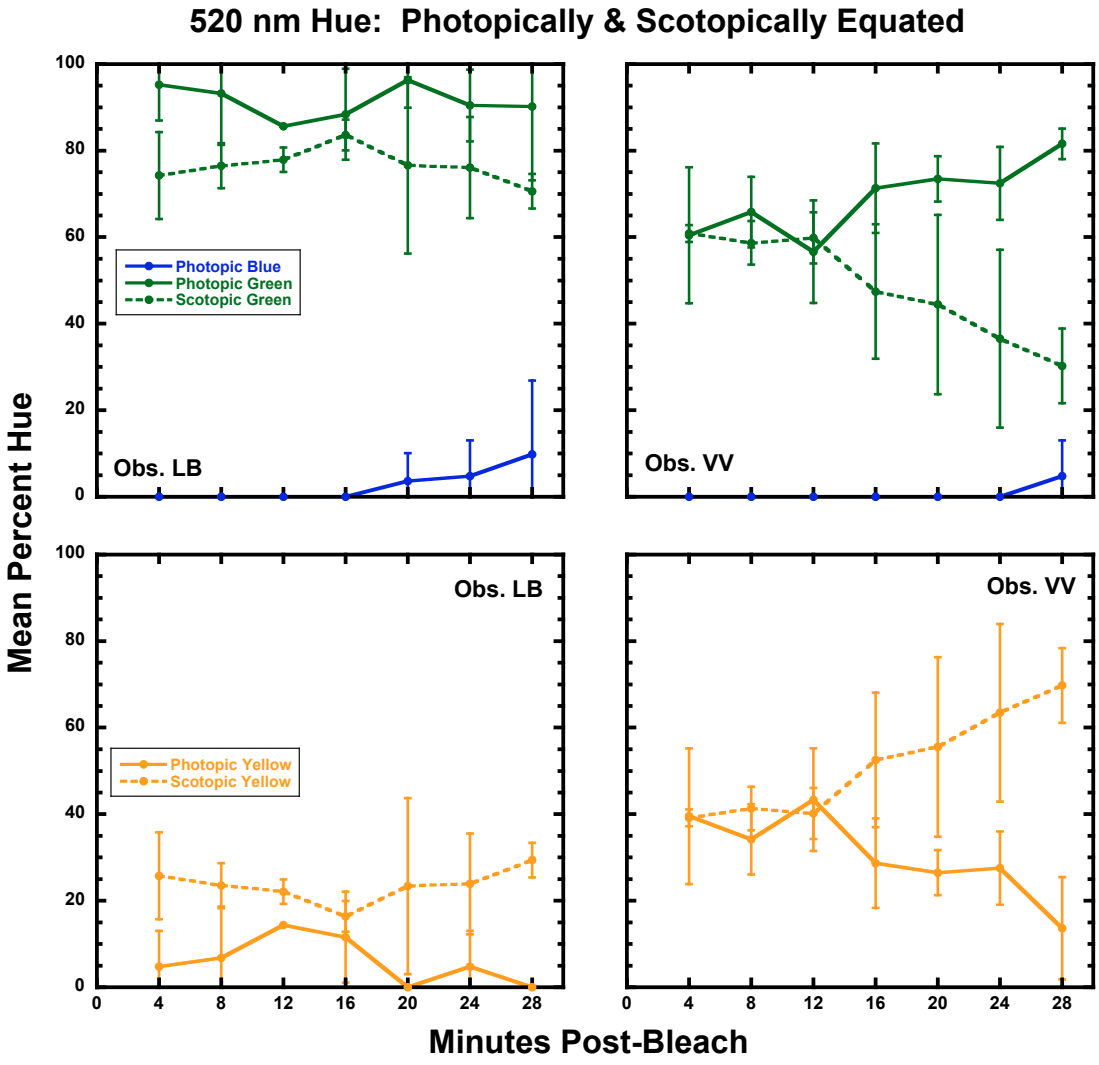

Figure 3.35: Mean percent hue (± 1 SD) for two observers is plotted as a function of minutes post-bleach for the 520 nm stimulus. Dashed lines are data from stimuli equated to 100 scot tds (65 phot tds equivalent), and solid lines are data from stimuli equated to 20 phot tds (30.5 scot tds equivalent). Each column of panels denotes a different observer.

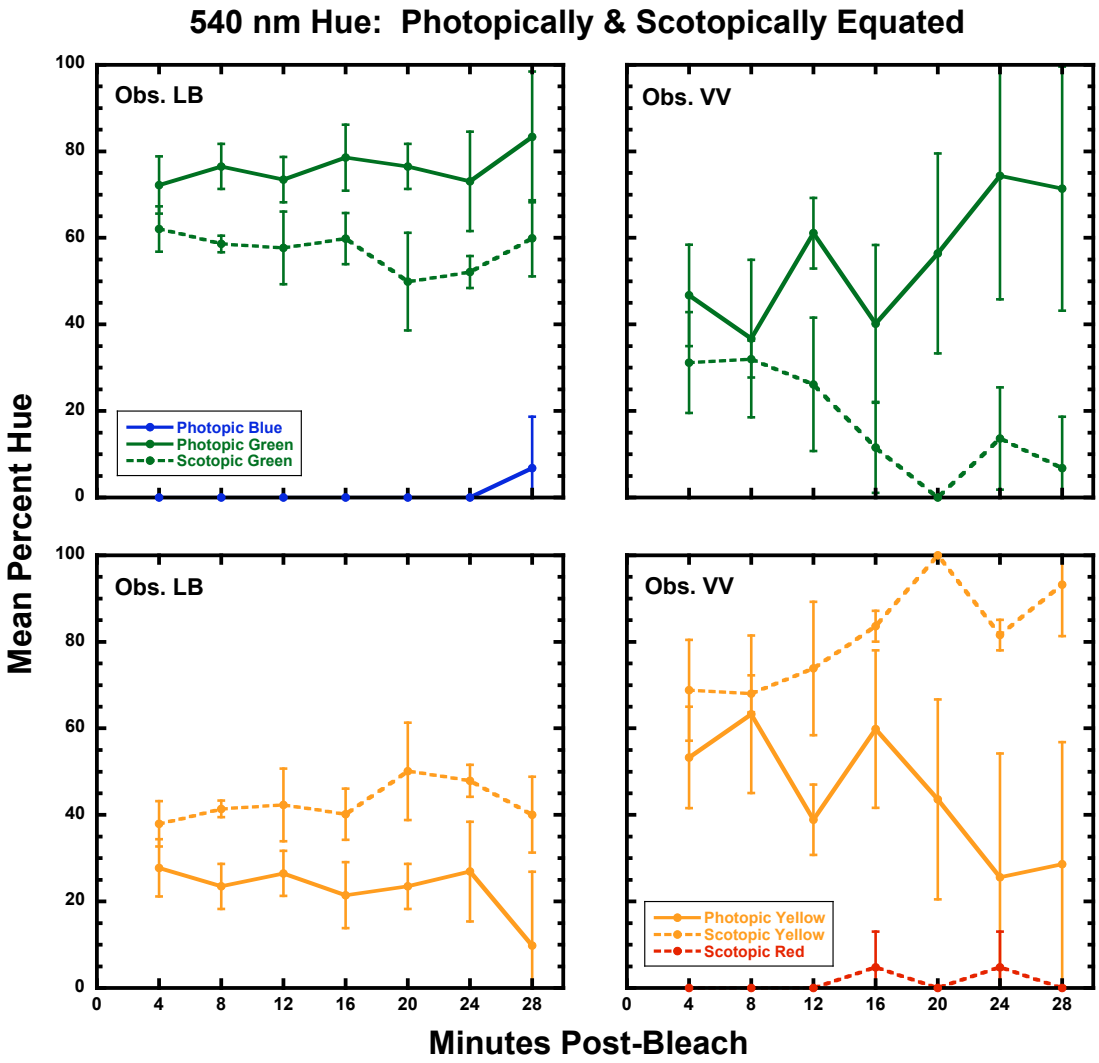

Figure 3.36: Mean percent hue (± 1 SD) for two observers is plotted as a function of minutes post-bleach for the 540 nm stimulus. Dashed lines are data from stimuli equated to 100 scot tds (34 phot tds equivalent), and solid lines are data from stimuli equated to 20 phot tds (59 scot tds equivalent). Each column of panels denotes a different observer.

hue values under both conditions were the same. VV described this wavelength as reddish-blue only during the last three time-points under both conditions, when rod

contribution would be increasing. Thus in both conditions VV's hue data indicate a perceptual shift towards a shorter wavelength stimulus (from greenish-blue to reddish-blue) with post-bleach time.

Figure 3.34 illustrates observers LB and VV's hue descriptions for the 500 nm stimulus at the seven post-bleach times, from both retinal illuminance conditions. There were no notable intra-observer hue differences reported under the two retinal illuminance conditions. Observer LB reported a larger mean percentage of green than VV did on nearly all trials at all time-points. Under both conditions observer VV reported a yellow hue component on some of the trials for all post-bleach times and the mean percentage of blue increased across time; thus the pattern of results also suggests a shift in perception towards a shorter wavelength with post-bleach time, which is more pronounced in the photopic than in the scotopic condition.

Figure 3.35 presents observers LB and VV's mean hue percentages for the 520 nm stimulus across post-bleach time for both retinal illuminance conditions. When the stimulus was scotopically equated, observer LB reported a yellowish-green hue experience that did not change across time. In the photopic condition, LB reported the green hue component to be about 20% greater than in the scotopic condition, and a blue hue component was reported on some trials during the last three time-points, consistent with a perceptual shift towards a shorter wavelength. Under the scotopic condition, observer VV described the stimulus as yellowish-green during the first three time-points, but hue perception shifted towards greenish-yellow as time and rod contribution increased, consistent with a perceptual shift towards a longer wavelength. In the photopic condition, VV described a yellowish-green stimulus that became greener

as time and rod contribution increased. Scotopic vs. photopic illuminance level appears to have an effect on the hue perception of this stimulus, as the between-observer differences in the scotopic condition indicate different patterns of results (no hue change vs. perceptual shift towards a longer wavelength) that are different from the pattern of results when the stimulus was equated photopically (perceptual shift towards a shorter wavelength for both observers).

In **Figure 3.36** mean hue percentages for the two observers (LB and VV) are shown for the 540 nm stimulus at the seven post-bleach times for both retinal illuminance conditions. This stimulus was described as yellowish-green (about 60% green and 40% yellow) by observer LB under the scotopic condition, with no change in hue perception across time. Under the photopic condition, LB also described the stimulus as yellowish-green at all time-points, but there was more green and less yellow than the percentages reported under the scotopic condition (70% green and 30% yellow). In the scotopic condition observer VV described this wavelength as predominantly yellow. During the first three time-points there was a green hue component, and no change in the hue percentages. Beginning at 16 min the percentage of yellow reported increased, and a smaller component of either green or red was reported. This is consistent with a perceptual shift to a longer wavelength with increasing time and rod input. Under the photopic condition, VV reported highly variable percentages of yellow and green at all time-points, and there was no identifiable pattern of change in hue perception across time. Once again there were large inter-observer differences in the hue percentages reported, as well and intra-observer differences in perception of hue under the two retinal illuminance conditions. For LB this wavelength

appeared perceptually shorter (more green, less yellow) under the photopic condition, but there was no hue change across time in either condition. This is similar to LB's results for the 520 nm stimulus. VV's hue percentages are also consistent with a perceptually shorter wavelength in the photopic condition, with only green and yellow components used to describe the stimulus, while there were larger percentages of yellow, and on some later trials, red hue components detected, when the stimulus was scotopically equated. VV described the 560 nm stimulus as a longer wavelength (less green, more yellow, some red, no blue), compared to LB's hue descriptions under both retinal illuminance conditions.

In summary, there were small intra-observer hue differences reported for the 480 and 500 nm stimuli between the two retinal illuminance conditions. There were greater, more interesting differences in the hue percentages reported in the two retinal illuminance conditions for the 520 and 540 nm stimuli for both observers. When these wavelengths were scotopically equated, both observers reported less (or no) blue, less green, and more yellow in both wavelengths. The hue reports for these wavelengths are similar to those provided for longer, photopically-equated wavelengths, e.g., VV's hue scaling data for the 520 nm stimulus (scotopically equated) is quite similar to the hue scaling data reported for the 540 nm stimulus (photopically equated). The results of this comparison support the idea that rods alter peripheral color perception in complex ways, but the most obvious thing they illustrate is that there were considerable differences in the hue experiences of these two observers when viewing these stimuli under the different retinal illuminance conditions. It is also important to note that when the stimuli were equated scotopically and viewed, the rods and M and L cones were all

being stimulated at much higher retinal illuminance levels than when the stimuli were equated photopically. Yet there were not dramatic differences in the hue and saturation reports from LB and VV. Thus, no obvious differences in perception can be attributed to the retinal illuminance level chosen, and whether rod or cone stimulation was held constant.

Another factor to consider is the absorption peaks of the different opsins in these photoreceptor classes. Rods are maximally sensitive to wavelengths of light near 500 nm. Thus, we might expect the greatest rod effects across time for the 500 nm stimulus, with the 480 nm and 520 nm stimuli also providing considerable rod stimulation. The 540 nm stimulus, in contrast, would not stimulate rods as much as the shorter wavelength stimuli, but the peak absorption for M-cones is near 540 nm, and thus perception of this stimulus might be primarily a function of M-cone activity. The most notable changes in perception across time, for this subset of stimuli, were reported by VV for the hue of the 520 nm stimulus, and for saturation and hue of the 540 nm stimulus. But there is reason to suspect that M-cone input may have exerted more influence here than rod input.

These results support the choice to use photopically equated stimuli for the studies described here, as there are no strong differences in blueness or saturation perception reported between the two retinal illuminance conditions, and these are the two aspects of peripheral color vision that have historically been proposed to change with rod input.

CHAPTER 4: UNIQUE AND BINARY HUES RESULTS

These studies compared unique and binary hue loci derived from hue scaling functions with loci measured using a staircase procedure. The derived wavelengths were used to predict the effect of rod input on unique and binary hue loci in the peripheral retina. Like the hue scaling results reported in Chapter 3, the unique and binary hue loci reported here are from the fovea and the peripheral retina, at 10° along the horizontal meridian of the temporal retina. The loci measured with the staircase procedure in the periphery were measured under two different adaptation conditions, bleach and no-bleach, which correspond to the 4 min and 28 min post-bleach times of the hue scaling study.

Unique Hues

Unique hues (UH) are defined physiologically as null points of the yellow/blue (Y/B) and red/green (R/G) opponent color channels. When both portions of the opponent Y/B channel are receiving equal stimulation, they will cancel each other out; thus we never perceive a colored stimulus as simultaneously yellow and blue. In this case a stimulus will only appear red, green, or achromatic (black, gray, or white). The locus of unique green (UG), for example, is thought to be the null point of the Y/B mechanism, when there is neither blue nor yellow perceived in a green stimulus. Psychologically, we might also think of a unique hue as a pure hue, one that does not contain any component of the neighboring spectral hues.

UH Predictions

Using the hue scaling results reported in Chapter 3, predictions for each observer's unique blue (UB), unique green (UG), and unique yellow (UY) loci were identified by determining the wavelength from graphs of the hue scaling functions, at which hues of the opponent color channels crossed over, or were in equilibrium. Because the shortest wavelength presented in the hue scaling study was 480 nm, it was not possible to predict a UB locus in most cases, since the locus of UB generally occurs at wavelengths shorter than 480 nm. Examples of these UH crossover points are shown in **Figure 4.1**, which presents hue scaling functions from observer VV's responses after viewing stimuli in the fovea. Vertical black lines on each graph indicate the equilibrium (crossover) points for the Y/B and R/G mechanisms for observer VV. The predicted locus for VV's UG in the fovea, for example, is 537 nm, as indicated by the vertical black line that marks the crossing over, or equilibrium, of the Y/B color channel in **Figure 4.1**. This process was completed for each observer, for the foveal and 4 min and 28 min post-bleach peripheral data. All of the UH loci wavelengths derived from the hue scaling functions are presented below in **Table 4.1**.

Predicted Rod Effects on UH Loci

Comparing the predicted UH loci from the 4 min (minimal rod input) and 28 min (maximal rod input) time-point data gives an indication of the effect rod input has on UH measurements. Because most of the UB loci were shorter than 480 nm, it is difficult to make predictions about the rod effect except for observers LB and VV. In both cases, the 28 min UB locus is at a longer wavelength than the 4 min UB locus. Thus, it is expected that with the staircase procedure this relationship should be found between

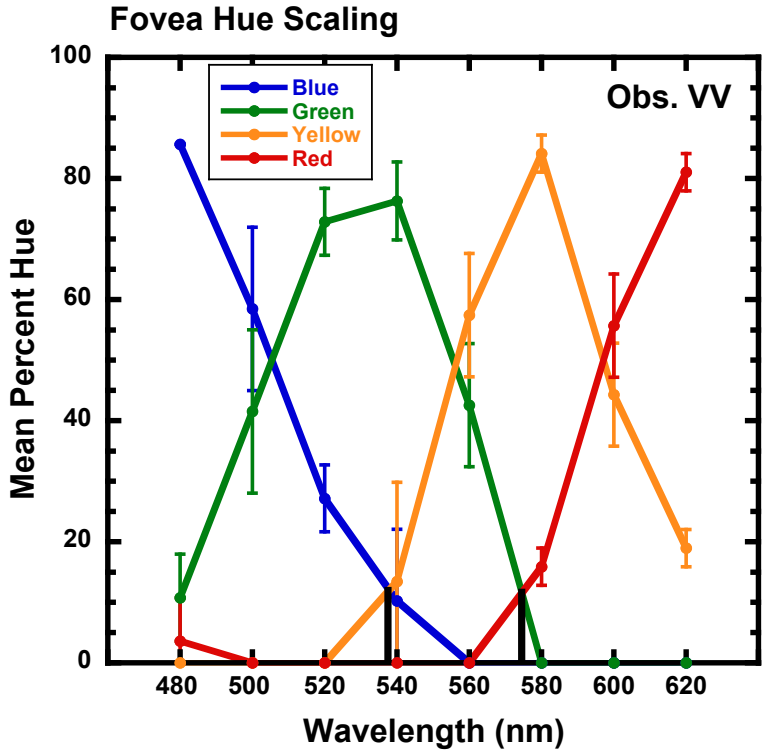

Figure 4.1: Mean hue percentages for eight wavelengths presented to the fovea of observer VV. Null points are indicated by vertical black lines. Error bars represent ±1 standard deviation (SD). UH wavelength values are reported in **Table 4.1**.

Table 4.1: Predicted Unique Hue (UH) loci from crossover points for the four observers in the hue scaling study. All wavelengths are reported in nm.

Observer	Unique Blue			Unique Green			Unique Yellow		
	Fovea	10° Temporal		Fovea	10° Temporal		Fovea	10° Temporal	
		4 min	28 min		4 min	28 min		4 min	28 min
AK	-	-	-	510	495	527	572	568	558
KY	-	-	-	527	499	497	568	564	566
LB	482	-	482	518	500	535	576	570	570
VV	-	-	483	537	494	509	573	554	563

UB loci measured with bleach (minimal rod input) and no-bleach (maximal rod input) conditions for observers LB and VV.

For observer KY the UG locus is predicted to be the same under the bleach and no-bleach conditions in the peripheral retina, right around 498 nm. For the other three observers the UG locus, computed from the 28 min function, when rods are contributing, is predicted to be a longer wavelength than the 4 min locus. Thus, the expectation when directly measuring UG with the staircase procedure is that three of four observers will show UG loci at longer wavelengths for the no-bleach condition than the bleach condition.

The computed UY loci from the hue scaling results are approximately the same for KY and LB, while the UY locus from the 28 min function for AK is shorter than the locus computed from the 4 min hue scaling function. UY loci from VV, however, show the opposite pattern from AK. The 28 min UY locus is longer than the 4 min locus.

Besides the effect of rods on UH loci, the loci measured in the fovea can be compared to loci derived from the 4 min hue scaling functions. Since rod input is minimal at 4 min post-bleach, this permits a comparison of whether cones are operating in a similar manner at both retinal locations. It should be noted at both retinal locations there is probably some rod input, since the stimulus size (2.55°) in the fovea is greater that the central rod-free area, and stimuli are above rod threshold at 4 min post-bleach in the peripheral retina. LB shows that the foveal UB locus is longer than the 4 min post-bleach locus; unfortunately, no other relationships can be noted since the UB loci were at shorter wavelengths (<480 nm) for both the fovea and 4 min post-bleach conditions for the other three observers. For all four observers the foveal UG locus is at

a longer wavelength than the 4 min post-bleach locus in the peripheral retina, and a similar pattern is observed for UY, although for three of the observers the shift is only 4-6 nm.

UH Loci Results

For each staircase, a mean was taken of the observer's last four response reversals (staircase mean), and then a mean was taken of the two means produced from each double-random staircase (trial mean). Each observer had three to four trial means for each UH locus for each retinal location and adaptation (bleach and no-bleach) condition. Means taken of those values produced the overall means and standard errors of the means (SEMs) that are reported for each observer's UH loci, and provided in Appendix B.

The criterion used to determine if there is a difference between UH loci is $\pm$ 3 nm difference or greater, with non-overlapping error bars. This criterion was selected based on results from the literature regarding wavelength discrimination in the fovea and in the peripheral retina (Stabell & Stabell, 1984), as well as between-session variability of unique hue loci (Nerger et al., 1995).

The first set of UB, UG, and UY hue loci were measured for observers AK, KY, LB, and VV immediately following the hue scaling sessions. Stimuli of two different diameters (1° and 2.55°) were viewed in the fovea for each UH in this first set of measurements, while stimuli viewed in the peripheral retina were 2.55° in diameter for all measurements. In **Figures 4.2-4.4** the UH loci derived from the hue scaling functions (black markers) are compared to UH loci measured with the staircase procedure (blue markers). "Temp. Bleach" in the figures refers to the bleach condition

from the staircase procedure, and 4 min post-bleach period from the hue scaling procedures. Similarly, “Temp. No-Bleach” refers to the no-bleach condition from the staircase procedure, and the 28 min post-bleach period from the hue scaling procedure. Each panel represents a different observer.

Unique Blue

Shown in **Figure 4.2** are the UB loci. As indicated in **Table 4.1**, UB loci could not be derived for all observers from the hue scaling functions. For both observers LB and VV, UB loci in the no-bleach condition were longer wavelengths than UB loci measured in the bleach condition. Similarly, LB’s foveal UB locus was longer than the peripheral locus measured under the bleach condition. KY’s UB loci values from the staircase procedure showed the same pattern as those of LB and VV when comparing the two peripheral conditions; and similar to LB, both VV and KY showed the foveal UB locus at a longer wavelength than the 4 min post-bleach locus. While the relative relationship between conditions is similar in the hue scaling-derived values and staircase values for LB (the only observer to have values from each procedure), the absolute value of the loci wavelengths differs by about 8 nm, much more than the $\pm$ 3 nm criterion for loci to be similar.

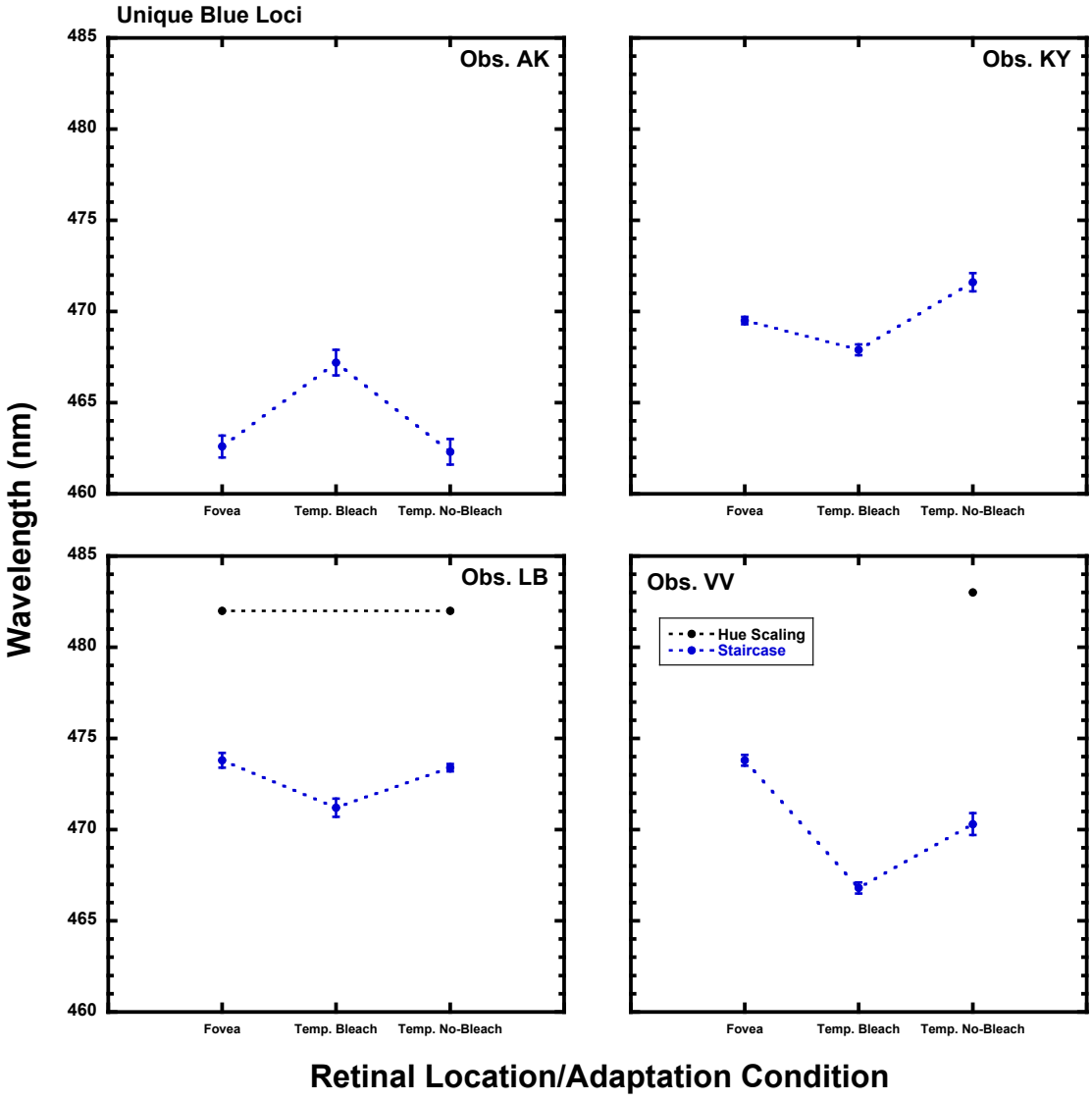

Figure 4.2: Mean derived UB loci from hue scaling (black markers) and mean UB loci from the staircase procedure (blue markers) are specified as a function of experimental condition for each observer. Error bars represent ± 1 standard error of the mean (SEM). All stimuli were 2.55° in diameter.

Unique Green

Shown in **Figure 4.3** are the UG wavelengths predicted from the hue scaling results (black markers), and the UG loci measured with the staircase procedure (green markers). Three observers show that the no-bleach loci are longer than the bleach loci in the peripheral retina, although the difference between the loci is greater with values derived from the hue scaling functions. All four observers show the same pattern between the fovea and the bleach conditions, i.e., the foveal locus is longer than the bleach condition locus. In general, the loci derived from the hue scaling functions are longer than those measured with the staircase procedure.

Unique Yellow

Shown in **Figure 4.4** are the UY wavelengths measured with the staircase procedure, with stimuli presented to the fovea, and to the temporal retina under a bleach and a no-bleach condition. AK and LB showed the same pattern of results between the bleach and no-bleach conditions, with both the derived values and those measured with the staircase procedure. For VV and KY, the pattern of results from the derived loci were opposite to those measured with the staircase procedure. In comparisons of the foveal and bleach condition loci, three of the four observers showed the same pattern from both procedures: foveal loci are at longer wavelengths than peripheral bleach condition loci. In some cases, the values from the two procedures were quite similar to each other, but in other instances the results were similar to those found for UB and UG, i.e., the absolute values of the loci differed.

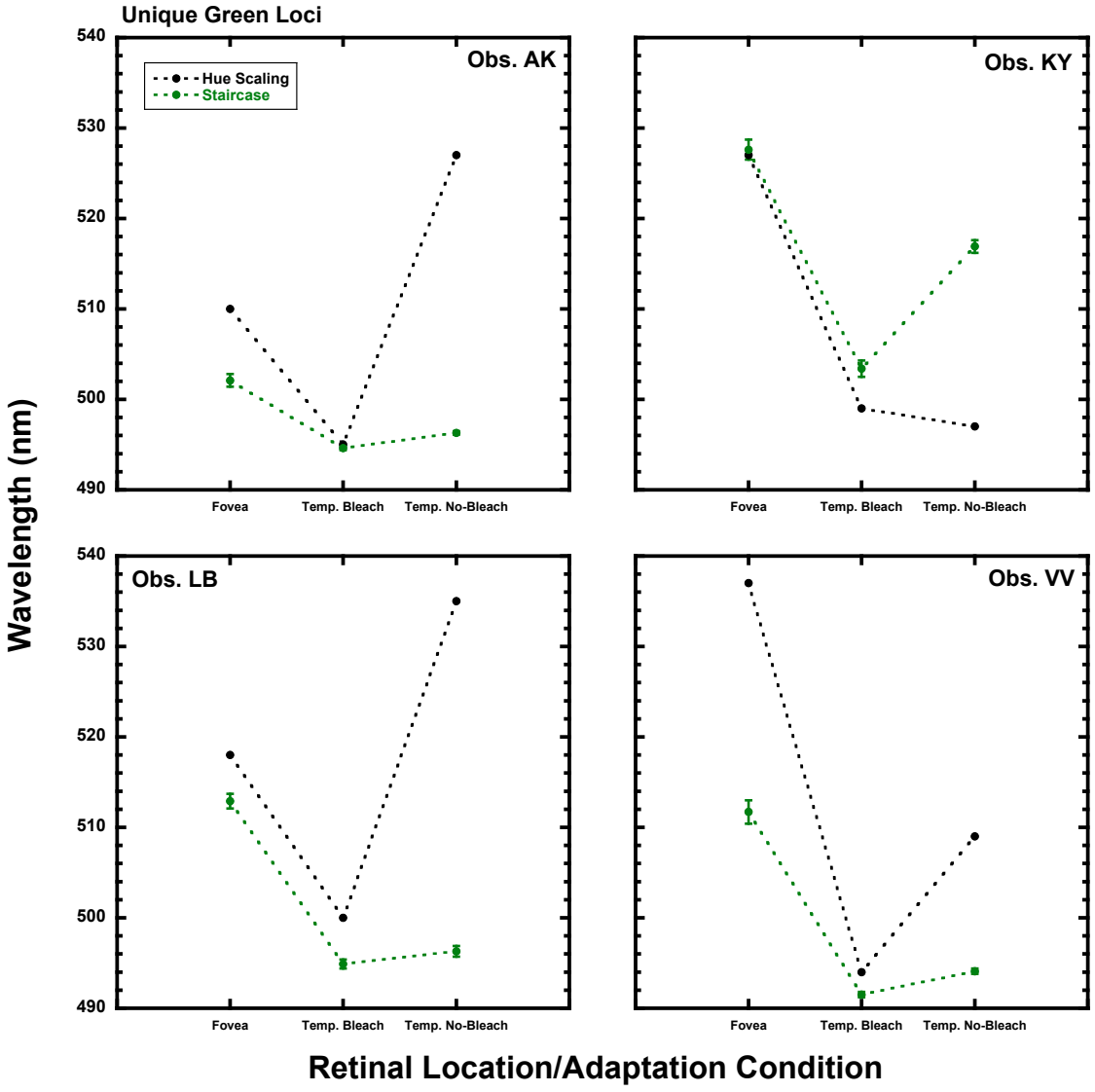

Figure 4.3: Mean derived UG loci from hue scaling (black markers) and mean UG loci from the staircase procedure (green markers) are specified as a function of experimental condition for each observer. Error bars represent ± 1 standard error of the mean (SEM). All stimuli were 2.55° in diameter.

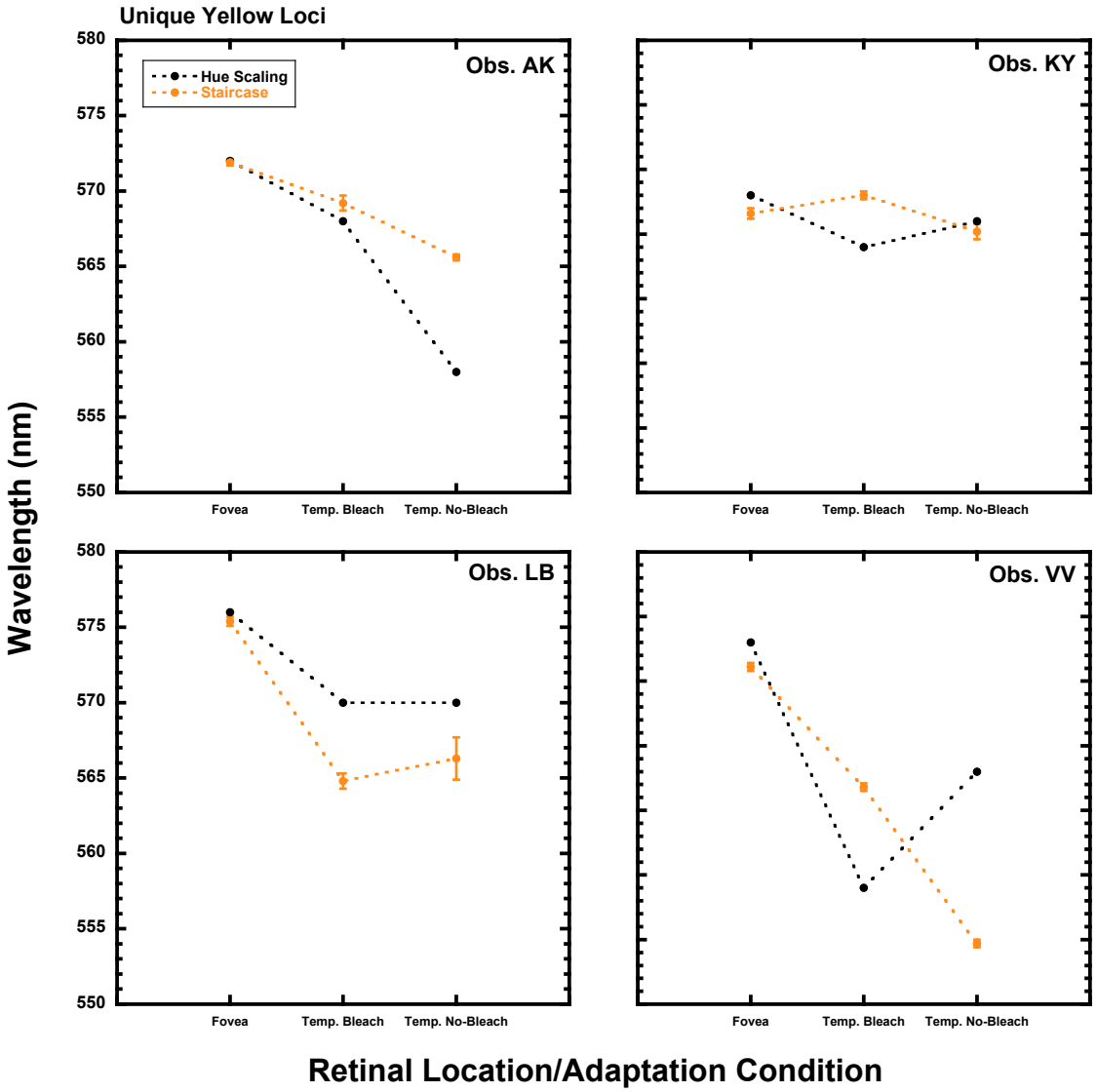

Figure 4.4: Mean derived UY loci from hue scaling (black markers) and mean UY loci from the staircase procedure (yellow markers) are specified as a function of experimental condition for each observer. Error bars represent ± 1 standard error of the mean (SEM). All stimuli were 2.55° in diameter.

Effect of Stimulus Size on Foveal UH Loci

As discussed for the UH results figures above, the presentation of a 2.55° stimulus to the fovea would most certainly overlie areas of the retina containing rod photoreceptors, as well as more S cones, which are extremely sparse in the fovea. A 1° stimulus was also viewed in the fovea, which was expected to impinge on no or very few rod photoreceptors. Thus, a comparison of the UH loci measured by the staircase procedure for these two different stimulus sizes in the fovea could give additional information about the effects of rod input on these loci measurements. These comparisons are shown in **Figures 4.5-4.7** below, with each panel representing a different observer. An asterisk in the figure indicates that the UH loci measured with the two stimulus sizes differed by more than 3 nm.

Unique Blue

For KY and VV the UB locus measured with a 1° stimulus (minimal rod input) was a shorter wavelength than the UB locus measured with the 2.55° stimulus (rod input). For AK the pattern was reversed, while for LB the UB loci were within 3 nm of each other. This supports the idea of rod input changing color perception, as measured by a UH determination, but there is no consistent, across-observer pattern of change.

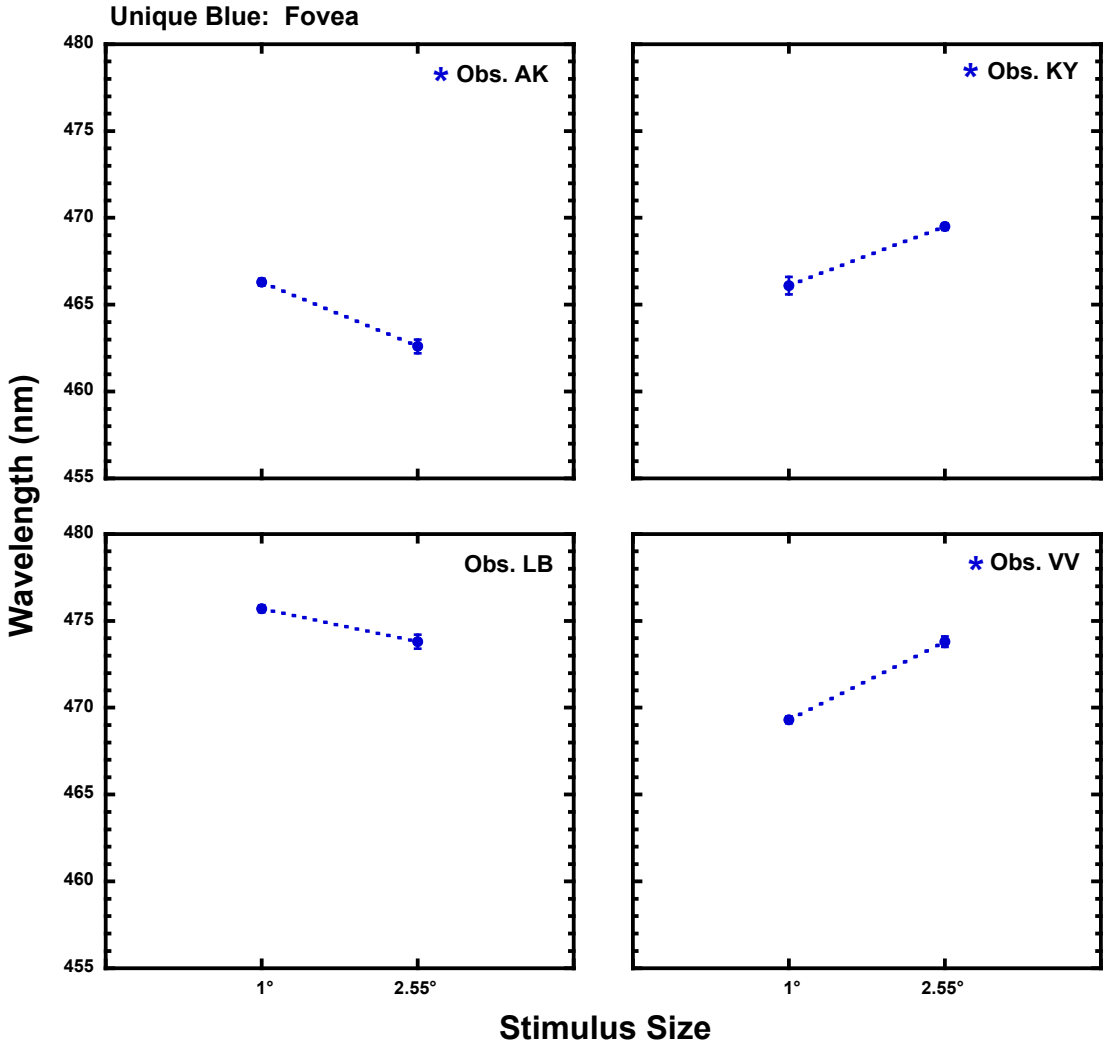

Figure 4.5: Mean UB loci (± 1 SEM) measured in the fovea for four observers with two different stimulus sizes. Asterisk (*) indicates those observers whose loci differed by at least ± 3 nm.

Unique Green

Figure 4.6 below illustrates that the foveal UG loci measured for each observer with two different stimulus sizes differed by more than 3 nm for three of the four observers (indicated by an *). For observers AK and VV the locus with the larger stimulus size was a shorter wavelength than that with the smaller stimulus size, while for observer KY the locus shifted to a longer wavelength with the larger stimulus size. Similar to the UB results, LB again identified UG loci that were within 3 nm of each other in the fovea with the different stimulus sizes. If the UG locus with the smaller stimulus size is thought of as rod-free, and analogous to the UG locus measured in the periphery under bleach condition, then we might expect the difference between the foveal UG loci measured with the smaller and larger stimulus sizes to mirror any differences found between the peripheral bleach condition and no-bleach condition UG loci. As shown in **Figure 4.3** however, there was no (i.e., $\leq$ 3 nm) difference in the two peripheral UG loci for three of the four observers. Observer KY's UG locus in the periphery under the no-bleach condition was a longer wavelength than the bleach condition UG locus, and the same pattern is found between the two foveal UG loci, i.e., the rod-free loci (1° foveal stimulus and bleach peripheral condition) are at shorter wavelengths than the loci which are assumed to have rod input (2.55° foveal stimulus and peripheral no-bleach condition).

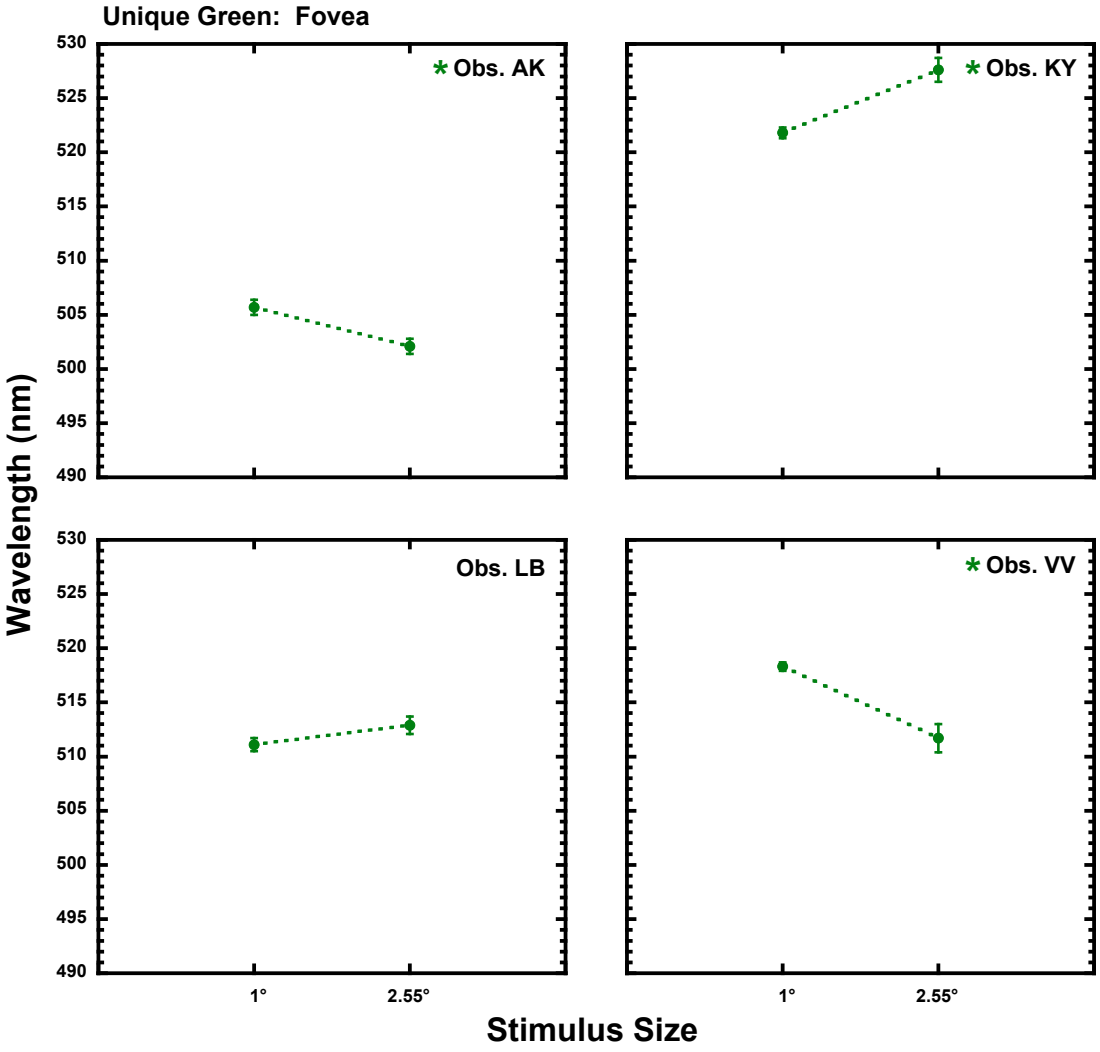

Figure 4.6: Mean UG loci (± 1 SEM) measured in the fovea for four observers with two different stimulus sizes. Asterisk (*) indicates those observers whose loci differed by at least ± 3 nm.

Unique Yellow

Figure 4.7 depicts the foveal UY loci measured for each observer with two different stimulus sizes. There are essentially no changes in the locus of UY for the two different stimulus sizes for any observer. These UY loci measurements offer no support for the influence of rods on UY perception.

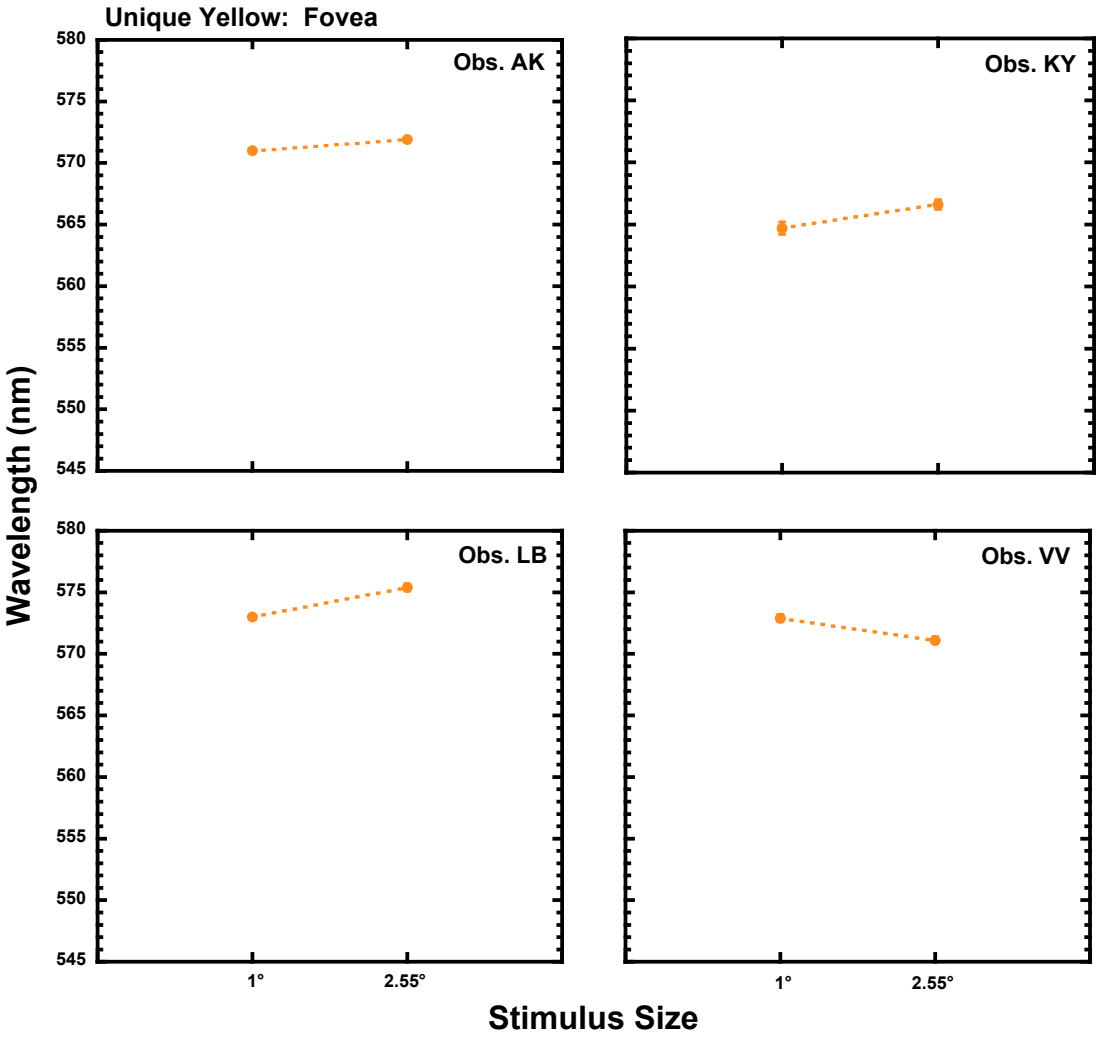

Figure 4.7: Mean UY loci (± 1 SEM) measured in the fovea for four observers with two different stimulus sizes. For each observer, the UY loci for the two stimulus sizes were within 3 nm of each other.

Second Set of UB Loci

A second set of UB loci were measured for observers JN, LB, and VV at the time that the binary hue measurements, described below, were made. During the second set of UB measurements, only a 1° stimulus was viewed in the fovea, while the stimulus size was 2.55° in the periphery. Thus, both the foveal UB loci and the peripheral loci measured under the bleach condition may be thought of as relatively rod-free. **Figure 4.8**, below, depicts the second set of UB measurements. The UB loci measured in the peripheral retina under the two adaptation conditions for all observers did not shift, although the observers differed from each other in the actual value of UB loci, indicating no rod effect on these peripheral UB loci. The UB locus measured for each observer in the fovea differed by more than 3 nm from the loci measured in the peripheral retina. For observer JN the peripheral UB loci were at a shorter wavelength than the foveal locus, but for observers LB and VV the peripheral UB loci were at a longer wavelength.

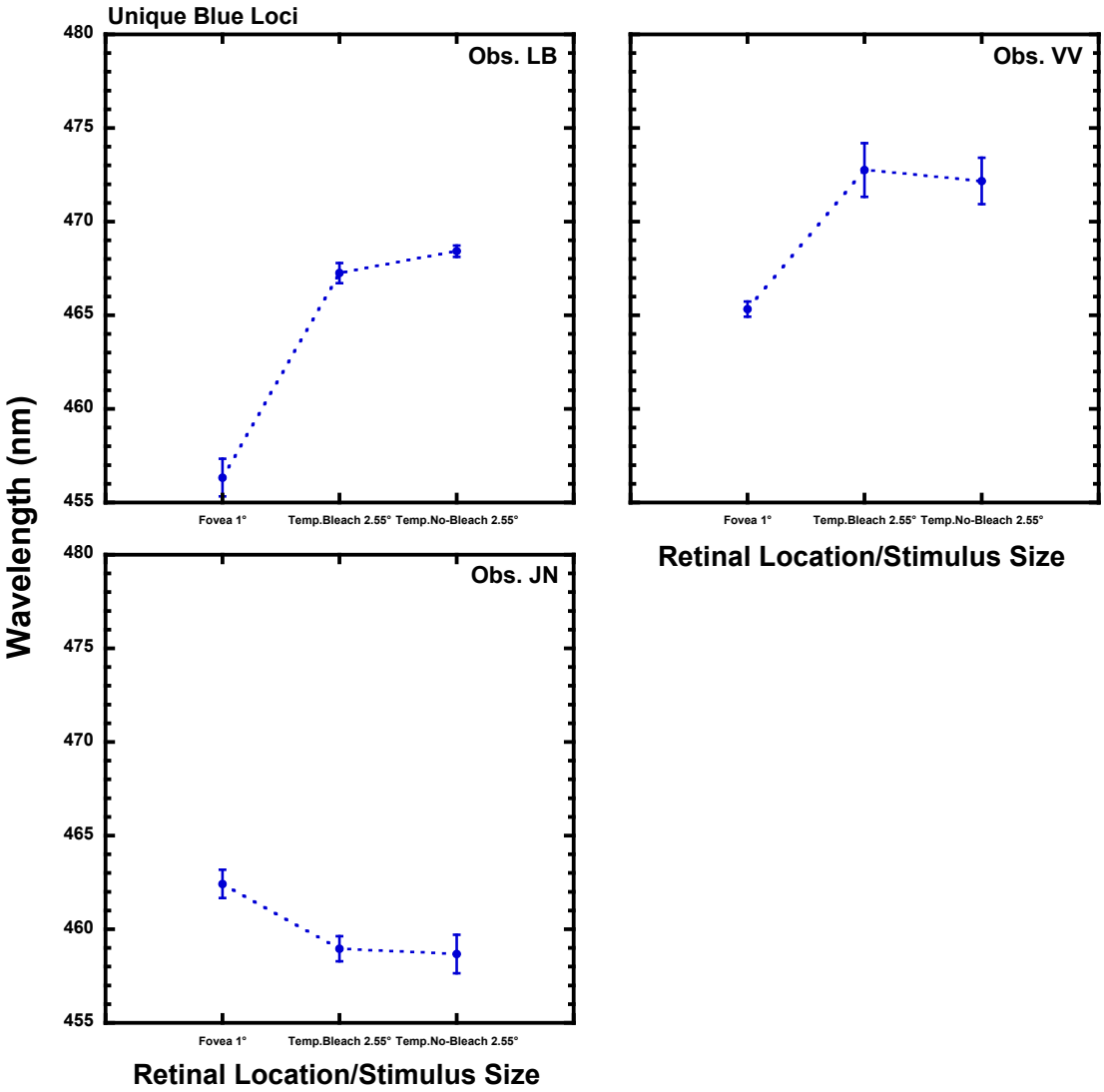

Figure 4.8: Mean UB loci (± 1 SEM) measured in the fovea and the peripheral retina for three observers. The stimulus viewed in the fovea was 1°, while the stimulus viewed at 10° temporal eccentricity was 2.55°.

Figure 4.9, below, presents LB's and VV's UB loci (from **Figure 4.2** and **Figure 4.8**) measured at two different time points, which were about two years apart. Five of the six comparisons of UB loci measured under identical conditions vary greatly, with shifts that exceed 3 nm, and with a shift of 19 nm in the most extreme case. Only VV's

peripheral no-bleach loci are the same from these two sets of UB loci. Except for the comparison between LB's bleach and no-bleach UB loci, the pattern of results between conditions also varied from the two time points.

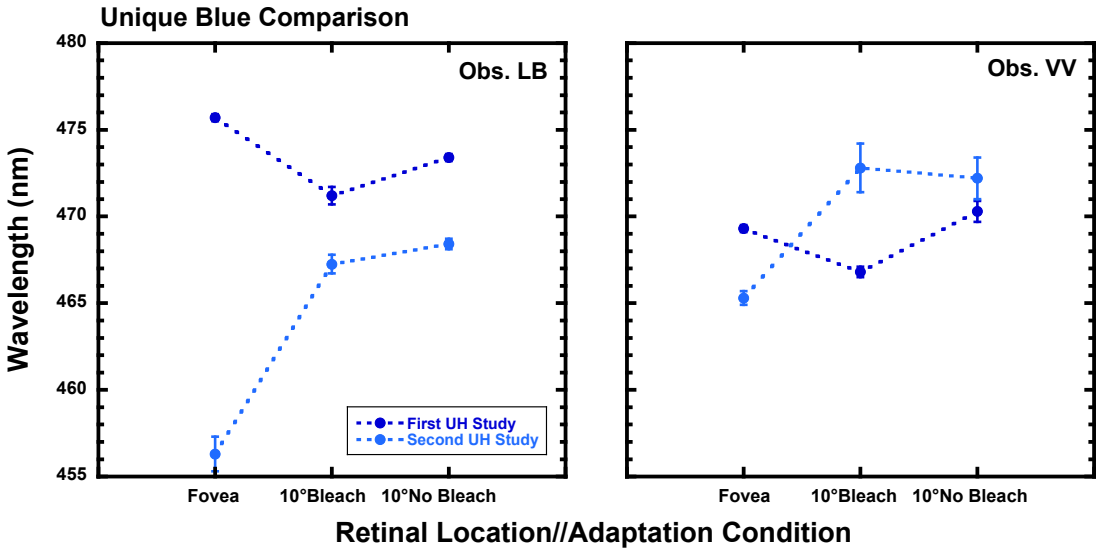

Figure 4.9: Comparison of mean UB loci (± 1 SEM) for observers LB and VV from the two sets of studies. The stimulus viewed in the fovea was 1°, while the stimulus viewed at 10° temporal eccentricity was 2.55°.

The present results suggest that UB at least, and perhaps all of the UHs, are subject to change across time. Since UG and UY loci were not measured at the second time point, a similar comparison between loci measured at two time points cannot be made.

Binary Hues

Binary hues are perceived as being equal mixtures of two neighboring spectral hues, and thus each contains input from both the Y/B and R/G opponent color channels. Four binary hues, red/blue (R/B), blue/green (B/G), green/yellow (G/Y), and yellow/red

(Y/R), were measured using a staircase method and were derived from the hue scaling functions of LB and VV. The binary R/B hue could not be derived from the hue scaling functions, since the shortest wavelength in that study was 480 nm. Observer JN did not participate in the hue scaling study, so no derivations of her binary hue loci were possible, but they were measured with the staircase procedure as an additional source of possible information about the influence of rod photoreceptor input on peripheral color perception.

Binary Hues Predictions

As shown in **Figure 4.10** below, the hue scaling functions for the foveal data (and the peripheral data from the bleach and no-bleach conditions, data not shown) were used to identify the wavelengths at which equal amounts of neighboring hues were reported by observers LB and VV. Black vertical lines indicate the wavelengths at which equal amounts of neighboring hues were reported by VV. All of the wavelengths identified by this method are listed in **Table 4.2**, below.

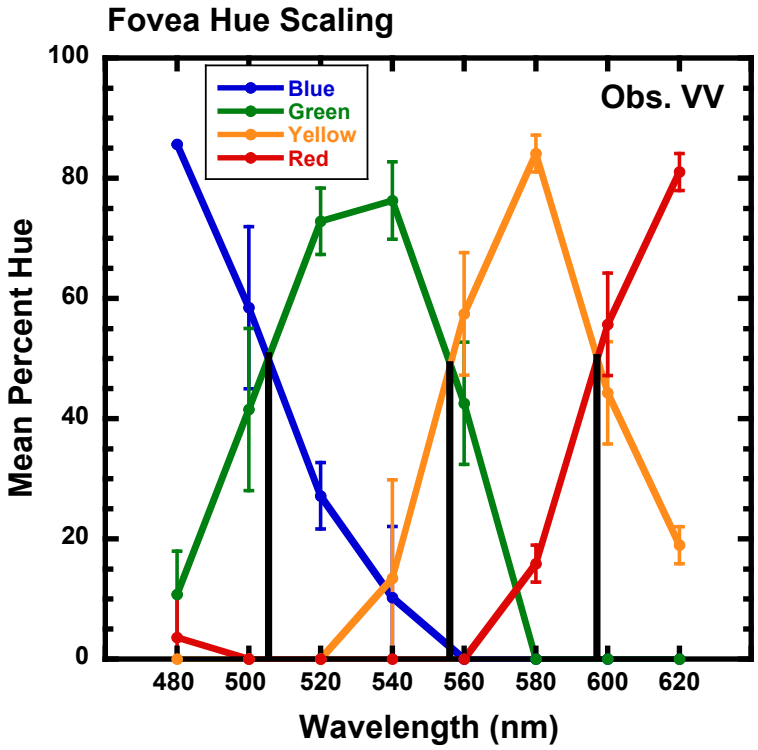

Figure 4.10: Mean hue percentages as a function of wavelength for eight stimuli presented to the fovea of observer VV. Wavelengths indicating equal percentages of neighboring hues are indicated by vertical black lines. Error bars represent ±1 standard deviation (SD). Binary hue wavelength values are reported in **Table 4.2**.

Table 4.2: Predicted Binary Hue loci for observers LB and VV, computed from hue scaling data. All wavelengths reported are in nm.

Observer	Binary B/G			Binary G/Y			Binary Y/R		
	Fovea	10° Temporal		Fovea	10° Temporal		Fovea	10° Temporal	
		4 min	28 min		4 min	28 min		4 min	28 min
LB	492	489	491	564	558	555	592	577	588
VV	506	487	492	554	536	547	597	584	591

Predicted Rod Effects on Binary Hue Loci

As listed in **Table 4.2**, when rods are active (peripheral no-bleach condition), the binary hue loci are predicted to shift to a longer wavelength, although the predicted shifts are very small in some cases. For B/G, G/Y, and Y/R, observer VV shows that the foveal locus is longer than the 28 min post-bleach locus, while the 28 min post-bleach locus is longer than the 4 min post-bleach locus. LB shows the same pattern for Y/R only. For B/G, LB shows no difference for the three conditions, and for G/Y, the foveal locus is a longer wavelength than the peripheral loci, which are the same (3 nm apart).

Binary Hue Loci Results

Appendix C lists the binary hue loci results obtained using the staircase method.

Binary Red/Blue

Figure 4.11 depicts the binary R/B loci for each observer under the three different viewing conditions tested. Each observer's loci are presented in a separate panel. The mean binary R/B locus measured in the fovea was the same for observers LB and VV (415 nm), but JN perceived binary R/B at a wavelength more than 21 nm longer. In the peripheral retina, under the bleach condition, all observers' binary loci differed from those measured in the fovea by at least 9 nm. In the periphery, JN and VV identified binary R/B at a shorter wavelength than in the fovea, while LB's peripheral bleach locus was at a longer wavelength. When rods were contributing to color perception in the peripheral retina (no-bleach), the binary hue locus did not change from that identified under bleach conditions for JN and LB, but for VV the locus was approximately 15 nm longer. It should be noted that for observer VV, the 400 nm

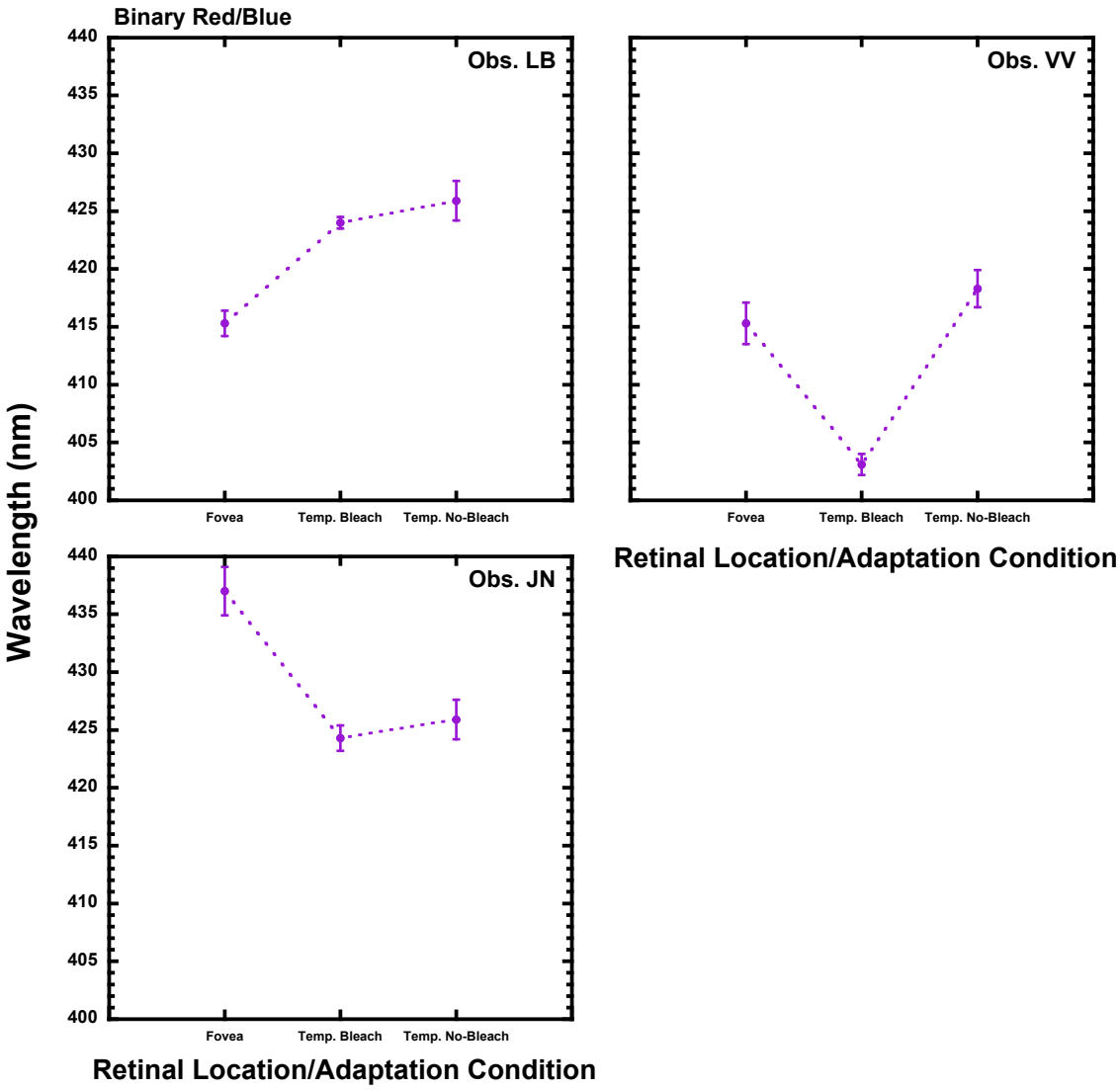

Figure 4.11: Comparison of the mean binary R/B loci (± 1 SEM) measured in the fovea (1° stimulus) and at 10° temporal eccentricity (2.55° stimulus) for three observers.

stimulus often appeared blue. The staircase could not be shifted to a shorter range of wavelengths without pushing beyond the limits of the visible spectrum into the range of ultraviolet wavelengths.

Binary Blue/Green

Figure 4.12 depicts the binary B/G loci for each observer for the three different viewing conditions with the staircase procedure (blue/green markers). For observers LB and VV, the values derived from the hue scaling functions are shown with black markers. Recall the 4 min post-bleach measure corresponds to the "Temporal Bleach" label in the figure, while the 28 min post-bleach measure corresponds to the "Temporal No-Bleach" label. For all observers the foveal B/G locus was at a longer wavelength than the peripheral loci. The same pattern of results is shown for observer VV with the loci derived from the hue scaling functions, and for LB for the foveal and peripheral bleach conditions (black markers).

The range of wavelengths from the staircase procedure identified as binary B/G in the fovea covered 11 nm, and both LB's and VV's B/G loci were measured at shorter wavelengths in the staircase procedure than those computed from the hue scaling functions. The comparison of loci measured in the periphery under bleach and no-bleach conditions showed no change for LB, while JN and VV both perceived the B/G locus at a longer wavelength when rods contributed in the no-bleach condition. Because the error bars on JN's graph overlap, indicating a fair amount of variability in responses, only VV's loci, from both experimental procedures, show a rod effect, whereby rods shift the B/G locus to a longer wavelength. For observers LB and VV, the pattern of binary B/G loci resembles the pattern of results found for UG.

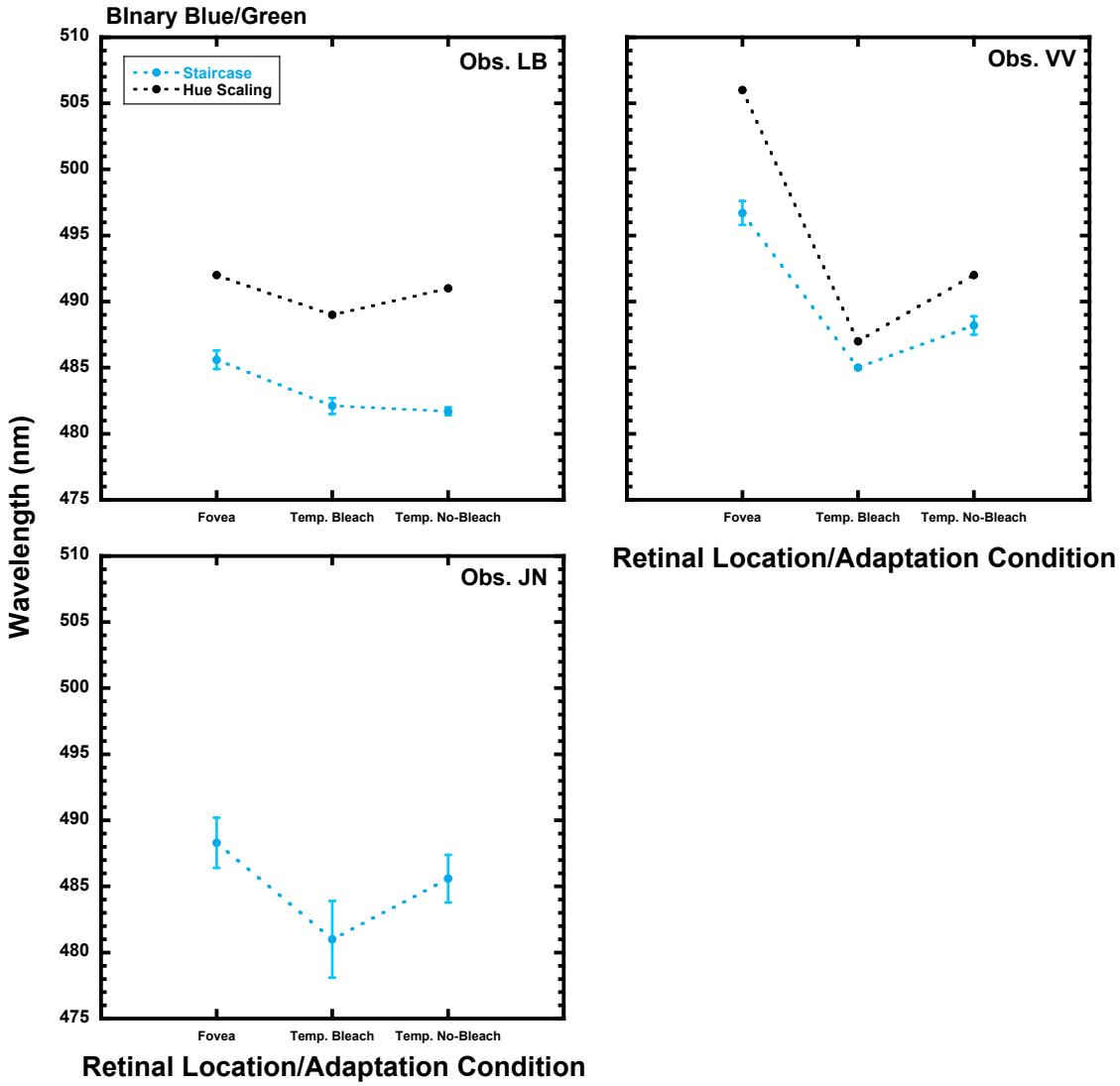

Figure 4.12: Comparison of the mean binary B/G loci (± 1 SEM) measured in the fovea (1° stimulus) and at 10° temporal eccentricity (2.55° stimulus) for three observers.

Binary Green/Yellow

Figure 4.13 presents the results for binary G/Y. It is interesting to note that the range of wavelengths measured for the foveal G/Y locus with the staircase was >22 nm across observers. For observers JN and LB the within-observer loci measured with the

staircase procedure under all three conditions were all within 8 nm, and the three loci measured using the staircase procedure for LB were within 5 nm of the G/Y loci computed from the hue scaling functions. For observer VV, the peripheral loci measured with the staircase procedure were approximately 20 nm shorter than the locus in the fovea. When the foveal loci from both experimental procedures are compared to the peripheral loci under bleach conditions, only VV shows the same pattern, i.e., G/Y at a shorter wavelength in the peripheral retina compared to the fovea. For LB there is no difference between the foveal and peripheral bleach condition loci with the staircase procedure and for JN the locus identified under bleach condition is 5 nm longer than the foveal locus.

For LB the peripheral binary G/Y loci measured with the staircase method closely matched those predicted from the hue scaling results, but the foveal locus was much longer than predicted. The pattern of results for binary G/Y for LB did not resemble the pattern of results found for either UG or UY. For VV, the binary G/Y loci measured in the fovea and in the periphery under the bleach condition closely matched the hue scaling results, but the binary G/Y locus measured with the staircase procedure in the peripheral retina under the no-bleach condition was essentially the same as that measured under the bleach condition, and was much shorter than the locus from the hue scaling results. Thus, the pattern of results for binary G/Y for VV closely resembles the pattern of results found for UG, but differs considerably from the results found for UY.

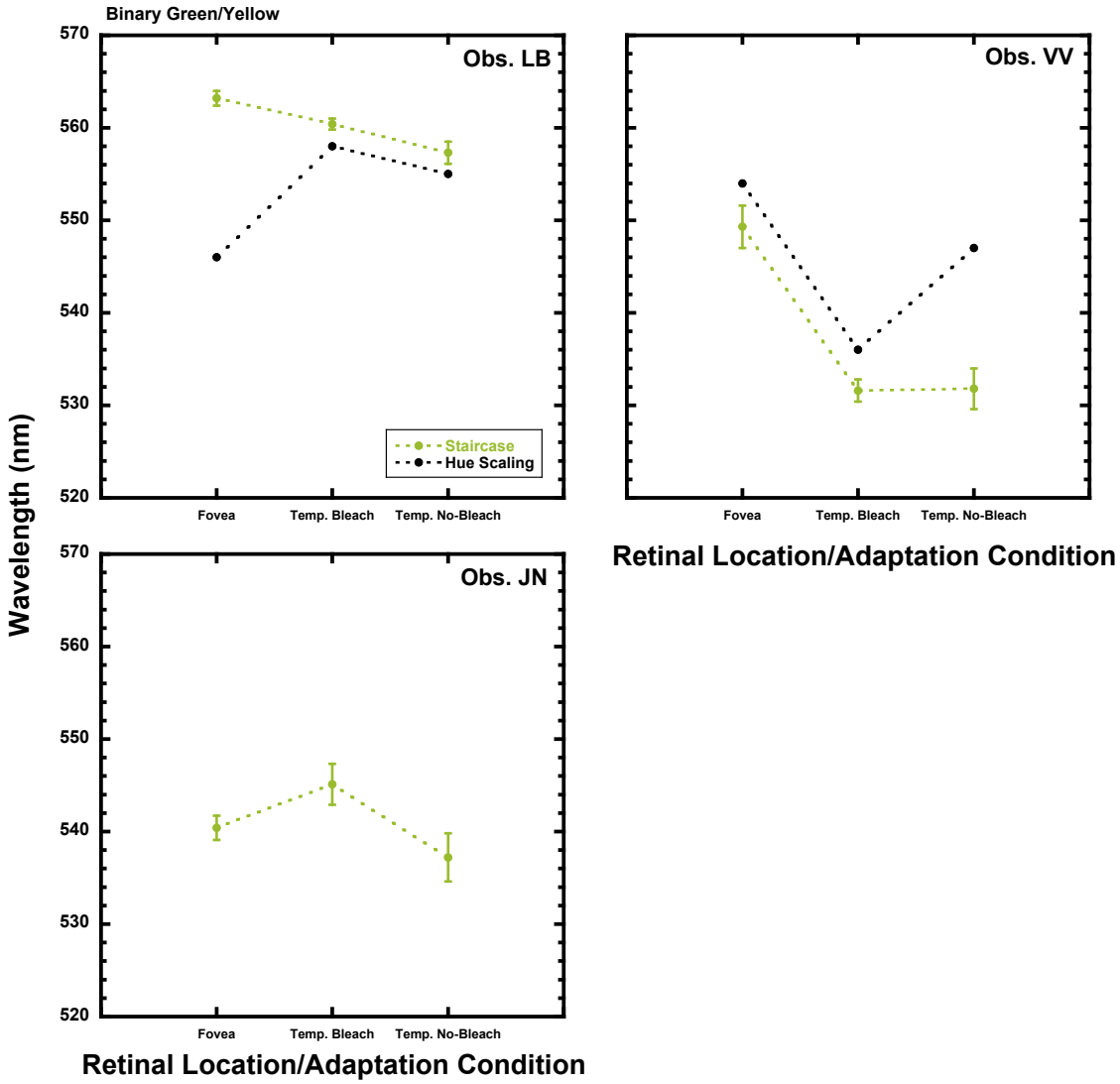

Figure 4.13: Comparison of the mean binary G/Y loci (± 1 SEM) measured in the fovea (1° stimulus) and at 10° temporal eccentricity (2.55° stimulus) for three observers.

Binary Yellow/Red

Figure 4.14 shows the binary Y/R loci for each observer under the three different viewing conditions tested. The range of wavelengths identified for this binary hue locus in the fovea was only 6 nm across the three observers. The pattern of results from the

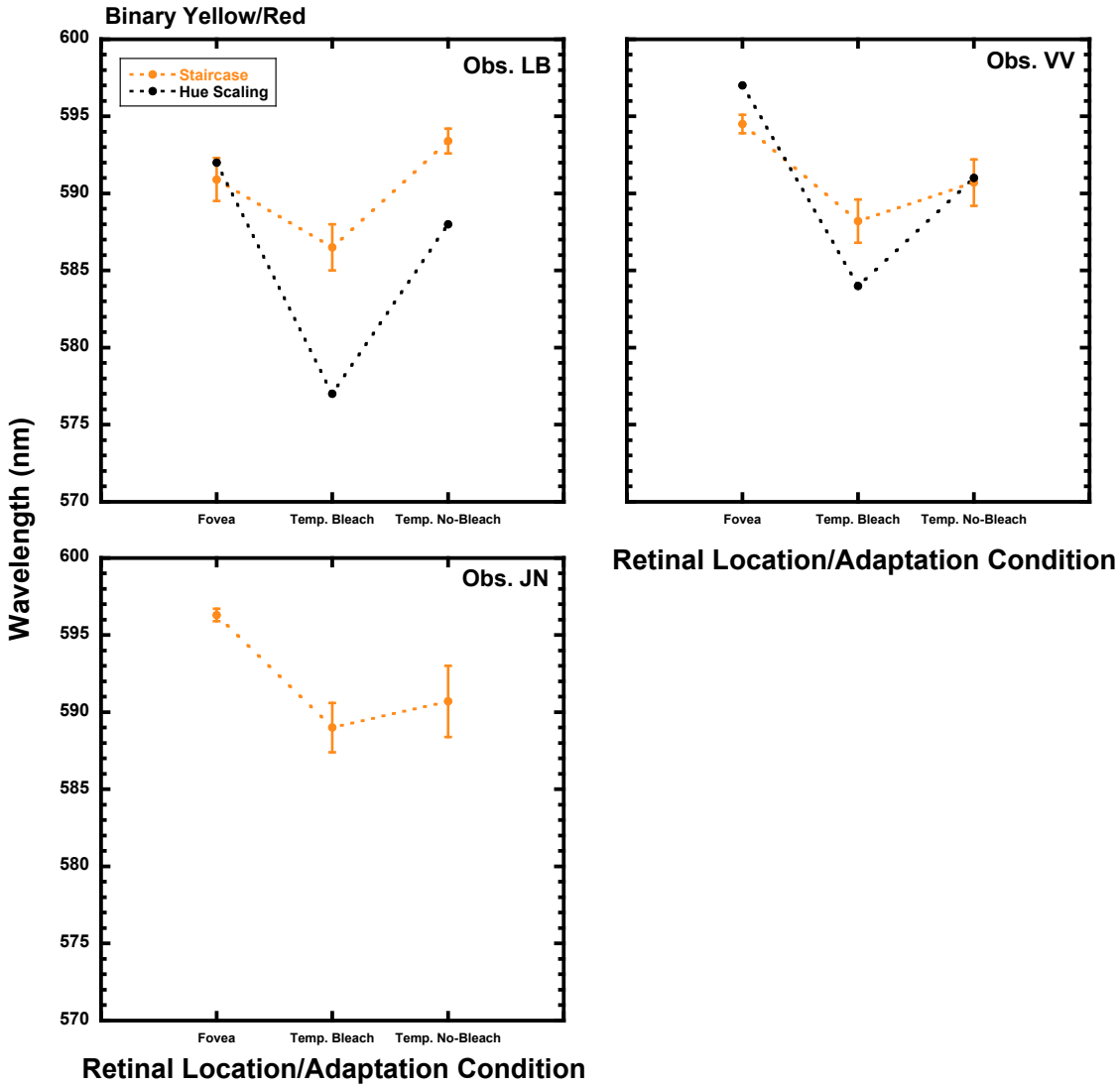

Figure 4.14: Comparison of the mean binary Y/R loci (± 1 SEM) measured in the fovea (1° stimulus) and at 10° temporal eccentricity (2.55° stimulus) for three observers.

staircase procedure for this binary hue is very similar for all three observers: the locus identified in the peripheral retina under bleach condition was shorter (more than 3 nm different) than the other two loci for all observers, a result consistent with the hue scaling data. The locus measured with the staircase procedure in the peripheral no-

bleach condition for each observer was a longer wavelength than the locus measured under the bleach condition, but only the shift to the longer wavelength for LB met the 3 nm criterion. This shift was greater for both LB and VV with the hue scaling loci. All of the Y/R loci measured with the staircase procedure fell within 6 nm of the loci computed from the hue scaling functions.

Overall, the hue scaling data did not predict the absolute values of the staircase binary hue loci well for observers LB and VV. Only seven of the 18 binary hue loci measured with the staircase procedure were within 3 nm of the values derived from the hue scaling functions. In general, the pattern of the binary hue loci observed among the foveal and peripheral bleach and no-bleach conditions from the hue scaling results was maintained when loci were measured with the staircase procedure for LB and VV.

CHAPTER 5: DISCUSSION

The studies reported here investigated the influence of rod photoreceptor input on color perception in the peripheral retina and compared foveal and peripheral color perception. A hue scaling study was designed to detect changes in color perception across the time course of dark adaptation, as rod function recovered from inactivation by a photobleaching stimulus. Two assertions that have been in the literature for decades are that rod input leads to a desaturated appearance for chromatic stimuli (Gordon & Abramov, 1977; Lembessis, 1997), and that rod input leads to an increased perception of blue in short-wavelength stimuli (Ambler & Proctor, 1976; Trezona, 1970; cf. Nerger et al., 2003). Rod input has been reported to influence peripheral color perception in more complex ways, including increasing the perception of yellow for long-wavelength stimuli (Stabell & Stabell, 1975; Buck et al., 1998). The results reported here were only partially consistent with these claims. Just under 50% of the saturation responses reported for the stimulus wavelengths show a pattern of decreasing saturation with increased rod activity (see **Figures 3.4** through **3.10**), while half of the responses suggest that rod input does not alter saturation perception in a predictable manner (see **Figure 3.3, Figures 3.4** through **3.10**. Observer LB reported no change in saturation perception across time for all stimuli, and other observers reported no change for specific wavelengths. This effect is wavelength specific.) While there was a modest trend in the hue response data consistent with the claim that rod input leads to increased perception of blue (see **Figures 3.14** through **3.16**), additional data would need to be collected for shorter wavelengths that appear more blue than those viewed in the hue scaling study. Likewise, there was also a trend towards increased perception

of yellow in long-wavelength stimuli with increasing rod participation (see **Figures 3.19** and **3.20**). Overall, the hue and saturation responses from this hue scaling study show clear between-observer variability, but no consistent, across-observer pattern of rod effects on peripheral color perception.

It was expected that there would be a clear pattern of rod influence on color perception detected in the hue scaling data, and that these results could be used to predict the loci of UHs and binary hues that would be measured under bleach and no-bleach conditions in the peripheral retina using a staircase method. Because the shortest wavelength presented in the hue scaling study was 480 nm, predictions about UB and binary R/B were not possible, but specific predictions were made for UG and UY, as well as the other binary hues. The UG loci measured using the staircase procedure did not match the predicted wavelengths in half of the measurements. In general the loci measured with the staircase procedure under the no-bleach condition, that were predicted to be at longer wavelengths than those in the bleach condition, were essentially the same as those in the bleach condition (see **Figure 4.3**). For UY, it was predicted that the peripheral loci would be the same under both conditions for two observers. For three of the four observers the measured UY loci were essentially the same under both conditions, suggesting that rod input, as manipulated by the no-bleach paradigm, does not alter the perception of UY (see **Figure 4.4**).

Predictions for the binary hues, for observers LB and VV, did not match the majority of measured loci, and in only one case, binary Y/R for observer LB (**Figure 4.14**), was there a difference between the loci in the bleach and no-bleach conditions.

Thus, these results fail to support the claim that rod input is associated with a change in peripheral color perception.

Individual Differences in Observers' Perceptions

While previous research (e.g., Nerger et al., 2003) suggests that at wavelengths shorter than 520 nm observers would perceive the hue scaling stimuli as less saturated as time in the dark increased, for two stimuli (480 nm and 620 nm, see **Figures 3.3** and **3.10**) none of the observers reported any change in saturation across time. It can be argued that, based on the spectral sensitivity function for rod photoreceptors, perception of a 620 nm stimulus would not be expected to be affected by rod input. For the other six stimuli, VV always reported a decrease in saturation across time. KY reported a decrease in saturation across time for five of the stimuli, and AK reported a decrease in saturation across time for four (50%) of the stimuli. Observer LB never reported a change in saturation across time for any of the stimuli, but all observers reported that the middle-wavelength stimuli were less saturated at all time-points than the shortest and longest wavelength stimuli, with the 560 nm stimulus described as the least saturated by all observers (see **Figures 3.4** through **3.9**). This pattern is consistent with reports in the literature (e.g., Abramov et al., 1991) that the middle wavelengths are perceived as less saturated than the shorter or longer wavelengths.

Gordon and Abramov, whose "4 + 1" protocol was followed in the hue scaling study, typically report group averages for hue scaling data (1990; Abramov et al., 1991), and claim that the "4 + 1" method is characterized by both within-subject and between-subjects reliability. In their 1990 publication, they offer as support for the within-subjects

consistency, data from one observer's hue scaling test-retest responses. In support of the between-subjects consistency claim, they offer a comparison between the data of a single observer, and the mean data of a group of four observers, noting that the SEM error bars on the data points are of approximately the same magnitude, and therefore we can assume that the variability in the population is on the same order as a single observer's variability on test-retest (Gordon & Abramov, 1990). This argument, based on data from a very small number of observers, does not provide convincing evidence of the homogeneity of the group data, and yet the practice of reporting mean data for the small groups of observers who typically participate in these psychophysical experiments has been the norm. Gordon et al. (1994) report "very little variability among subjects in hue and saturation scaling", so that "group averages nicely reflect behavior and serve to reduce noise." (p. 40). When the hue scaling results obtained in the present study were analyzed as group means this was not the case, as illustrated in **Figure 5.1**. Closer reading of Gordon et al. indicates that observers in the 1994 study viewed each stimulus 32 times, whereas in the present study each stimulus was viewed three or four times in each condition.

Additionally, Gordon et al. report a two-fold difference in the individual variances of responses between experienced and inexperienced observers (Gordon et al., 1994). The literature tends to be built on the perceptual data reported by a small number of observers overall, and many of the same observers participated in multiple studies in various labs, and they are therefore highly experienced. This is a general problem in many of the psychophysical studies published about color perception—there are very small numbers of observers in each study, and it is likely that the authors are among the

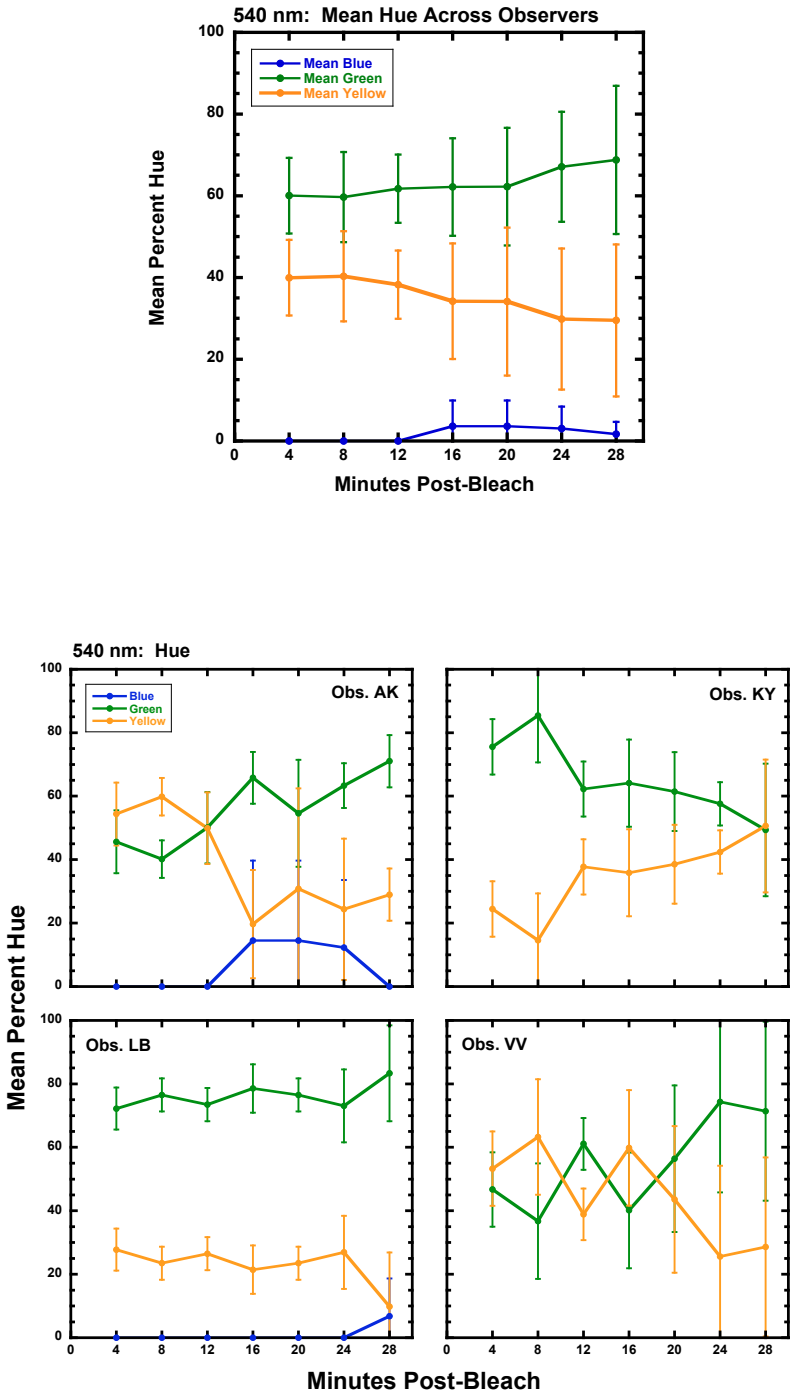

Figure 5.1: Top panel presents mean hue percentages across observers for the 540 nm stimulus presented to the peripheral retina at seven post-bleach times. Lower four panels are **Figure 3.16** reprinted, showing mean hue percentages (±1 SD) reported by four individual observers for the 540 nm stimulus. Results presented as group means do not closely reflect any of the individual observers' descriptions.

observers. For example, in what may the extreme case, results published by the Stabells report on the perceptions of the two authors as the only subjects in many of their studies (e.g., Stabell & Stabell, 1975; Stabell & Stabell, 1979; Stabell & Stabell, 1984; Stabell & Stabell, 1998, Stabell & Stabell, 1999; Stabell & Stabell, 2002). Therefore, the question arises of how accurately the results of these studies generalize to the general population.

McKeefry et al. (2007) reported on hue and saturation shifts in the peripheral retina during an asymmetric color matching task, and published the mean data as well as the individual data for their nine observers. There were very clear differences between the individual results and the mean data graphs. Buck et al. (2008) also presented individual observers' data in a study of time course effects on rod input (i.e., a range of stimulus durations), and these authors devoted part of their discussion to the unexpected differences in the UH loci measured for their three observers. The measured loci did not match the pattern predicted by Buck et al.'s model, and the results obtained were "puzzling" and "unexplained." Perhaps the convention of reporting mean data from small groups of observers in human vision psychophysics studies has tended to obscure the variability that is obvious in the hue scaling saturation and hue data reported here.

What the hue scaling data do illustrate is that in many cases different observers' perceptions of the monochromatic stimuli are not described in the same way by these four observers at any given time-point, or across the time-course of dark adaptation. The 480 nm stimulus, for example (see **Figure 3.13**), was described as greenish-blue at all time-points by observer KY, greenish-blue at six time-points and 100% blue at 20

min post-bleach by AK, and reddish-blue or greenish-blue at various time-points by observers LB and VV. LB tended to alternate between perceiving the stimulus as reddish- or greenish-blue across the time-course, while VV's descriptions clearly switched from greenish-blue to reddish-blue after 20 min post-bleach. Can we attribute this change in perception to rod influence? Why don't the other observers show a clear change across time in the perception of this stimulus? From these data we predict that the locus of UB will be at a wavelength shorter than 480 nm for AK and KY, given that this wavelength is always described as greenish-blue, or perceptually a longer wavelength than UB. VV and LB, on the other hand, would be predicted to perceive UB at a wavelength closer to 480 nm, given that they sometimes perceive this stimulus as reddish-blue (perceptually shorter) and at other times perceive it as greenish-blue (perceptually longer). When the UB loci were measured with the staircase method, AK did perceive UB at a wavelength shorter than the other observers (bleach and no-bleach conditions), but the UB loci for the other observers all overlapped.

One additional example of individual perceptual differences can be appreciated by examining the descriptions of the 560 nm stimulus (see **Figure 3.17**). This is the stimulus that all observers found to be the least saturated under all viewing conditions. The hue perceptions reported by AK and LB alternate between greenish-yellow and yellowish-green, with some reddish-yellow perceptions during the later time-points. This would suggest that the locus for binary G/Y should be near 560 nm, and for LB this was the binary G/Y locus measured under both bleach and no-bleach conditions. Observers KY and VV described the 560 nm stimulus as predominantly yellow, sometimes with some green, sometimes with some red. VV described this stimulus as 100% yellow on

all trials at 24 min post-bleach, which suggests that the locus of UY under the no-bleach condition should be approximately 560 nm for VV, but the UY yellow locus measured with the staircase method was 550 nm. Thus, LB described the 560 nm stimulus as approximately equally yellow and green, and identified 560 nm as the locus of binary G/Y. VV described the 560 nm stimulus as predominantly yellow, sometimes greenish, sometimes reddish, yet identified 550 nm as UY under no-bleach condition, and perceived 562 nm as UY under the bleach condition. VV's binary G/Y locus was 531 nm under both conditions, which is 19 nm (no-bleach) and 31 nm (bleach) shorter than the UY loci. LB identified 560 nm as the locus of binary G/Y, and perceived UY at 565 nm (bleach) and 566 nm (no-bleach), so that there was only a 5-6 nm distance between LB's binary G/Y and UY loci. Thus, what appeared equally green and yellow to LB (560 nm stimulus) was a longer wavelength stimulus than the locus that VV perceived as UY under the no-bleach condition (see **Figure 5.2** below). Perhaps the idea that finding consistent patterns of change in color perception across time, assumed to be correlated with rod input, was naïve, and did not take into consideration the possibility that these test wavelengths would not appear the same or even similar to the four observers in this study. Given that the previous literature typically reported mean data across all observers, this point may not have been obvious. If an increase in perception of blue was expected with rod input, but the stimuli were not initially perceived as equally blue by all observers, or if different portions of the spectrum appear blue to different observers, then a study such as the present one could not detect such a phenomenon.

Observers LB and VV participated in all of the hue loci studies described here, and **Figure 5.2**, below, illustrates the UH and binary hue loci for these two observers in

the fovea and in the periphery under the two different bleach conditions. We can see that the range of wavelengths each observer identified for each locus, particularly for the middle wavelengths, differs noticeably. The UH and binary hue loci in each viewing condition are not equidistant across the spectrum for each observer, and in most cases, while the loci differ for the fovea vs. the peripheral retina (bleach condition), there is little difference between the loci identified in the peripheral retina under the bleach and no-bleach conditions. The greatest between-observer differences are for the loci of binary G/Y and UY.

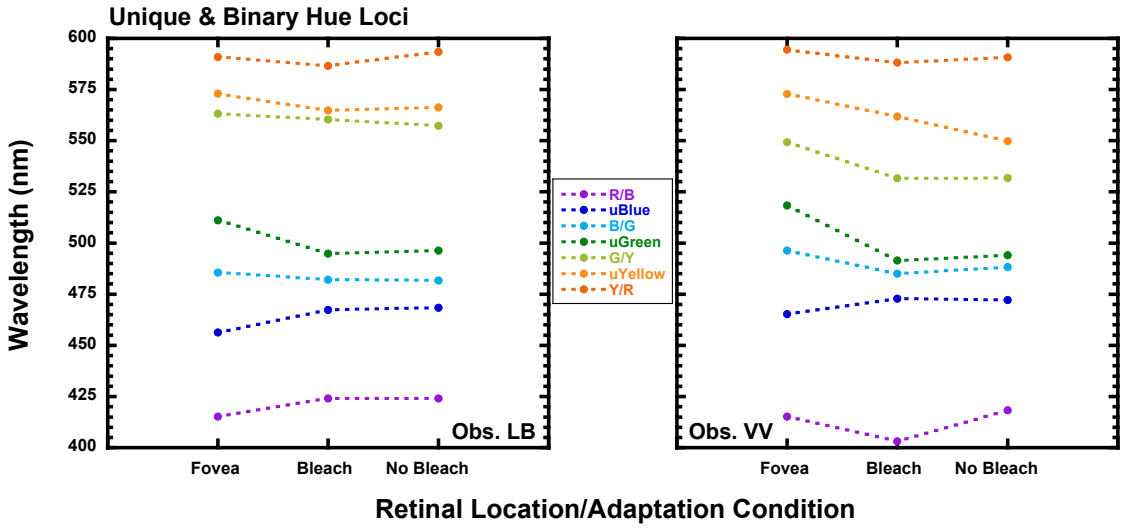

Figure 5.2: Mean UH and binary hue loci measured for observers LB and VV in the fovea (1° stimulus) and peripheral retina (2.55° stimulus) under bleach and no bleach conditions. The UG and UY loci were measured during the first study, the UB and binary hue loci are from the second study.

The change over time in the two sets of UB loci for observers LB and VV, shown in **Figure 4.9**, is also puzzling. As discussed in Chapter 4, a shift of 3 nm or more represents a perceptible hue difference. The UB locus was measured in the fovea twice,

and in the peripheral retina twice under the two bleach conditions, for LB and VV, with about two years separating the measurements. The second set of UB loci identified by LB under the three conditions all differed from the first set of loci by more than three nm. The loci identified by VV differed by more than 3 nm in two of the conditions (fovea and bleach condition in the periphery), and only the two UB loci measured in the periphery under the no-bleach condition were within 3 nm of each other. Cross-sectional data that examined the effect of aging on the locus of UB indicated that it remains relatively constant over the life span (Schefrin & Werner, 1990), but these measurements, taken two years apart, disagree with those findings. It is not clear whether individual changes in the locus of UB in the same observer over time has previously been reported.

Including the UH and binary hue loci studies here was intended to provide a more complete picture of observers' color perception. UHs have been thought of as the null points in the opponent color mechanisms, and as such are thought of as having a special status, a defining aspect of one's individual color perceptions. Results from an interesting study just published undermine the very concept of UHs as distinct from other hues (Bosten & Boehm, 2014). It was found that the specific instructions given to observers in a UH locus study had the effect of altering where the UH loci were measured. One group of observers were given instructions using the primary hue terms blue, green, yellow, and red while the other group were given instructions that included binary hue terms such as teal, lime, orange, and purple. Observers indicated by a key press which of the neighboring hues was present in the stimulus, and altering the color terms used in the instructions led to a significant shift in the UH loci identified. These

results seem to suggest that top-down influences from language-processing areas of the cortex are moderating observers' color perceptions.

Like the UHs, measurements of the loci of each observer's binary hues was meant to add to the story of rod effects on peripheral color perception. While one might intuitively expect that the binary hues would fall midway between the unique hues, the predicted loci based on the hue scaling data suggested otherwise, and as shown in **Figure 5.1**, this is not the pattern that was found. For both observers a distance of more than 30 nm separates the loci for binary R/B and UB in all conditions. UB, binary B/G and UG are clustered close together across the spectrum for both observers, under all viewing conditions. For VV the locus of binary B/G in the fovea (497 nm) is at a longer wavelength than the loci of UG identified in the peripheral retina under bleach (492 nm) and no-bleach conditions (494 nm). Binary G/Y and UY are also clustered together for both observers, and VV's binary G/Y locus in the fovea (549 nm) is nearly identical to the UY locus in the peripheral retina under no-bleach condition (550 nm). For LB the binary G/Y and UY loci were also nearly identical in some cases. In the fovea, binary G/Y was measured at 563 nm, while UY in the peripheral retina under bleach conditions was 565 nm. LB's binary G/Y locus was 560 nm when measured in the peripheral retinal under bleach conditions, and differed from UY by only 5 nm.

Desaturating Effect of Rods?

The failure to find a consistent desaturating effect of rods in the present studies might be explained by two factors that are known to influence rod effects on hue scaling: stimulus size and stimulus intensity. The parameters chosen for the present

study, 2.55° stimulus with a 20 (1.3 log) phot td illuminance level, were known to adequately fill the perceptive fields for the four elemental hues in the peripheral retina (Troup et al., 2005), and stimulate both rods and cones. Previous studies (e.g., Abramov et al., 1991), whose results suggest that rods impart a desaturated appearance to stimuli in the periphery have included the use of smaller stimulus sizes, e.g., Nerger et al. (2003) presented a 1.5° stimulus at 8° nasal retina, with a 25 phot td illuminance level. This smaller stimulus certainly did not fill the perceptive field for green (Troup et al., 2005). The mosaic of the nasal retina is also likely to differ from the temporal retina, given that the optic nerve exits the eye at approximately 12° eccentricity in the nasal retina ("Facts and Figures," 2014), interrupting the neural retina and forming a blind spot upon which there are no photoreceptors. Curcio et al. (1987) report this type of asymmetry in their examination of primate retinas. Subsequent research from this laboratory has shown by the presentation of a stimulus, with a given illuminance level and size at different retinal locations, that the perceptive field sizes for green in the nasal vs. temporal retina differ considerably (Volbrecht, Clark, Nerger & Randell, 2009). Thus, the differences between experimental conditions may have led to an incompletely filled perceptive field, and decreased rod activity, and may explain the different patterns of results, including reports of desaturated color perception in the peripheral retina when rods are active.

Rod Effects on Hue Perception

As expected, observers' hue perception for most stimuli did change across the time course of dark adaptation (see **Figures 3.13-3.20**). Four observers describing

eight stimulus wavelengths generated 32 graphic representations of color perception across time, and only ten of these graphs showed essentially no change in the hue percentages. In those ten cases, the descriptions were almost exclusively of either the shortest wavelength (480 nm) or the longer wavelengths (580-620 nm). The interesting pattern in these hue changes across time was that color perception later in the time-course, when rods were likely to be contributing to perception, was of a perceptually shorter wavelength than the descriptions early in the time-course. For example, for the 500 nm stimulus, all observers reported that the predominant hue was green, but during the early time points (4 min and 8 min post-bleach) a yellow hue component was also perceived. During the later time points (16 min post- bleach and later) all observers perceived a blue hue component on at least some viewing trials (see **Figure 3.14**). So this wavelength was described as yellowish-green during the early time-points, but it came to be perceived as bluish-green as time passed and more rods began to affect color perception. For the shorter-wavelength stimuli (480-540 nm) this shift to describing the stimuli with hue terms consistent with shorter wavelengths as time in the dark increased was found for half of the responses, suggesting the effect of rod signals is to add a blue component to hues. For the 560 nm stimulus, two observers' hue descriptions were consistent with a longer wavelength appearance with rod input (i.e., a greenish-yellow appearance during the first time-points, then less green perception, increased yellow perception, and some red perceived during the later time-points). The hue perceptions were essentially unchanged across time for the 580 nm stimulus for all observers, but for the longer-wavelength stimuli (600-620 nm), three of the eight descriptions show a pattern of increasing yellow perception with time and rod input,

which is consistent with perceiving a shorter wavelength at the later time-points. Other authors have indicated that rod input is associated with an increase in signals from the Y/B mechanism (e.g., Parry et al., 2006; Stabell & Stabell, 1975), and these results lend some support to that claim.

There was also a noticeable pattern in about 20% of the graphs in which the hue and saturation percentages changed during the earlier time-points, but seemed to stabilize at or after 16 min post-bleach. This suggests that after rods reach a minimum level of activation, additional rod input does not change color perception. Examples of this pattern can be seen in **Figures 3.7** (saturation for 560 nm stimulus, observers AK, KY, VV), **Figure 3.16** (hue for 540 nm stimulus, observer AK), and **Figure 3.20** (hue for 620 nm stimulus, observer AK). The same pattern of results is present in work of other researchers who examined rod effects on saturation and hue across time (e.g., Lembessis, 1997; Stabell & Stabell, 1998), but this time course phenomenon has not been widely illustrated or discussed in the literature concerning rods and color perception.

Two hypotheses regarding hue were evaluated: that rod input leads to increased perception of blue in shorter-wavelength stimuli and increased perception of yellow in longer-wavelength stimuli. These effects would be detected by comparing the hue scaling responses from 4 min and 28 min post-bleach stimulus presentations, as well as the unique and binary hue loci measurements from the bleach and no-bleach conditions. It was possible that another pattern of change in hue perception would be revealed, but no consistent pattern of hue change was found between the cone-dominant (4 min post-

bleach, or bleach condition) and rod and cone mediated (28 min post-bleach, or no-bleach condition) stimulus descriptions.

Examination of the UH loci results (see **Figures 4.2-4.4**, and **Figure 4.8**) showed that in more than 50% of the measurements there was no difference (i.e., the loci did not differ by more than 3 nm) in the locus measured under bleach and no-bleach conditions. When there was a difference, approximately half of the loci in the no-bleach condition were at shorter wavelengths than the locus in the bleach condition, but about the same number were in the opposite direction. No discernable rod influence on color perception was found in this study.

For the binary hue loci, more than half of the results showed no difference between the loci in the bleach and no-bleach conditions, one third of the bleach/no-bleach comparisons showed a longer wavelength locus for the no-bleach condition, and in only one case (binary G/Y for JN) the locus in the no-bleach condition was at a shorter wavelength than the bleach condition locus. Again, these data do not present a consistent rod influence on peripheral color perception.

Comparing Foveal and Peripheral Color Perception

Noticeable and consistent differences were found between observers' descriptions of the 480-580 nm stimuli presented foveally, compared to peripherally under the bleach condition. This comparison was made to show differences in cone-mediated color perception at two retinal locations.

Figure 3.11 shows the saturation responses from the fovea and 4 min post-bleach trials, and there is no distinct difference between the responses. The saturation

values overlap for the most part for individual observers, and when they differ there are equal numbers of descriptions of the foveally-viewed and peripherally-viewed stimuli as more saturated, across observers. Only observer LB described the stimuli as less saturated when they were viewed in the peripheral retina. The other observers described the stimuli, particularly the middle wavelengths, as less saturated when they were viewed in the fovea. This pattern of results is consistent with other data collected in this laboratory, and recently reanalyzed (Opper, Douda, Volbrecht & Nerger, 2014).

As shown in **Figures 3.21-3.26**, and described in Chapter 3, there is a consistent pattern in the hue responses of stimuli appearing as if they were of longer wavelengths when viewed in the peripheral retina. What looks blue when viewed in the fovea looks greenish-blue when viewed in the periphery, etc. For example, the 520 nm stimulus imaged on the fovea was described as either bluish-green or yellowish-green by all observers (or sometimes as both bluish-green on some trials and yellowish-green on different trials by a single observer). When this same stimulus was viewed in the peripheral retina under bleach conditions, all observers reported a larger yellow component, and no blue component (see **Figure 3.23**). It might have been expected that color appearance for stimuli under these two viewing conditions would be very similar, as they are both "cone vision," but these results tell a different story.

As described in Chapter 1, the topography of the human retina varies markedly between the fovea and peripheral retinal areas. Stimuli imaged on the fovea (1° stimuli in these studies), and those that would be imaged on the fovea and surrounding parafoveal retina (2.55° stimuli), would lead to photon capture primarily in the specialized midget cone photoreceptors that exclusively populate the 1° central fovea

(Kolb, 2012). There are very few S-cones in the fovea, and the foveal midget M- and L-cones are thinner and morphologically different than the cones found in the peripheral retina. There is no neural convergence in the retinal processing for the central fovea, midget cones synapse one-to-one onto midget bipolar cells, which synapse one-to-one onto midget ganglion cells. Outside the fovea, rods begin to be interspersed among the cones, there are relatively more S-cones present in the peripheral mosaic than there are in the fovea, and there begins to be convergence of the neural signals through the layers of the retina, so that ganglion cells have increasingly larger receptive fields the further away from the fovea they lie, and they receive synaptic input from ever larger numbers of retinal cells (Kolb, 2012). Neural processing through the horizontal and amacrine cell layers also occurs outside of the fovea, as the size of individual cells, density of photoreceptors, and degree of neural convergence changes with eccentricity across the retina.

Both psychophysical (Mullen & Kingdom, 2002) and fMRI (Vanni, Henriksson, Viikari & James, 2006) studies have also revealed differences in the strength of the R/G and Y/B channels, as well as the luminance channel, in different regions of the retina The strength of the R/G opponent channel is greatest in the central retina, and then R/G sensitivity declines in the peripheral retina, while the strength of both the luminance and Y/B channels remains relatively constant across the retina. Therefore, when comparing descriptions of color perception for a wavelength of light viewed in the fovea vs. 10° temporal retinal eccentricity under the bleach condition, we should expect differences, related to where in the spectrum a given wavelength falls.

Comparison of Psychophysical Tasks

It was expected that the pattern of results from the two different types of psychophysical tasks, hue scaling and staircase, would be similar. While hue scaling and hue locus identification both require observers to provide a verbal response after each stimulus presentation, there are some important differences between the two procedures, and the types of verbal responses requested. Hue scaling responses follow the "4 + 1" technique described by Gordon and Abramov (1988), in which observers assigned hue and saturation percentages to describe their color perception experience. Therefore, the responses collected for each stimulus were percentage values, observers' verbal estimates of the hue and saturation composition of their perception of each stimulus, and these numerical estimates were then averaged. Graham and Ratoosh (1962) raised objections to averaging verbal estimates as though they are quantities, when in fact they are learned verbal responses that observers use to describe their own subjective perceptions. This method suggests that the observer is reporting some internal, private measurements, but in fact there is no way of knowing how observers' verbal estimates correlate with measurable variables (e.g., amount of blue) related to one's sensations and perceptions, elicited by specific wavelengths of light. There is no way to ascertain that a given observer's use of percentage descriptions, based on reference to his or her "internal standards" (Gordon et al., 1994) in any way correspond to another observer's descriptions. Therefore, this procedure might be expected to produce data with greater between-observer variability, and the data would not necessarily be expected to correlate directly with quantitative measurements.

In contrast, in the hue loci studies, the observer's task after stimulus presentation was to respond with one of two alternative forced-choices. In a UH determination, the observer was to report which of the adjacent hues was present in the stimulus, e.g., for UB, did the stimulus appear reddish-blue or greenish-blue? In a binary hue determination, the observer's task was to report which of the two binary hue components was predominant, e.g., for a B/G determination, did the stimulus appear to contain more blue or more green? The verbal responses guided the experimenter in selecting the successive stimulus wavelengths presented, and the final datum obtained was a wavelength (± 1 nm) about which an observer reversed his or her perceptual description. Thus the data here are numeric wavelength values, identified from verbal responses, which are quantitative data. After considering these differences in the types of verbal reports given in each study, it does not seem surprising that the results do not agree.

Another important difference between the types of data collected in the two procedures is that the variable of saturation was not assessed in the staircase procedure, but only in hue scaling. Observers were expected to register their hue and saturation perceptions during the 500 msec stimulus presentations in the hue scaling study, but only hue needed to be assessed during the hue loci stimulus presentations. fMRI data suggest that language regions of the brain are active during color perception, and top-down influences may operate when observers must verbally describe color perceptions, such that activation of color vision cortical areas is modulated by activation of the language areas (Siok et al., 2009). While the exact cortical locations that might process the color information that observers reported in these studies is not known, one

might imagine that different locations in the visual pathway might be active when assessing hue content of a stimulus vs. the degree of saturation of a stimulus. The entire visual pathway may be operating differently in these two different tasks.

The fMRI data also support a point having to do with lateralization of visual processing. Siok et al. (2009) found that the (top-down) effects of language on color categorization were stronger for stimuli presented in the right visual field than in the left visual field. Given that the major language processing regions of the cortex are located in the left hemisphere for most humans (Pinel, 2014), and that visual information from the right visual field is processed in the left hemisphere's visual cortical areas, this makes sense. There would be no need for additional neural communication between the two hemispheres in this case, the language and visual processing would all occur in the same hemisphere. In the studies reported here, peripheral stimuli were all presented to the temporal retina of observers' right eyes, upon which impinge images from the left visual field. This input would remain ipsilateral through the primary visual pathway, and be processed in the visual cortices of the right hemisphere. There would need to be additional synaptic communication to forward this visual information to the left hemisphere language cortical areas, or to carry modulating language input to the right visual cortical areas. Foveal stimulus presentations, on the other hand, would be processed in both hemispheres of the brain. Differences in results between studies of rod effects on color vision might also be due to the portion of the visual field to which stimuli were presented. For example, Nerger et al. (2003) presented monochromatic stimuli to the nasal retina of observers' right eyes, which processes images from the right visual field. The mean hue scaling data reported in that study showed a decrease

in saturation across the time-course of dark adaptation, and all observers described the 480 nm stimulus as bluish-green, whereas all observers described this same wavelength of light as greenish- (or sometimes reddish-) blue in the present study. The retinal location of stimulus presentation was one variable that was different between the two studies. The stimulus size for peripheral stimuli was smaller in the Nerger et al. (2003) study: 1.5° vs. 2.55° in the present study, and the retinal illuminance level was 25 phot tds vs. 20 phot tds in the present study. So the perceptive fields for green and possibly yellow and blue were not filled in the earlier study in the no-bleach condition (Pitts, Troup, Volbrecht & Nerger, 2005). In any case, the results obtained in these two similar studies were quite different, and perhaps the difference in visual hemifield contributes to the differences. The majority of right-handed and left-handed individuals process language primarily in the left hemisphere (Mazoyer et al., 2014), so visual hemifield of stimulus presentation, and handedness of observers, might also be important variables to consider in hue scaling and hue loci studies.

Normal Vision Across the Entire Retina

When considering the results obtained in the studies presented here, it is important to remember that the human visual system did not evolve to perceive small, brief, monochromatic stimuli imaged only on a small region of one peripheral retina. When a salient stimulus appears in our visual field, we automatically shift our gaze so that the visual input is imaged on the fovea of both eyes. This visual input is then processed bilaterally in the greatly magnified region of primary visual cortex devoted to foveal images. The stimuli presented to the peripheral retina in the present studies did

not allow normal processing, the way that our visual system has evolved to do its job. We can't know what normally operating, higher-level mechanisms were bypassed in processing minimal input only from one peripheral retina. We cannot know which parts of normal visual processing are not functional during these experimental tasks, and what effect this minimal stimulus presentation exerts on visual perception. In normal human vision, for example when looking at a brightly-colored wall, we don't perceive the portion of the wall which is imaged on the fovea to be of a different hue or saturation than the portions of the wall that are being imaged on the peripheral retina. We perceive the wall to be of a uniform hue and saturation. It is likely that there is a summative cortical mechanism that ensures that our color perception for large surfaces is homogeneous, not unlike the mechanism that fills in the blind spots in each of our visual fields (Kulikowski et al., 2009). When visual stimuli are not imaged on the fovea, this putative mechanism would presumably not operate. The fact that foveal hue scaling responses differ from the responses when the same stimulus is viewed in the peripheral retina, whether or not rods are contributing, leads to the interesting question of how we tend to perceive homogeneous color in our vision in the real world, when foveal and peripheral color perception are somehow seamlessly blended. It would seem logical that the foveal perceptions somehow outweigh the peripheral, given that the foveal input is processed in a greatly magnified region of primary visual cortex. Finding the neural substrate for this function would be an ambitious aim for future imaging studies.

In a number of studies both the fovea (or parafoveal region) and the peripheral retina were simultaneously stimulated, and observers were asked to manipulate one of

the stimuli until both stimuli matched. For example, Ambler & Proctor (1976) used a binocular color matching task to test for rod effects. For the color matching task, the observer's left eye viewed a 500 nm stimulus either in the fovea or at 8° nasal eccentricity. The stimuli were tiny, about 0.5°, and stimulus presentations were 150 msec. The fovea of the observer's right eye viewed a mixture of 470 nm and 510 nm lights, and the task was to adjust the amounts of these two wavelengths to make a color match to the light in the left eye. Differences in the amount of 470 nm light needed for the match in the fovea compared to in the periphery form the basis for these authors' claim that rods in the periphery add a blue sensation, and more blue light must be added to make a match. This was a binocular task, and at least one fovea was being stimulated in all trials. The different streams of input being processed in this task make it very different from the tasks used in the present studies. Also, no verbal responses were required, only a manual adjustment of the lights, so this factor might also lead to differences in the results and conclusions that can be drawn. More recently Parry et al. (2006) presented a test and a probe stimulus simultaneously to the left eye of observers, and asked them to make a color match. The test stimulus was presented at various nasal eccentricities, while the probe was always at 1° nasal eccentricity in the left eye, so processing would be contralateral, in the right hemisphere. On some trials observers indicated whether the two stimuli were the same or different by means of a lever press. On other trials observers adjusted the parameters of the test stimulus until a match was achieved, so again no verbal responses were required, and possible top-down, language effects would not be operating. The results of these studies were consistent with a shift towards blue or yellow with increasing retinal eccentricity, but this was not

automatically attributed to rod input, as there was no specific manipulation of rod vs. cone activity. These authors describe a variety of hue changes of varying magnitudes at differing retinal eccentricities, which is in agreement with the present results. If a summating mechanism operates in the visual system, as suggested above, then results from matching studies involving presentation of two simultaneous stimuli would not be directly comparable to the results obtained when an observer views only a single, peripheral stimulus, since this mechanism would not be operational in the second situation.

Kulikowski et al. (2009) suggest that some form of spatial or temporal integration of chromatic signals from the entire visual field occurs, based on the results of color matching studies, and they describe this as "panoramic viewing." It is worth remembering that the human visual system is wired for binocular, stereoscopic vision, with binocular neurons in primary visual cortex (V1) receiving inputs from both eyes. The presentation of stimuli that don't activate this aspect of visual processing may lead to any number of unusual color effects.

In summary, the studies reported here had the aim of extending our knowledge of the contribution of rod photoreceptors to color perception in the peripheral retina. Psychophysical data were collected, and analysis of these data led to the conclusion that perhaps in the experimental conditions used, rod input was not the only relevant variable that differed in the bleach and no-bleach viewing conditions. Many of the results reported here, and in previous literature, concerning rod effects, might be explained by other aspects of the experimental conditions, or other aspects of visual processing in the peripheral retina. It is likely impossible to isolate rod input as a

variable. The rod bleach technique used in the present studies is sufficient to temporarily minimize rod function, but once a critical number of rods are actively capturing photons, rod signals in the peripheral retina combine with cone signals, and are processed through all the levels of the visual system. Several experimental results, discussed above, also suggest that top-down influences can alter color perception. Even though the human visual system is the most studied of the sensory systems, it still remains a highly complex, elusive, and incompletely understood system.

REFERENCES

Abramov, I., & Gordon, J. (2005). Seeing unique hues. *Journal of the Optical Society of America A 22(10),* 2143-2153.

Abramov, I., Gordon, J., & Chan, H. (1991). Color appearance in the peripheral retina: effects of stimulus size. *Journal of the Optical Society of America A 2,* 404-414.

Abramov, I., Gordon, J., & Chan, H. (1992). Color appearance across the retina: effects of a white surround. *Journal of the Optical Society of America A 9(2),* 195-202.

Abramov, I., Gordon, J., & Chan, H. (2009). Color appearance: properties of the uniform appearance diagram derived from hue and saturation scaling. *Attention, Perception & Psychophysics 71*, 632-643.

Ahnelt, P., Kerl, C., & Kolb, H. (1990). Identification of Pedicles of Putative Blue-Sensitive Cones in the Human Retina. *Journal of Comparative Neurology 293,* 39-53.

Ahnelt, P., & Kolb, H. (1994). Horizontal cells and cone photoreceptors in human retina: a Golgi-electron microscopic study of spectral connectivity. *Journal of Comparative Neurology 343,* 406-427.

Ahnelt, P.K., Kolb, H., & Pflug, R. (1987). Identification of a subtype of cone photoreceptor likely to be blue sensitive, in the human retina. *Journal of Comparative Neurology 255,* 18-34.

Alpern, M. (1971). Rhodopsin Kinetics in the Human Eye. *Journal of Physiology 217*, 447-471.

Ambler, B.A., & Proctor, R.W. (1976). Rod involvement in peripheral color processing. *Scandinavian Journal of Psychology 17,* 142-148.

Bosten, J.M., & Boehm, A.E. (2014). Empirical evidence for unique hues? *Journal of the Optical Society of America A 31(4),* A385-A393.

Bowmaker, J.K., & Dartnall, H.J.A. (1980). Visual pigment of rods and cones in a human retina. *Journal of Physiology 298,* 501-511.

Brouwer, G.J., & Heeger, D.J. (2009). Decoding and Reconstructing Color from Responses in Human Visual Cortex. *The Journal of Neuroscience 29(44)*, 13992-14003.

Buck, S.L. (2001). What Is the Hue of Rod Vision? *Color Research and Application 26 Supplement,* S57-S59.

Buck, S.L., & Knight, R.F. (1997). Modeling rod contributions to extrafoveal hue perception. In *IS&TIOSA Optics in the Information Age* (pp. 16-18), Springfield, VA: IS&T.

Buck, S.L., Knight, R.F., & Bechtold, J. (2000). Opponent-color models and the influence of rod signals on the loci of unique hues. *Vision Research 40*, 3333-3344.

Buck, S.L., Knight, R., Fowler, G., & Hunt, B. (1998). Rod influence on hue-scaling functions. *Vision Research 38*, 3259-3263.

Buck, S.L., Thomas, L.P., Connor, C.R., Green, K.B., & Quintana, T. (2008). Time course of rod influences on hue perception. *Visual Neuroscience 25,* 517-520.

Calkins, D.J. (2004). Linking Retinal Circuits to Color Opponency. In L.M. Chalupa & J.S. Werner (Eds.) *The Visual Neurosciences, Volume 2*, Ch. 64. Cambridge: The MIT Press.

Chaudhuri, A. (2011). *Fundamentals of Sensory Perception.* Don Mills, Ontario: Oxford University Press Canada.

Cook, J.E., & Becker, D. (1995). Gap junctions in the vertebrate retina. *Microscopy Research and Technique 31,* 408-419.

Curcio, C.A., Sloan, K.R., Kalina, R.E., & Hendrickson, A.E. (1990). Human photoreceptor topography. *Journal of Comparative Neurology 292,* 497-523.

Curcio, C.A., Sloan, K.R., Packer, O., Hendrickson, A.E., & Kalina, R.E. (1987). Distribution of cones in human and monkey retina: individual variability and radial asymmetry. *Science 236,* 579-582.

Dacey, D. (2004). Origins of Perception: Retinal Ganglion Cell Diversity and the Creation of Parallel Visual Pathways. In M.S. Gazzaniga (Ed.) *The Cognitive Neurosciences III*, Ch. 20. Cambridge: The MIT Press.

De Monasterio, F.M., & Gouras, P. (1975). Functional properties of ganglion cells of the rhesus monkey retina. *Journal of Physiology 251,* 167-195.

DeValois, R.L., & DeValois, K.K. (1993). A Multi-Stage Color Model. *Vision Research 13(8),* 1053-1065.

DeValois, R.L., Smith, C.J., Kitai, S.T., & Karoly, A.J. (1958). Response of Single Cells in Monkey Lateral Geniculate Nucleus to Monochromatic Light. *Science 127(3292)*, 238-239.

Dkhissi-Benyahya, O., Rieux, C., Hut, R.A., & Cooper, H.M. (2006). Immunohistochemical evidence of a melanopsin cone in human retina. *Investigative Ophthalmology and Visual Science 47(4),* 1636-1641.

Facts and Figures concerning the human retina. (2013). Retrieved June 23, 2014, from Webvision online textbook: http://webvision.med.utah.edu/

Field, G.D., Greschner, M., Gauthier, J.L., Rangel, C., Shlens, J., Sher, A., Marshak, D.W., Litke, A.M., & Chichilnisky, E.J. (2009). High-sensitivity rod photoreceptor input to the blue-yellow color opponent pathway in macaque retina. *Nature Neuroscience 12(9),* 1159-1164.

Gordon, J., & Abramov, I. (1977). Color vision in the peripheral retina. II. Hue and saturation. *Journal of the Optical Society of America, 67(2),* 202-207.

Gordon, J., & Abramov, I. (1988). Scaling procedures for specifying color appearance. *Color Research and Application, 13,* 146-152.

Gordon, J., Abramov, I., & Chan, H. (1994). Describing color appearance: Hue and saturation scaling. *Perception & Psychophysics, 56,* 27-41.

Graham, C.H., & Ratoosh, P. (1962). Notes on some interrelations of sensory psychology, perception, and behavior. In S. Koch (Ed.), *Psychology: A study of a science: Vol. 4* (pp. 483-524). New York: McGraw-Hill.

Granit, R. (1947). *Sensory Mechanisms of the Retina.* London: Oxford University Press.

Hadjikhani, N., Liu, A.K., Dale, A.M., Cavanagh, P., & Tootell, R.B. (1998). Retinotopy and color sensitivity in human visual cortical area V8. *Nature Neuroscience 1(3),* 235-241.

Hecht, S., Haig, C., & Chase, A.M. (1937). The influence of light adaptation on subsequent dark adaptation of the eye. *Journal of General Physiology 20,* 831-850.

Helmholtz, H. von (1910/1924). In J.P.C. Southall (Ed.) *Physiological optics, Vol. 2.* Rochester, NY: Optical Society of America. (Original work published 1910)

Hering, E. (1964). *Outlines of a theory of the light sense.* Translated by L.M. Hurvich and D. Jameson. Cambridge: Harvard University Press. (Original work published 1920)

Hofer, H., Carroll, J., Neitz, J., Neitz, M., & Williams, D.R. (2005). Organization of the human trichromatic cone mosaic. *Journal of Neuroscience 25,* 9669-9679.

Hubel, D.A. (1988). *Eye, Brain and Vision,* Ch. 6. New York: Scientific American Library.

Hurvich, L.M., & Jameson, D. (1957). An opponent-process theory of color vision. *Psychological Review 64,* 384-404.

Jameson, D., & Hurvich, L.M. (1955). Some quantitative aspects of an opponent-colors theory: I. Chromatic responses and spectral saturation. *Journal of the Optical Society of America, 45,* 546-552.

Jameson, D., & Hurvich, L.M. (1967). Fixation-light bias: An unwanted by-product of fixation control. *Vision Research, 7,* 805-809.

Kaiser, P.K., & Boynton, R.M. (1996). Science of Color Vision: A Brief History. In P. K. Kaiser and R. M. Boynton, (Eds.) *Human Color Vision, Second Edition*, Ch. 1. Washington, DC: Optical Society of America.

Knight, R., & Buck, S.L. (2002). Time-dependent changes of rod influence on hue perception. *Vision Research 42*, 1651-1662.

Kolb, H. (2012). Midget pathways of the primate retina underlie resolution and red green color opponency. In *Webvision: The Organization of the Retina and Visual System.* Retrieved July 9, 2014 from http://webvision.med.utah.edu/ book/part-iii-retinal-circuits/midget-pathways-of-the-primate-retina-underly-resolution/

Kolb, H. (2011). Outer plexiform layer. In *Webvision: The Organization of the Retina and Visual System.* Retrieved September 27, 2013 from http://webvision.med.utah.edu/ book/part-ii-anatomy-and-physiology-of-the-retina/oute-plexiform/.

Kolb, H., Linberg, K.A., & Fisher, S.K. (1992). Neurons of the human retina: A Golgi study. *Journal of Comparative Neurology 31,* 147-187.

Kries, J. von (1905). Die Gesichtsempfindungen. In W. Nagel (Ed.) *Handbuch der Physiologie des Menschen, Vol. 3.* Vieweg: Braunschweig.

Kuehni, R.G. (2004). Variability in unique hue selection: a surprising phenomenon. *Color Research and Application 29,* 158-162.

Kulikowski, J.J., Daugirdiene, A., Panorgias, A., Murray, I.J., Stanikunas, R., & Vaitkevicius, H. (2009). Stages for extracting colour information: how the brain processes colour. *Psichologija 39,* 71-92.

Lamb, T.D., & Pugh, E.N. (2004). Dark adaptation and the retinoid cycle of vision. *Progress in Retinal and Eye Research 23*, 307-380.

Lamb, T.D., & Pugh, E.N. (2006). Phototransducton, Dark Adaptation, and Rhodopsin Regeneration, The Proctor Lecture. *Investigative Ophthalmology and Visual Science 47 (12),* 5138-5152.

Larimer, J., Krantz, D.H., & Cicerone, C.M. (1975). Opponent process additivity. II. Yellow/blue equilibria and nonlinear models. *Vision Research 15(6),* 723-731.

Lembessis, E. (1997). The Influence of Dark-adapted Rods Upon Color Vision. (Doctoral dissertation, City University of New York, 1997). Dissertation Abstracts International-B, 58/05, 2294.

Lie, I. (1963). Dark adaptation and the photochromatic interval. *Documenta Ophthalmologica 17,* 411-510.

Loeser, L. (1904). Uber den einfluss der Dunkeladaptation auf die spezifische Farbenschwelle. *Zeitschrift fur Psychologie und Physiologie der Sinnesorgane 36,* 1-18.

Lueck, C.J., Zeki, S., Friston, K.J., Deiber, M.P., Cope, P., Cunningham, V.J., Lammerstsma, A.A., Kennard, C., & Frackowiak, R.S. (1989). The colour centre in the cerebral cortex of man. *Nature 340(6232),* 386-389.

Marks, W.B., Dobelle, W.H., & MacNichol, M.F.Jr. (1964). Visual pigments of single primate cones. *Science 143,* 1181-1183.

Masland, R.H. (2001). The fundamental plan of the retina. *Nature Neuroscience 4(9),* 877-886.

Maxwell, J.C. (1855). Experiments on colour, as perceived by the eye, with remarks on colour blindness. *Transactions of the Royal Society, Edinburgh 21,* 275-298.

Mazoyer, B., Zago, L., Jobard, G., Crivello, F., Joliot, M., Perchey, G., Mellet, E., Petit, L., & Tzourio-Mazoyer, N. (2014). Gaussian Mixture Modeling of Hemispheric Lateralization for Language in a Large Sample of Healthy Individuals Balanced for Handedness. *PLoS ONE.* doi: 10.1371/journal.pone.0101165

McKeefry, D.J., & Zeki, S. (1997). The position and topography of the human colour centre as revealed by functional magnetic resonance imaging. *Brain 120(Pt 12),* 2229-2242.

McKeefry, D.J., Murray, I.J., & Parry, N.R.A. (2007). Perceived shifts in saturation and hue of chromatic stimuli in the near peripheral retina. *Journal of the Optical Society of America A 24(10),* 3168-3179.

Mullen, K.T., & Kingdom, F.A. (2002). Differential distributions of red-green and blue-yellow cone opponency across the visual fields. *Visual Neuroscience 19,* 109-118.

Nathans, J. (1987). Molecular biology of visual pigments. *Annual Review of Neuroscience 10,* 163-194.

Nathans, J., Merbs, S.L., Sung, C-H., Weitz, C.J., & Wang, Y. (1992). Molecular Genetics of Human Visual Pigments. *Annual Review of Genetics 26,* 403-424.

Nathans, J., Thomas, D., & Hogness, D.S. (1986). Molecular genetics of human color vision: genes encoding blue, green, and red pigments. *Science 232,*193-202.

Nerger, J.L., Volbrecht, V.J., & Ayde, C.J. (1995). Unique hue judgments as a function of test size in the fovea and at 20-deg temporal eccentricity. *Journal of the Optical Society of America A 12,* 1225-1232.

Nerger, J.L., Volbrecht, V.J., Ayde, C.J., & Imhoff, S.M. (1998) Effect of the S-cone mosaic and rods on red/green equilibria. *Journal of the Optical Society of America A 15(11),* 2816-2826.

Nerger, J.L., Volbrecht, V.J., & Haase, K.A. (2003). The influence of rods on colour naming during dark adaptation. In J. Mollon, J. Pokorny, & K. Knoblauch, (Eds.) *Normal and Defective Colour Vision*, Ch. 19. Oxford: Oxford University Press.

Opper, J.K., Douda, N.D., Volbrecht, V.J., & Nerger, J.L. (2014). Supersaturation in the peripheral retina. *Journal of the Optical Society of America A 31(4)*, A148-A158.

Østerberg, G. (1935). Topography of the layer of rods and cones in the human retina. *Acta Ophthalmologica (Suppl.) 6*, 1-103.

Packer, O.S., Verweij, J., Li, P.H., Schnapf, J.L., & Dacey, D.M. (2010). Blue-Yellow Opponency in Primate S Cone Photoreceptors. *The Journal of Neuroscience 30(2)*, 568-572.

Pang, J.-J., Gao, F., Lem, J., Bramblett, D.E., Paul, D.L., & Wu, S.M. (2010). Direct rod input to cone BCs and direct cone input to rod BCs challenge the traditional view of mammalian BC circuitry. *Proceedings of the National Academy of Sciences USA 107(1),* 395-400.

Parry, N.R., McKeefry, D.J., & Murray, I.J. (2006). Variant and invariant color perception in the near peripheral retina. *Journal of the Optical Society of America A 23 (7),* 1586-1597.

Perlman, I., Kolb, H., & Nelson, R. (2011). S-Potentials and Horizontal Cells. In Kolb, H., Fernandez, E., & Nelson, R., (Eds.) *Webvision: The Organization of the Retina and Visual System* [Internet] Salt Lake City (UT): University of Utah Health Sciences Center.

Pinel, J.P.J. (2014). *Biopsychology, Ninth Edition.* Ch. 16. Boston: Pearson.

Pitts, M.A., Troup, L.J., Volbrecht, V.J., & Nerger, J.L. (2005). Chromatic perceptive field sizes change with retinal illuminance. *Journal of Vision 5*, 435-443.

Polyak, S.L. (1941). *The Retina.* Chicago: University of Chicago Press.

Raviola, E., & Gilula, N.B. (1975). Intramembrane organization of specialized contacts in the outer plexiform layer of the retina: A freeze-fracture study in monkeys and rabbits. *Journal of Cell Biology 65*, 192-222.

Reeves, A. (2004). Visual Adaptation. In L.M. Chalupa & J.S. Werner (Eds.) *The Visual Neurosciences, Volume 1*, Ch. 54. Cambridge: The MIT Press.

Roorda, A., & Williams, D.R. (1999). The arrangement of the three cones classes in the living human eye. *Nature 397,* 520-522.

Rushton, W.A.H. (1957). Physical measurement of cone pigment in the living human eye. *Nature 179,* 571-573.

Rushton, W., & Powell, D. (1972). The rhodopsin content and the visual threshold of human rods. *Vision Research 12,* 1073-1081.

Schefrin, B.E., & Werner, J.S. (1990). Loci of spectral unique hues throughout the life span. *Journal of the Optical Society of America A 7(2),* 305-311.

Schmolesky, M. (2000). The Primary Visual Cortex. In *Webvision: The Organization of the Retina and Visual System.* Retrieved March 14, 2010 from http://webvision.med.utah.edu/.

Schultze, M. (1866). Zur anatomie und physiologie der Retina. *Arch. Mikrosk. Anat. 9*, 176-286.

Sharpe, L.T., Stockman, A., Jagle, H., & Nathans, J. (1999). Opsin genes, cone photopigments, color vision, and color blindness, in K.R. Gegenfurtner & L.T. Sharpe (Eds.) *Color Vision: From Genes to Perception,* Ch. 1. Cambridge: Cambridge University Press.

Siok, W.T., Kay, P., Wang, W.S.Y., Chan, A.H.D., Chen, L., Luke, K.-K., & Tan, L.H. (2009). Language regions of brain are operative in color perception. *Proceedings of the National Academy of Sciences 106 (20)*, 8140-8145.

Solomon, S.G., & Lennie, P. (2007). The machinery of colour vision. *Nature Reviews/Neuroscience 8(4)*, 276-286.

Sparkes, R.S., Klisak, I., Kaufman, D., Mohandas, T., Tobin, A.J., & McGinnis, J.F. (1986). Assignment of the rhodopsin gene to human chromosome three, region 3q21-3q24 by *in situ* hybridization studies. *Current Eye Research 5, (10),* 797-798.

Stabell, B., & Stabell, U. (1976). Rod and cone contribution to peripheral colour vision. *Vision Research 16(10),* 1099-1104.

Stabell, B., & Stabell, U. (1998). Chromatic rod-cone interaction during dark adaptation. *Journal of the Optical Society of America A 15 (11)*, 2809-2815.

Stabell, B., & Stabell, U. (2002). Effects of rod activity on color perception with light adaptation. *Journal of the Optical Society of America A 19(7),* 1249-1258.

Stabell, B., & Stabell, U. (2009). *Duplicity Theory of Vision: From Newton to the Present.* New York: Cambridge University Press.

Stabell, U. (1967). Rods as color receptors in photopic vision. *Scandinavian Journal of Psychology 8,* 139-144.

Stabell, U., & Stabell, B. (1965). Rods as color receptors. *Scandinavian Journal of Psychology 6,* 195-200.

Stabell, U., & Stabell, B. (1975). The Effect of Rod Activity on Colour Matching Functions. *Vision Research 15*, 1119-1123.

Stabell, U., & Stabell, B. (1979). Change in Hue with Rod Intrusion During Dark-Adaptation. *Vision Research 19*, 1127-1131.

Stabell, U., & Stabell, B. (1984). Color-vision mechanisms of the extra-foveal retina. *Vision Research 24,* 1969-1975.

Stabell, U., & Stabell, B. (1999). Rod-cone color mixture: effect of size and exposure time. *Journal of the Optical Society of America A 16 (11),* 2638-2642.

Trezona, P.W. (1970). Rod Participation in the 'Blue' Mechanism and its Effect on Color Matching. *Vision Research 10,* 317-332.

Troup, L.J., Pitts, M.A., Volbrecht, V.J., & Nerger, J.L. (2005). Effect of stimulus intensity on the sizes of chromatic perceptive fields. *Journal of the Optical Society of America A 22,* 2137-2142.

Valberg, A. (2005). Physiology of the Eye. In *Light Vision Color,* Ch. 3. Hoboken: John Wiley & Sons, Ltd.

Vanni, S., Henriksson, L., Viikari, M., & James, A.C. (2006). Retinotopic distribution of chromatic responses in human primary visual cortex. *European Journal of Neuroscience 24*, 1821-1831.

Volbrecht, V.J., Clark, C.L., Nerger, J.L., & Randell, C.E. (2009). Chromatic perceptive field sizes measured at 10° eccentricity along the horizontal and vertical meridians. *Journal of the Optical Society of America A 26(5),* 1167-1177.

Volbrecht, V.J., Nerger, J.L., Baker, L.S., Trujillo, A.R., & Youngpeter, K. (2010). Unique hue loci differ with methodology. *Opthalmic and Physiological Optics 30*, 545-552.

Volbrecht, V.J., Nerger, J.L., Imhoff, S.J., & Ayde, C.J. (2000). Effect of the short-wavelength-sensitive-cone mosaic and rods on the locus of unique green. *Journal of the Optical Society of America A 17(3),* 628-634.

Vos, J.J., & Walraven, P.L. (1971). On the derivation of the foveal receptor primaries. *Vision Research 11*, 799-818.

Wald, G. (1935). Carotenoids and the visual cycle. *Journal of General Physiology 38,* 351-371.

Wald, G. (1964). The receptors of human color vision. *Science 145,* 1007-1016.

Wang, J-S., & Kefalov, V.J. (2009). An Alternative Pathway Mediates the Mouse and Human Cone Visual Cycle. *Current Biology 19*, 1665-1669.

Westheimer, G. (1966). The Maxwellian view. *Vision Research, 6,* 669-682.

Williams, D.R., & Hofer, H. (2004). Formation and Acquisition of the Retinal Image. In L.M. Chalupa & J.S. Werner (Eds.) *The Visual Neurosciences, Volume 1*, Ch. 50. Cambridge: The MIT Press.

Willmer, E.N. (1946). *Retinal Structure and Colour Vision.* Cambridge: Cambridge University Press.

Willmer, E.N. (1950). Low threshold rods and the perception of blue. *Journal of Physiology 11,* 17P.

Wright, W.D. (1946). *Researches on Normal and Defective Colour Vision.* London: Henry Kimpton.

Young, T. (1802). On the theory of light and colours. *Philosophical Transactions*, 12-48.

APPENDIX A: HUE SCALING DATA

Fovea All λ	Sat* mean	Sat SD	Blue mean	Blue SD	Green mean	Green SD	Yellow mean	Yellow SD	Red mean	Red SD
AK fovea										
480 nm	82.58	3.54	94.88	10.24	5.12	10.24	0.00	0.00	0.00	0.00
500 nm	82.90	5.48	17.94	15.28	78.48	10.65	3.59	7.18	0.00	0.00
520 nm	78.63	5.20	3.59	7.18	78.79	6.25	17.62	12.50	0.00	0.00
540 nm	68.67	4.01	0.00	0.00	60.27	12.84	39.73	12.84	0.00	0.00
560 nm	64.16	5.99	0.00	0.00	46.01	14.12	53.99	14.12	0.00	0.00
580 nm	65.57	10.23	0.00	0.00	0.00	0.00	69.69	4.82	30.31	4.82
600 nm	77.26	4.52	0.00	0.00	0.00	0.00	43.52	5.35	56.48	5.35
620 nm	81.05	3.06	0.00	0.00	0.00	0.00	26.99	12.70	73.01	12.70
KY fovea										
480 nm	82.58	3.54	100.0	0.00	0.00	0.00	0.00	0.00	0.00	0.00
500 nm	74.84	3.69	20.68	15.41	74.20	7.75	5.12	10.24	0.00	0.00
520 nm	73.48	9.42	24.05	16.13	70.83	6.06	5.12	10.24	0.00	0.00
540 nm	47.58	11.74	0.00	0.00	70.58	3.27	29.42	3.27	0.00	0.00
560 nm	32.38	1.91	0.00	0.00	34.45	10.55	65.55	10.55	0.00	0.00
580 nm	36.55	9.15	0.00	0.00	0.00	0.00	50.82	8.46	49.18	8.46
600 nm	63.31	6.41	0.00	0.00	0.00	0.00	36.82	4.02	63.18	4.02
620 nm	76.05	4.35	0.00	0.00	0.00	0.00	0.00	0.00	100.0	0.00
LB fovea										
480 nm	81.05	3.06	94.15	7.09	0.00	0.00	0.00	0.00	5.85	7.09
500 nm	85.64	0.00	18.95	3.06	81.05	3.06	0.00	0.00	0.00	0.00
520 nm	84.11	3.06	2.26	4.52	94.15	7.09	3.59	7.18	0.00	0.00
540 nm	71.53	2.10	0.00	0.00	83.91	12.40	16.09	12.40	0.00	0.00
560 nm	72.58	2.42	0.00	0.00	64.16	5.99	35.84	5.99	0.00	0.00
580 nm	69.53	1.91	0.00	0.00	0.00	0.00	78.31	2.42	21.69	2.42
600 nm	77.26	4.52	0.00	0.00	0.00	0.00	28.37	3.85	71.63	3.85
620 nm	82.58	3.54	0.00	0.00	0.00	0.00	5.85	7.09	94.15	7.09
VV fovea										
480 nm	81.05	3.06	85.64	0.00	10.77	7.18	0.00	0.00	3.59	7.18
500 nm	76.05	4.35	58.47	13.49	41.53	13.49	0.00	0.00	0.00	0.00
520 nm	80.32	7.17	27.16	5.53	72.84	5.53	0.00	0.00	0.00	0.00
540 nm	70.58	3.27	10.24	11.83	76.30	6.43	13.45	16.40	0.00	0.00
560 nm	58.08	3.34	0.00	0.00	42.56	10.17	57.44	10.17	0.00	0.00
580 nm	72.74	4.52	0.00	0.00	0.00	0.00	84.11	3.06	15.89	3.06
600 nm	72.74	4.52	0.00	0.00	0.00	0.00	44.30	8.52	55.70	8.52
620 nm	85.64	0.00	0.00	0.00	0.00	0.00	18.95	3.06	81.05	3.06

*Saturation

480 nm	Sat mean	Sat SD	Blue mean	Blue SD	Green mean	Green SD	Yellow mean	Yellow SD	Red mean	Red SD
AK periphery										
4 minutes	88.39	10.51	80.32	17.04	19.68	17.04	0.00	0.00	0.00	0.00
8 minutes	86.34	11.83	83.33	15.12	16.67	15.12	0.00	0.00	0.00	0.00
12 minutes	88.39	10.51	83.33	15.12	16.67	15.12	0.00	0.00	0.00	0.00
16 minutes	77.91	2.79	83.33	15.12	16.67	15.12	0.00	0.00	0.00	0.00
20 minutes	86.34	11.83	100.0	0.00	0.00	0.00	0.00	0.00	0.00	0.00
24 minutes	88.39	10.51	81.56	3.54	18.44	3.54	0.00	0.00	0.00	0.00
28 minutes	88.39	10.51	81.56	3.54	18.44	3.54	0.00	0.00	0.00	0.00
KY periphery										
4 minutes	69.76	8.64	58.73	7.56	41.27	7.56	0.00	0.00	0.00	0.00
8 minutes	80.59	8.75	64.73	9.24	35.27	9.24	0.00	0.00	0.00	0.00
12 minutes	77.00	14.98	86.34	11.83	13.66	11.83	0.00	0.00	0.00	0.00
16 minutes	71.94	13.03	73.76	20.58	26.24	20.58	0.00	0.00	0.00	0.00
20 minutes	78.13	13.02	86.78	12.70	13.22	12.70	0.00	0.00	0.00	0.00
24 minutes	77.00	14.98	95.21	8.29	4.79	8.29	0.00	0.00	0.00	0.00
28 minutes	76.09	11.66	68.80	27.21	31.20	27.21	0.00	0.00	0.00	0.00
LB periphery										
4 minutes	83.60	3.54	81.56	3.54	13.66	11.83	0.00	0.00	4.79	8.29
8 minutes	79.95	5.49	83.60	3.54	6.83	11.83	0.00	0.00	9.57	8.29
12 minutes	77.91	2.79	78.13	13.02	17.09	18.60	0.00	0.00	4.79	8.29
16 minutes	83.60	3.54	74.36	22.79	25.64	22.79	0.00	0.00	0.00	0.00
20 minutes	77.91	2.79	90.43	8.29	4.79	8.29	0.00	0.00	4.79	8.29
24 minutes	77.91	2.79	95.21	8.29	4.79	8.29	0.00	0.00	0.00	0.00
28 minutes	76.29	2.79	90.43	8.29	0.00	0.00	0.00	0.00	9.57	8.29
VV periphery										
4 minutes	76.29	2.79	74.89	4.52	25.11	4.52	0.00	0.00	0.00	0.00
8 minutes	78.55	7.63	76.51	5.22	23.49	5.22	0.00	0.00	0.00	0.00
12 minutes	69.21	2.20	74.68	0.00	25.32	0.00	0.00	0.00	0.00	0.00
16 minutes	70.61	4.01	83.33	15.12	16.67	15.12	0.00	0.00	0.00	0.00
20 minutes	71.88	2.42	83.60	3.54	6.83	11.83	0.00	0.00	9.57	8.29
24 minutes	71.88	2.42	93.17	11.83	0.00	0.00	0.00	0.00	6.83	11.83
28 minutes	74.89	4.52	88.39	10.51	0.00	0.00	0.00	0.00	11.61	10.51

500 nm	Sat mean	Sat SD	Blue mean	Blue SD	Green mean	Green SD	Yellow mean	Yellow SD	Red mean	Red SD
AK periphery										
4 minutes	78.55	7.63	0.00	0.00	68.02	4.26	31.98	4.26	0.00	0.00
8 minutes	83.60	3.54	9.84	17.04	73.08	11.49	17.09	18.60	0.00	0.00
12 minutes	78.55	7.63	0.00	0.00	65.79	8.13	34.21	8.13	0.00	0.00
16 minutes	69.21	2.20	31.20	27.21	60.36	12.81	8.44	14.62	0.00	0.00
20 minutes	81.72	15.97	31.62	15.32	68.38	15.32	0.00	0.00	0.00	0.00
24 minutes	71.03	8.22	19.13	18.49	69.76	8.64	11.11	19.25	0.00	0.00
28 minutes	82.06	16.81	29.06	25.17	61.10	8.13	9.84	17.04	0.00	0.00
KY periphery										
4 minutes	78.55	7.63	6.83	11.83	83.60	3.54	9.57	8.29	0.00	0.00
8 minutes	79.95	5.49	6.83	11.83	81.56	3.54	11.61	10.51	0.00	0.00
12 minutes	73.28	2.42	15.27	13.44	76.29	2.79	8.44	14.62	0.00	0.00
16 minutes	69.21	2.20	25.11	4.52	74.89	4.52	0.00	0.00	0.00	0.00
20 minutes	73.49	5.22	35.57	5.51	64.43	5.51	0.00	0.00	0.00	0.00
24 minutes	72.22	6.60	13.43	23.27	81.78	20.43	4.79	8.29	0.00	0.00
28 minutes	68.80	11.64	0.00	0.00	86.78	12.70	13.22	12.70	0.00	0.00
LB periphery										
4 minutes	77.91	2.79	4.79	8.29	90.43	8.29	4.79	8.29	0.00	0.00
8 minutes	81.56	3.54	4.79	8.29	90.43	8.29	4.79	8.29	0.00	0.00
12 minutes	83.60	3.54	14.36	0.00	85.64	0.00	0.00	0.00	0.00	0.00
16 minutes	78.55	7.63	9.57	8.29	83.60	3.54	6.83	11.83	0.00	0.00
20 minutes	79.95	5.49	0.00	0.00	100.0	0.00	0.00	0.00	0.00	0.00
24 minutes	83.60	3.54	9.57	8.29	90.43	8.29	0.00	0.00	0.00	0.00
28 minutes	83.60	3.54	18.01	6.33	81.99	6.33	0.00	0.00	0.00	0.00
VV periphery										
4 minutes	79.95	5.49	0.00	0.00	75.23	7.42	24.77	7.42	0.00	0.00
8 minutes	78.34	6.33	6.83	11.83	76.29	2.79	16.88	14.62	0.00	0.00
12 minutes	82.06	16.81	6.83	11.83	84.73	13.44	8.44	14.62	0.00	0.00
16 minutes	68.02	4.26	20.05	5.49	79.95	5.49	0.00	0.00	0.00	0.00
20 minutes	63.10	0.00	23.49	5.22	76.51	5.22	0.00	0.00	0.00	0.00
24 minutes	69.21	2.20	26.38	6.49	73.62	6.49	0.00	0.00	0.00	0.00
28 minutes	59.85	6.74	15.27	13.44	77.91	2.79	6.83	11.83	0.00	0.00

520 nm	Sat mean	Sat SD	Blue mean	Blue SD	Green mean	Green SD	Yellow mean	Yellow SD	Red mean	Red SD
AK periphery										
4 minutes	67.94	2.20	0.00	0.00	61.52	15.53	38.48	15.53	0.00	0.00
8 minutes	77.91	2.79	0.00	0.00	77.86	19.53	22.14	19.53	0.00	0.00
12 minutes	76.73	20.86	0.00	0.00	61.52	15.53	38.48	15.53	0.00	0.00
16 minutes	71.03	8.22	31.20	27.21	60.36	12.81	8.44	14.62	0.00	0.00
20 minutes	65.21	12.50	0.00	0.00	62.92	16.87	37.08	16.87	0.00	0.00
24 minutes	65.56	4.26	24.37	22.25	65.79	8.13	9.84	17.04	0.00	0.00
28 minutes	65.56	4.26	24.37	22.25	68.80	11.64	6.83	11.83	0.00	0.00
KY periphery										
4 minutes	72.43	8.44	0.00	0.00	77.91	2.79	22.09	2.79	0.00	0.00
8 minutes	68.02	4.26	0.00	0.00	81.99	6.33	18.01	6.33	0.00	0.00
12 minutes	63.15	3.48	0.00	0.00	73.62	6.49	26.38	6.49	0.00	0.00
16 minutes	45.67	9.30	0.00	0.00	79.74	20.15	20.26	20.15	0.00	0.00
20 minutes	48.73	18.61	6.83	11.83	71.30	10.33	21.87	20.37	0.00	0.00
24 minutes	38.03	1.96	0.00	0.00	64.34	4.02	35.66	4.02	0.00	0.00
28 minutes	57.73	10.07	0.00	0.00	61.12	8.74	38.88	8.74	0.00	0.00
LB periphery										
4 minutes	77.91	2.79	0.00	0.00	95.21	8.29	4.79	8.29	0.00	0.00
8 minutes	77.91	2.79	0.00	0.00	93.17	11.83	6.83	11.83	0.00	0.00
12 minutes	76.29	2.79	0.00	0.00	85.64	0.00	14.36	0.00	0.00	0.00
16 minutes	81.56	3.54	0.00	0.00	88.39	10.51	11.61	10.51	0.00	0.00
20 minutes	83.60	3.54	3.69	6.40	96.31	6.40	0.00	0.00	0.00	0.00
24 minutes	81.56	3.54	4.79	8.29	90.43	8.29	4.79	8.29	0.00	0.00
28 minutes	76.94	7.83	9.84	17.04	90.16	17.04	0.00	0.00	0.00	0.00
VV periphery										
4 minutes	81.56	3.54	0.00	0.00	60.46	15.71	39.54	15.71	0.00	0.00
8 minutes	88.39	10.51	0.00	0.00	65.79	8.13	34.21	8.13	0.00	0.00
12 minutes	73.62	6.49	0.00	0.00	56.65	11.84	43.35	11.84	0.00	0.00
16 minutes	64.43	5.51	0.00	0.00	71.30	10.33	28.70	10.33	0.00	0.00
20 minutes	64.52	7.28	0.00	0.00	73.49	5.22	26.51	5.22	0.00	0.00
24 minutes	61.97	1.96	0.00	0.00	72.43	8.44	27.57	8.44	0.00	0.00
28 minutes	55.37	4.93	4.79	8.29	81.56	3.54	13.66	11.83	0.00	0.00

540 nm	Sat mean	Sat SD	Blue mean	Blue SD	Green mean	Green SD	Yellow mean	Yellow SD	Red mean	Red SD
AK periphery										
4 minutes	74.89	4.52	0.00	0.00	45.63	9.91	54.37	9.91	0.00	0.00
8 minutes	91.56	14.62	0.00	0.00	40.17	5.92	59.83	5.92	0.00	0.00
12 minutes	69.42	5.86	0.00	0.00	50.09	11.26	49.91	11.26	0.00	0.00
16 minutes	54.37	9.91	14.53	25.17	65.79	8.13	19.68	17.04	0.00	0.00
20 minutes	50.00	6.41	14.53	25.17	54.60	16.86	30.87	31.57	0.00	0.00
24 minutes	42.04	15.73	12.30	21.30	63.33	7.04	24.37	22.25	0.00	0.00
28 minutes	44.00	18.89	0.00	0.00	71.03	8.22	28.97	8.22	0.00	0.00
KY periphery										
4 minutes	58.64	3.86	0.00	0.00	75.54	8.75	24.46	8.75	0.00	0.00
8 minutes	66.67	0.00	0.00	0.00	85.38	14.76	14.62	14.76	0.00	0.00
12 minutes	45.63	7.56	0.00	0.00	62.26	8.68	37.74	8.68	0.00	0.00
16 minutes	35.15	10.86	0.00	0.00	64.13	13.71	35.87	13.71	0.00	0.00
20 minutes	31.71	7.73	0.00	0.00	61.46	12.43	38.54	12.43	0.00	0.00
24 minutes	36.67	7.04	0.00	0.00	57.60	6.80	42.40	6.80	0.00	0.00
28 minutes	27.76	14.77	0.00	0.00	49.37	20.90	50.63	20.90	0.00	0.00
LB periphery										
4 minutes	68.15	5.93	0.00	0.00	72.22	6.60	27.78	6.60	0.00	0.00
8 minutes	71.88	2.42	0.00	0.00	76.51	5.22	23.49	5.22	0.00	0.00
12 minutes	73.28	2.42	0.00	0.00	73.49	5.22	26.51	5.22	0.00	0.00
16 minutes	67.19	9.57	0.00	0.00	78.55	7.63	21.45	7.63	0.00	0.00
20 minutes	65.79	8.13	0.00	0.00	76.51	5.22	23.49	5.22	0.00	0.00
24 minutes	67.53	11.58	0.00	0.00	73.08	11.49	26.92	11.49	0.00	0.00
28 minutes	73.08	11.49	6.83	11.83	83.33	15.12	9.84	17.04	0.00	0.00
VV periphery										
4 minutes	81.56	3.54	0.00	0.00	46.73	11.72	53.27	11.72	0.00	0.00
8 minutes	83.60	3.54	0.00	0.00	36.74	18.20	63.26	18.20	0.00	0.00
12 minutes	73.49	5.22	0.00	0.00	61.10	8.13	38.90	8.13	0.00	0.00
16 minutes	61.98	15.53	0.00	0.00	40.16	18.21	59.84	18.21	0.00	0.00
20 minutes	43.59	0.00	0.00	0.00	56.42	23.09	43.58	23.09	0.00	0.00
24 minutes	37.80	7.36	0.00	0.00	74.37	28.55	25.63	28.55	0.00	0.00
28 minutes	36.67	7.04	0.00	0.00	71.36	28.21	28.64	28.21	0.00	0.00

560 nm	Sat mean	Sat SD	Blue mean	Blue SD	Green mean	Green SD	Yellow mean	Yellow SD	Red mean	Red SD
AK periphery										
4 minutes	71.88	2.42	0.00	0.00	36.67	7.04	63.33	7.04	0.00	0.00
8 minutes	71.88	2.42	0.00	0.00	40.26	3.34	59.74	3.34	0.00	0.00
12 minutes	53.29	9.75	0.00	0.00	36.90	0.00	63.10	0.00	0.00	0.00
16 minutes	25.11	4.52	0.00	0.00	61.61	43.51	38.39	43.51	0.00	0.00
20 minutes	33.25	3.69	0.00	0.00	50.00	43.54	40.16	26.65	9.84	17.04
24 minutes	35.47	18.69	0.00	0.00	9.84	17.04	70.48	0.00	19.68	17.04
28 minutes	38.48	15.53	0.00	0.00	26.51	45.91	42.39	21.33	31.10	28.65
KY periphery										
4 minutes	42.21	12.42	0.00	0.00	24.60	21.30	65.56	4.26	9.84	17.04
8 minutes	51.07	4.89	0.00	0.00	33.33	28.87	66.67	28.87	0.00	0.00
12 minutes	42.49	1.90	0.00	0.00	29.05	7.42	70.95	7.42	0.00	0.00
16 minutes	26.72	2.42	0.00	0.00	31.93	15.83	68.07	15.83	0.00	0.00
20 minutes	25.96	9.48	0.00	0.00	9.84	17.04	70.48	0.00	19.68	17.04
24 minutes	25.11	4.52	0.00	0.00	22.14	19.53	69.42	5.86	8.44	14.62
28 minutes	29.39	4.01	0.00	0.00	25.11	4.52	74.89	4.52	0.00	0.00
LB periphery										
4 minutes	54.27	3.70	0.00	0.00	47.77	9.94	52.23	9.94	0.00	0.00
8 minutes	58.96	10.48	0.00	0.00	57.79	12.42	42.21	12.42	0.00	0.00
12 minutes	56.50	6.55	0.00	0.00	51.28	13.32	48.72	13.32	0.00	0.00
16 minutes	56.41	0.00	0.00	0.00	50.00	6.41	50.00	6.41	0.00	0.00
20 minutes	59.83	5.92	0.00	0.00	37.50	10.55	62.50	10.55	0.00	0.00
24 minutes	62.06	5.21	0.00	0.00	31.10	28.65	64.11	21.04	4.79	8.29
28 minutes	58.96	10.48	0.00	0.00	34.21	8.13	65.79	8.13	0.00	0.00
VV periphery										
4 minutes	79.52	0.00	0.00	0.00	0.00	0.00	81.56	3.54	18.44	3.54
8 minutes	83.60	3.54	0.00	0.00	16.40	3.54	83.60	3.54	0.00	0.00
12 minutes	74.26	10.04	0.00	0.00	0.00	0.00	95.21	8.29	4.79	8.29
16 minutes	43.50	6.55	0.00	0.00	4.79	8.29	90.43	8.29	4.79	8.29
20 minutes	44.24	12.85	0.00	0.00	0.00	0.00	90.43	8.29	9.57	8.29
24 minutes	38.90	8.13	0.00	0.00	0.00	0.00	100.0	0.00	0.00	0.00
28 minutes	37.50	10.55	0.00	0.00	14.62	14.76	85.38	14.76	0.00	0.00

580 nm	Sat mean	Sat SD	Blue mean	Blue SD	Green mean	Green SD	Yellow mean	Yellow SD	Red mean	Red SD
AK periphery										
4 minutes	81.72	15.97	0.00	0.00	0.00	0.00	58.64	3.86	41.36	3.86
8 minutes	76.29	2.79	0.00	0.00	0.00	0.00	58.73	7.56	41.27	7.56
12 minutes	63.26	18.20	0.00	0.00	0.00	0.00	50.00	0.00	50.00	0.00
16 minutes	61.10	8.13	0.00	0.00	0.00	0.00	48.94	1.84	51.06	1.84
20 minutes	71.03	8.22	0.00	0.00	0.00	0.00	56.41	0.00	43.59	0.00
24 minutes	59.84	17.04	0.00	0.00	0.00	0.00	46.37	14.69	53.63	14.69
28 minutes	53.23	5.60	0.00	0.00	0.00	0.00	64.52	7.28	35.48	7.28
KY periphery										
4 minutes	56.50	6.55	0.00	0.00	0.00	0.00	59.74	3.34	40.26	3.34
8 minutes	55.43	6.83	0.00	0.00	0.00	0.00	52.14	3.70	47.86	3.70
12 minutes	47.86	10.38	0.00	0.00	0.00	0.00	57.57	5.06	42.43	5.06
16 minutes	38.54	12.43	0.00	0.00	0.00	0.00	63.04	14.36	36.96	14.36
20 minutes	33.25	3.69	0.00	0.00	0.00	0.00	62.20	7.36	37.80	7.36
24 minutes	36.67	7.04	0.00	0.00	0.00	0.00	65.62	5.47	34.38	5.47
28 minutes	35.15	10.86	0.00	0.00	0.00	0.00	55.34	1.86	44.66	1.86
LB periphery										
4 minutes	57.69	8.41	0.00	0.00	0.00	0.00	46.67	15.12	53.33	15.12
8 minutes	63.25	5.92	0.00	0.00	0.00	0.00	60.25	14.55	39.75	14.55
12 minutes	54.27	3.70	0.00	0.00	0.00	0.00	49.00	12.32	51.00	12.32
16 minutes	59.83	5.92	0.00	0.00	0.00	0.00	47.77	9.94	52.23	9.94
20 minutes	66.75	3.69	0.00	0.00	0.00	0.00	54.37	9.91	45.63	9.91
24 minutes	67.94	2.20	0.00	0.00	0.00	0.00	56.50	6.55	43.50	6.55
28 minutes	64.52	7.28	0.00	0.00	0.00	0.00	60.92	5.24	39.08	5.24
VV periphery										
4 minutes	72.43	8.44	0.00	0.00	0.00	0.00	57.90	11.91	42.10	11.91
8 minutes	70.61	4.01	0.00	0.00	0.00	0.00	72.43	8.44	27.57	8.44
12 minutes	67.44	17.83	0.00	0.00	0.00	0.00	71.80	12.12	28.20	12.12
16 minutes	57.60	6.80	0.00	0.00	0.00	0.00	54.37	9.91	45.63	9.91
20 minutes	48.94	6.67	0.00	0.00	0.00	0.00	73.28	2.42	26.72	2.42
24 minutes	39.13	3.86	0.00	0.00	0.00	0.00	83.60	3.54	16.40	3.54
28 minutes	36.67	7.04	0.00	0.00	0.00	0.00	64.02	19.00	35.98	19.00

600 nm	Sat mean	Sat SD	Blue mean	Blue SD	Green mean	Green SD	Yellow mean	Yellow SD	Red mean	Red SD
AK periphery										
4 minutes	88.39	10.51	0.00	0.00	0.00	0.00	42.11	11.02	57.89	11.02
8 minutes	83.33	15.12	0.00	0.00	0.00	0.00	38.90	8.13	61.10	8.13
12 minutes	81.56	3.54	0.00	0.00	0.00	0.00	41.36	3.86	58.64	3.86
16 minutes	73.49	5.22	0.00	0.00	0.00	0.00	41.25	7.04	58.75	7.04
20 minutes	70.48	0.00	0.00	0.00	0.00	0.00	50.00	6.41	50.00	6.41
24 minutes	76.51	5.22	0.00	0.00	0.00	0.00	45.63	7.56	54.37	7.56
28 minutes	71.88	2.42	0.00	0.00	0.00	0.00	41.36	3.86	58.64	3.86
KY periphery										
4 minutes	72.22	6.60	0.00	0.00	0.00	0.00	23.71	2.79	76.29	2.79
8 minutes	68.59	10.55	0.00	0.00	0.00	0.00	27.76	14.77	72.24	14.77
12 minutes	58.79	8.37	0.00	0.00	0.00	0.00	35.15	10.86	64.85	10.86
16 minutes	59.83	5.92	0.00	0.00	0.00	0.00	38.89	9.62	61.11	9.62
20 minutes	55.44	8.19	0.00	0.00	0.00	0.00	43.50	6.55	56.50	6.55
24 minutes	58.66	5.04	0.00	0.00	0.00	0.00	45.51	10.66	54.49	10.66
28 minutes	58.66	5.04	0.00	0.00	0.00	0.00	43.50	6.55	56.50	6.55
LB periphery										
4 minutes	69.21	2.20	0.00	0.00	0.00	0.00	25.32	0.00	74.68	0.00
8 minutes	63.33	7.04	0.00	0.00	0.00	0.00	26.72	2.42	73.28	2.42
12 minutes	66.45	14.25	0.00	0.00	0.00	0.00	26.38	6.49	73.62	6.49
16 minutes	73.49	5.22	0.00	0.00	0.00	0.00	26.72	2.42	73.28	2.42
20 minutes	67.94	2.20	0.00	0.00	0.00	0.00	32.47	11.58	67.53	11.58
24 minutes	72.22	6.60	0.00	0.00	0.00	0.00	29.39	4.01	70.61	4.01
28 minutes	73.49	5.22	0.00	0.00	0.00	0.00	30.79	2.20	69.21	2.20
VV periphery										
4 minutes	74.68	0.00	0.00	0.00	0.00	0.00	26.72	2.42	73.28	2.42
8 minutes	73.28	2.42	0.00	0.00	0.00	0.00	28.97	8.22	71.03	8.22
12 minutes	73.62	6.49	0.00	0.00	0.00	0.00	31.62	15.32	68.38	15.32
16 minutes	73.28	2.42	0.00	0.00	0.00	0.00	31.98	4.26	68.02	4.26
20 minutes	67.53	11.58	0.00	0.00	0.00	0.00	45.63	9.91	54.37	9.91
24 minutes	70.61	4.01	0.00	0.00	0.00	0.00	40.20	5.72	59.80	5.72
28 minutes	69.21	2.20	0.00	0.00	0.00	0.00	40.17	5.92	59.83	5.92

620 nm	Sat mean	Sat SD	Blue mean	Blue SD	Green mean	Green SD	Yellow mean	Yellow SD	Red mean	Red SD
AK periphery										
4 minutes	88.39	10.51	0.00	0.00	0.00	0.00	6.83	11.83	93.17	11.83
8 minutes	90.43	8.29	0.00	0.00	0.00	0.00	4.79	8.29	95.21	8.29
12 minutes	88.39	10.51	0.00	0.00	0.00	0.00	6.83	11.83	93.17	11.83
16 minutes	93.17	11.83	0.00	0.00	0.00	0.00	30.58	5.86	69.42	5.86
20 minutes	76.51	5.22	0.00	0.00	0.00	0.00	36.67	7.04	63.33	7.04
24 minutes	80.32	17.04	0.00	0.00	0.00	0.00	34.44	4.26	65.56	4.26
28 minutes	86.34	11.83	0.00	0.00	0.00	0.00	33.04	6.69	66.96	6.69
KY periphery										
4 minutes	93.17	11.83	0.00	0.00	0.00	0.00	9.57	8.29	90.43	8.29
8 minutes	95.21	8.29	0.00	0.00	0.00	0.00	13.66	11.83	86.34	11.83
12 minutes	93.17	11.83	0.00	0.00	0.00	0.00	6.83	11.83	93.17	11.83
16 minutes	69.42	5.86	0.00	0.00	0.00	0.00	11.61	10.51	88.39	10.51
20 minutes	63.33	7.04	0.00	0.00	0.00	0.00	23.91	11.66	76.09	11.66
24 minutes	65.56	4.26	0.00	0.00	0.00	0.00	12.30	21.30	87.70	21.30
28 minutes	66.96	6.69	0.00	0.00	0.00	0.00	18.28	15.97	81.72	15.97
LB periphery										
4 minutes	69.76	8.64	0.00	0.00	0.00	0.00	18.44	3.54	81.56	3.54
8 minutes	73.28	2.42	0.00	0.00	0.00	0.00	15.27	13.44	84.73	13.44
12 minutes	74.89	4.52	0.00	0.00	0.00	0.00	20.05	5.49	79.95	5.49
16 minutes	76.51	5.22	0.00	0.00	0.00	0.00	20.48	0.00	79.52	0.00
20 minutes	74.89	4.52	0.00	0.00	0.00	0.00	20.48	0.00	79.52	0.00
24 minutes	79.52	0.00	0.00	0.00	0.00	0.00	18.44	3.54	81.56	3.54
28 minutes	77.91	2.79	0.00	0.00	0.00	0.00	11.61	10.51	88.39	10.51
VV periphery										
4 minutes	83.60	3.54	0.00	0.00	0.00	0.00	19.41	8.75	80.59	8.75
8 minutes	81.56	3.54	0.00	0.00	0.00	0.00	14.36	0.00	85.64	0.00
12 minutes	88.39	10.51	0.00	0.00	0.00	0.00	9.57	8.29	90.43	8.29
16 minutes	78.34	6.33	0.00	0.00	0.00	0.00	18.01	6.33	81.99	6.33
20 minutes	67.53	11.58	0.00	0.00	0.00	0.00	29.80	12.19	70.20	12.19
24 minutes	79.52	0.00	0.00	0.00	0.00	0.00	18.44	3.54	81.56	3.54
28 minutes	74.89	4.52	0.00	0.00	0.00	0.00	25.32	0.00	74.68	0.00

Scotopically Equated Stimuli

480 nm	Sat mean	Sat SD	Blue mean	Blue SD	Green mean	Green SD	Yellow mean	Yellow SD	Red mean	Red SD
LB periphery										
4 minutes	73.28	2.42	79.52	0.00	13.66	11.83	0.00	0.00	6.83	11.83
8 minutes	73.49	5.22	85.38	5.73	0.00	0.00	0.00	0.00	14.62	5.73
12 minutes	67.94	2.20	79.95	5.49	0.00	0.00	0.00	0.00	20.05	5.49
16 minutes	79.52	0.00	83.60	3.54	0.00	0.00	0.00	0.00	16.40	3.54
20 minutes	73.49	5.22	85.64	0.00	0.00	0.00	0.00	0.00	14.36	0.00
24 minutes	71.88	2.42	81.56	3.54	0.00	0.00	0.00	0.00	18.44	3.54
28 minutes	74.89	4.52	83.60	3.54	0.00	0.00	0.00	0.00	16.40	3.54
VV periphery										
4 minutes	83.60	3.54	88.39	10.51	11.61	10.51	0.00	0.00	0.00	0.00
8 minutes	77.91	2.79	86.78	12.70	13.22	12.70	0.00	0.00	0.00	0.00
12 minutes	77.91	2.79	86.34	11.83	13.66	11.83	0.00	0.00	0.00	0.00
16 minutes	72.01	4.63	90.43	8.29	9.57	8.29	0.00	0.00	0.00	0.00
20 minutes	73.49	5.22	95.21	8.29	4.79	8.29	0.00	0.00	0.00	0.00
24 minutes	67.94	2.20	90.43	8.29	4.79	8.29	0.00	0.00	4.79	8.29
28 minutes	66.75	3.69	85.64	0.00	0.00	0.00	0.00	0.00	14.36	0.00
500 nm										
LB periphery										
4 minutes	66.75	3.69	11.61	10.51	83.60	3.54	4.79	8.29	0.00	0.00
8 minutes	70.61	4.01	16.40	3.54	83.60	3.54	0.00	0.00	0.00	0.00
12 minutes	73.28	2.42	16.40	3.54	83.60	3.54	0.00	0.00	0.00	0.00
16 minutes	78.55	7.63	9.57	8.29	83.60	3.54	6.83	11.83	0.00	0.00
20 minutes	74.04	9.48	6.83	11.83	93.17	11.83	0.00	0.00	0.00	0.00
24 minutes	74.89	4.52	19.68	10.27	80.32	10.27	0.00	0.00	0.00	0.00
28 minutes	77.91	2.79	14.36	0.00	85.64	0.00	0.00	0.00	0.00	0.00
VV periphery										
4 minutes	83.60	3.54	0.00	0.00	78.34	6.33	21.66	6.33	0.00	0.00
8 minutes	83.60	3.54	0.00	0.00	75.23	7.42	24.77	7.42	0.00	0.00
12 minutes	76.51	5.22	6.83	11.83	77.91	2.79	15.27	13.44	0.00	0.00
16 minutes	71.03	8.22	12.30	21.30	69.42	5.86	18.28	15.97	0.00	0.00
20 minutes	64.29	2.06	15.27	13.44	77.91	2.79	6.83	11.83	0.00	0.00
24 minutes	63.10	0.00	6.83	11.83	76.51	5.22	16.67	15.12	0.00	0.00
28 minutes	66.75	3.69	4.79	8.29	86.78	12.70	8.44	14.62	0.00	0.00

520 nm	Sat mean	Sat SD	Blue mean	Blue SD	Green mean	Green SD	Yellow mean	Yellow SD	Red mean	Red SD
LB periphery										
4 minutes	66.75	3.69	0.00	0.00	74.26	10.04	25.74	10.04	0.00	0.00
8 minutes	69.34	4.63	0.00	0.00	76.51	5.22	23.49	5.22	0.00	0.00
12 minutes	71.88	2.42	0.00	0.00	77.91	2.79	22.09	2.79	0.00	0.00
16 minutes	72.01	4.63	0.00	0.00	83.60	3.54	16.40	3.54	0.00	0.00
20 minutes	66.75	3.69	0.00	0.00	76.59	20.35	23.41	20.35	0.00	0.00
24 minutes	70.61	4.01	0.00	0.00	76.09	11.66	23.91	11.66	0.00	0.00
28 minutes	67.19	9.57	0.00	0.00	70.61	4.01	29.39	4.01	0.00	0.00
VV periphery										
4 minutes	83.60	3.54	0.00	0.00	60.83	1.96	39.17	1.96	0.00	0.00
8 minutes	83.60	3.54	0.00	0.00	58.66	5.04	41.34	5.04	0.00	0.00
12 minutes	79.52	0.00	0.00	0.00	59.83	5.92	40.17	5.92	0.00	0.00
16 minutes	66.67	0.00	0.00	0.00	47.45	15.53	52.55	15.53	0.00	0.00
20 minutes	64.29	2.06	0.00	0.00	44.43	20.74	55.57	20.74	0.00	0.00
24 minutes	68.02	4.26	0.00	0.00	36.57	20.54	63.43	20.54	0.00	0.00
28 minutes	59.83	5.92	0.00	0.00	30.24	8.64	69.76	8.64	0.00	0.00

540 nm

LB periphery										
4 minutes	62.06	5.21	0.00	0.00	62.06	5.21	37.94	5.21	0.00	0.00
8 minutes	67.02	7.50	0.00	0.00	58.60	1.90	41.40	1.90	0.00	0.00
12 minutes	68.80	11.64	0.00	0.00	57.69	8.41	42.31	8.41	0.00	0.00
16 minutes	61.97	1.96	0.00	0.00	59.83	5.92	40.17	5.92	0.00	0.00
20 minutes	56.50	6.55	0.00	0.00	49.91	11.26	50.09	11.26	0.00	0.00
24 minutes	60.87	3.86	0.00	0.00	52.14	3.70	47.86	3.70	0.00	0.00
28 minutes	68.15	5.93	0.00	0.00	59.92	8.78	40.08	8.78	0.00	0.00
VV periphery										
4 minutes	85.64	0.00	0.00	0.00	31.20	11.64	68.80	11.64	0.00	0.00
8 minutes	85.64	0.00	0.00	0.00	31.98	4.26	68.02	4.26	0.00	0.00
12 minutes	81.56	3.54	0.00	0.00	26.14	15.42	73.86	15.42	0.00	0.00
16 minutes	68.29	7.73	0.00	0.00	11.61	10.51	83.60	3.54	4.79	8.29
20 minutes	71.88	2.42	0.00	0.00	0.00	0.00	100.0	0.00	0.00	0.00
24 minutes	68.15	5.93	0.00	0.00	13.66	11.83	81.56	3.54	4.79	8.29
28 minutes	68.02	4.26	0.00	0.00	6.83	11.83	93.17	11.83	0.00	0.00

APPENDIX B: UNIQUE HUE DATA

Unique Blue	Fovea Mean	Fovea SEM	Periph Mean	Periph SEM	Periph Mean	Periph SEM
			B* condition		NB** condition	
AK						
1° stimulus	466	0.6				
2.55° stimulus	463	0.6	467	0.7	462	0.7
KY						
1° stimulus	466	0.5				
2.55° stimulus	470	0.2	468	0.3	472	0.5
LB						
1° stimulus	476	0.2				
2.55° stimulus	474	0.4	471	0.5	473	0.2
VV						
1° stimulus	469	0.2				
2.55° stimulus	474	0.3	467	0.3	470	0.6
Unique Green						
AK						
1° stimulus	506	0.7				
2.55° stimulus	502	0.7	495	0.2	496	0.2
KY						
1° stimulus	522	0.5				
2.55° stimulus	528	1.1	503	0.9	517	0.7
LB						
1° stimulus	511	0.6				
2.55° stimulus	513	0.8	495	0.5	496	0.6
VV						
1° stimulus	518	0.4				
2.55° stimulus	512	1.3	492	0.3	494	0.3

*Bleach
**No bleach

Unique Yellow	Fovea Mean	Fovea SEM	Periph Mean	Periph SEM	Periph Mean	Periph SEM
			B condition		NB condition	
AK						
1° stimulus	571	0.0				
2.55° stimulus	572	0.2	569	0.5	566	0.2
KY						
1° stimulus	565	0.5				
2.55° stimulus	567	0.4	568	0.3	565	0.6
LB						
1° stimulus	573	0.2				
2.55° stimulus	575	0.3	565	0.5	566	1.4
VV						
1° stimulus	573	0.3				
2.55° stimulus	571	0.3	562	0.3	550	0.3
Second Set Unique Blue						
JN						
1° stimulus	462	0.7				
2.55° stimulus			459	0.7	459	1.0
LB						
1° stimulus	456	1.0				
2.55° stimulus			467	0.5	468	0.3
VV						
1° stimulus	465	0.4				
2.55° stimulus			473	1.4	472	1.2

APPENDIX C: BINARY HUE DATA

Binary Red/Blue	Fovea Mean	Fovea SEM	Periph Mean B* condition	Periph SEM	Periph Mean NB** condition	Periph SEM
JN						
1° stimulus	437	2.1				
2.55° stimulus			424	1.1	426	1.7
LB						
1° stimulus	415	1.8				
2.55° stimulus			424	0.5	424	0.9
VV						
1° stimulus	415	1.8				
2.55° stimulus			403	0.9	418	1.6
Binary Blue/Green						
JN						
1° stimulus	488	1.9				
2.55° stimulus			481	2.9	486	1.8
LB						
1° stimulus	486	0.7				
2.55° stimulus			482	0.6	482	0.3
VV						
1° stimulus	497	0.9				
2.55° stimulus			485	0.1	488	0.7
Binary Green/Yellow						
JN						
1° stimulus	540	1.3				
2.55° stimulus			545	2.2	537	2.6
LB						
1° stimulus	563	0.8				
2.55° stimulus			560	0.6	557	1.2
VV						
1° stimulus	549	2.3				
2.55° stimulus			532	1.2	532	2.2

*Bleach
**No bleach

Binary Yellow/Red	Fovea Mean	Fovea SEM	Periph Mean B condition	Periph SEM	Periph Mean NB condition	Periph SEM
JN						
1° stimulus	596	0.4				
2.55° stimulus			589	1.6	591	2.3
LB						
1° stimulus	591	1.4				
2.55° stimulus			587	1.5	593	0.8
VV						
1° stimulus	595	0.6				
2.55° stimulus			588	1.4	591	1.5

LIST OF ABBREVIATIONS

AC	amacrine cell
BC	bipolar cell
HC	horizontal cell
L cone	long-wavelength sensitive cone photoreceptor
LGN	lateral geniculate nucleus of the dorsal thalamus
M cone	middle-wavelength sensitive cone photoreceptor
Phot	photopic, referring to vision mediated by cone photoreceptors
RGC	retinal ganglion cell
RPE	retinal pigment epithelium
S cone	short-wavelength sensitive cone photoreceptor
SBC	small bistratified cell, a type of RGC
Scot	scotopic, referring to vision mediated by rod photoreceptors
SD	standard deviation
SEM	standard error of the mean
Td	Troland, a unit of retinal illuminance
UB	unique blue
UG	unique green
UH	unique hue
UY	unique yellow
V1	primary visual cortex (AKA striate cortex, Brodmann's area 17)
V4	fourth visual cortical area
VO1	first area of ventral occipital visual cortex